SAPIENZA
UNIVERSITÀ DI ROMA

Dipartimento di Ingegneria dell'Informazione, Elettronica e Telecomunicazioni

Dottorato di Ricerca in Elettromagnetismo del XXIX Ciclo

Attività di Ricerca:

Definizione, Studio e Progetto Preliminare di una Tecnica di Geo-Localizzazione di Sorgenti Interferenti per Satelliti Commerciali di Telecomunicazioni

Coordinatore del Corso: ***Prof. Daniele Andreucci***

Docente guida: ***Prof. Fabrizio Frezza***

Dottorando: ***Vincenzo Schena***

Novembre 2013 – Ottobre 2016

PREMESSA

Il lavoro descritto nel presente documento costituisce per me, da un lato, il giusto compendio dei miei studi, conclusi più di ventisette anni fa e dall'altro una nota d'onore, per una carriera spesa a fare ricerca e sviluppo nell'Azienda in cui lavoro da ormai diciannove anni, cioè Thales Alenia Space Italia (TAS-I), dopo aver iniziato la mia carriera in un Consorzio di Ricerca tra Università e Industria.

E' per questo che mi sento di dedicare il lavoro svolto nei tre anni di Dottorato a Thales Alenia Space Italia e in particolare al mio collega Ing. Giacinto Losquadro, oggi anche il mio Responsabile in Azienda. Con lui ho percorso tutti i diciannove anni di carriera aziendale, affrontando le tante difficoltà che in qualsiasi lavoro s'incontrano, ma anche condividendo tante soddisfazioni.

Spero di non saziare mai abbastanza la mia sete d'imparare e la mia curiosità nell'apprendere, non solo le "cose" tecniche, ma anche di altre discipline.

Penso che la vera ricchezza di un uomo sia la conoscenza e la consapevolezza di quanto altri uomini hanno fatto sia nel passato sia nel presente. Questo costituisce anche uno dei mezzi per conoscere gli altri e condividere con loro il dono prezioso del sapere.

TABLE OF CONTENTS

1 RESEARCH ACTIVITY SUMMARY 11

2 MOTIVATION: RADIO FREQUENCY INTERFERENCE CONTEXT DEFINITION (CONTEXT OF THE RESEARCH) 13

2.1 RFI ANALYSIS IN THE SATCOM CONTEXT 13

3 BACKGROUND: RADIO FREQUENCY INTERFERENCE CHARACTERISATION AND QUANTIFICATION 18

3.1 RADIO FREQUENCY INTERFERENCE IMPACT AND CHARACTERISATION 20

3.2 SATCOM RADIO FREQUENCY INTERFERENCE SCENARIO ANALYSIS AND QUANTIFICATION 28

4 METHODOLOGY: THE GEO-LOCALISATION TECHNIQUE FOR RFI MITIGATION 40

4.1 PHASE 1 - SPECTRUM MONITORING OPERATION APPROACH FOR INTERFERENCE INTERCEPTION 42

4.2 PHASE 2 – RFI GEO-LOCATION CONCEPTS AND TECHNIQUES, DEFINITION AND DESIGN 48

4.3 RFI GEO-LOCATION TECHNIQUE AND ALGORITHM: INTERFEROMETER GEO-LOCALISATION TECHNIQUE 55

4.3.1 System Dimensioning for Ku band scenario 61

5 PRELIMINARY ARCHITECTURAL DESIGN 73

5.1 ON-BOARD RFI GEO-LOCALISATION SYSTEM INTEGRATION 74

5.2 CALIBRATION TECHNIQUES 89

5.3 SIMULATION ACTIVITY 94

6 CONCLUSIONS AND FUTURE WORK 97

7 ANNEX 1 101

7.1 SUPER-RESOLUTION ALGORITHMS 101

7.1.1 Definition of the Spatial Covariance Matrix 102

7.1.2 MUSIC (MUltiple SIgnal Classification) 105

7.1.3 Algorithms based on spectral analysis 107

7.1.4 DOA Estimation Algorithm using Conventional Technique 108
7.1.5 DOA Estimation Algorithm using Capon Technique 109
7.1.6 Other super-resolution algorithms 111
8 ANNEX 2 112
8.1 ESTIMATION METHOD OF CHANNELS TRANSFER FUNCTION 112
9 ANNEX 3 114
9.1 CALIBRATION VIA TRANSFER FUNCTION PARAMETERS ESTIMATION 114
10 ANNEX 4 123
11 REFERENCE DOCUMENTS 129
12 LIST OF ACRONYMS 132

LIST OF FIGURES

Figure 2-1: SATCOM Service Mission Scenarios 15

Figure 3-1: Graphic Representation of the Statistical Analysis of the Interference Occurrence per Mont Percentage, [RD 5] 22

Figure 3-2: Around the Edge of Coverage 27

Figure 3-3: Inside Coverage 27

Figure 3-4: BSS/FSS Commercial SATCOM Scenario Victim Scenario 30

Figure 3-5: NTS and MSS SATCOM Victim Scenario 31

Figure 3-6: G/T Performance on the HB6 coverage [RD 14] 31

Figure 3-7: EIRP Performances on the HB6 Coverage [RD 14] 32

Figure 3-8: SATCOM Feeder Link Chain Details 37

Figure 4-1: RFI Management Strategy 41

Figure 4-2: Pirate Interference [RD 4] 44

Figure 4-3: CW Interference [RD 4] 45

Figure 4-4: Sweep CW Interference (Jammer) Spectrum Plot [RD 4] 46

Figure 4-5: Multi-Tone CW Interference (Jammer) Spectrum Plot [RD 4] 47

Figure 4-6: Radio Interferometer Principle Scheme 56

Figure 4-7: Interferometer Implementation Scheme 58

Figure 4-8: Ambiguity Resolution, Accuracy and FoV 59

Figure 4-9: Geo-Satellite Field-of-View 60

Figure 4-10: Link Geometry 60

Figure 4-11: Sensor Antenna Spatial Configuration and Possible Installation Layout on the Satellite 61

Figure 4-12: SpaceBus B2 and Related Deployed Satellite 61

Figure 4-13: Ambiguity Resolution, Accuracy and FoV 63

Figure 4-14: Electrical Angle Error Introduced by the Noise 65

Figure 5-1: Geo-Localisation Hybrid Technology Architecture 73

Figure 5-2: Feeds Layout on Earth Face Panel 74

Figure 5-3: Feeds Layout on Earth Face Panel 74

Figure 5-4: 10,00 -12,75 GHz 75

Figure 5-5: RaFISS payload RX section block diagram (baseline with H and V polarization) 76

Figure 5-6: RaFISS payload PL receiving section block diagram with the H or V polarization processing option 77

Figure 5-7: Interferometer Payload (RaFISS) transmission Section Block Diagram (PCC Link Channel Approach) 80

Figure 5-8: Block Diagram of signal acquisition chains of Digital Processor Operating in Single Polarisation 81

Figure 5-9: Narrow Band Analysis Approximation Concept 83

Figure 5-10: FPGA Poliphase FFT Channelizer Architecture 84

Figure 5-11: Schematic outline of a three layer QMF bank 85

Figure 5-12: Simulator Block Diagram 94

Figure 5-13: Simulation Scenario and Covariance Matrix Block Diagram 95

Figure 5-14: Simulation Result on the Spatial Spectrum 95

Figure 5-15: RFI signal vector referenced on the plane containing the sensors/antennas...96

Figure 5-16: Simulation flow to find the RFI sources position improving the positioning accuracy.....96

Figure 5-17: Result of the position of the RFI sources on the map.....96

Figure 6-1: SICRAL 2 Satellite [RD 17] 97

Figure 6-2: Laboratory Emulation Set-Up 98

Figure 7-1: Scheme of signals which affect from different directions on a generic antenna array 102

Figure 7-2: 3-dimensional array with arbitrary geometry.....103

Figure 7-3 Performance of MUSIC 107

Figure 7-4 Comparison of the three algorithms (red: conventional, black: Capon, blue: MUSIC).....107

Figure 7-5: Performance of conventional DOA Estimation algorithm.....109

Figure 7-6 Performance of Capon DOA Estimation algorithm.....110

Figure 9-1: Digital part of the Channel Processor coming from Company Heritage System 115

Figure 9-2: a) and b) estimated transfer functions in phase and module form; c) complex transfer function as to be synthesised on I and Q branches 115

Figure 9-3: Approximate standard deviation of Estimated Phase as a function of the Calibration Tone Power over Total Users Power ratio, i.e., $\mathbf{10 \cdot Log10 PcalPcTot}$ 116

Figure 9-4 : Estimated Module Standard Deviation (20*log10(1+sigma) 118

Figure 9-5: Simulated I&Q Amplitude Unbalance estimation.....120

Figure 9-6: Simulated I&Q Phase Unbalance estimation 120

Figure 9-7: Simulated Feed-to-Feed Amplitude Unbalance estimation 120

Figure 9-8: Simulated Feed-to-Feed Phase Unbalance estimation.....120

Figure 9-9: Simulated Phase Noise Source 121

Figure 9-10: Simulated Feed-to-Feed Overall Amplitude Unbalance estimation.....121

Figure 9-11 : Simulated Feed-to-Feed Overall Phase Unbalance estimation 122

LIST OF TABLES

Table 3-1: RFI Scenarios Definition Preliminary Guidelines [RD 6] 20

Table 3-2: Statistical Analysis of the Interference Events per Month.....21

Table 3-3: Interference classification and typology 23

Table 3-4: Unintentional Interferences [RD 6] 24

Table 3-5: Intentional RFI Scenarios Definition.....28

Table 3-6: Reference Scenario Parameters 29

Table 3-7: Service Area G/T and EIRP 32

Table 3-8: Frequency Plan and Channelization.....33

Table 3-9: Ku/Ku Band Scenario Preliminary C/(N+I) evaluation.....39

Table 4-1: Victim/Interferer Parameters.....46

Table 4-2: Victim/Interferer Parameters.....47

Table 4-3: Preliminary RFI Geo-Location Figure-of -Merit.....51

Table 4-4: RFI Geo-Location Concepts and algorithms characteristics.....53

Table 4-5: Ku/Ku Band RFI Scenario Preliminary System Dimensioning (sensors diameter 6 λ) 68

Table 4-6: Ku/Ku Band RFI Scenario Preliminary System Dimensioning (sensors diameter 13 λ) 69

Table 4-7: Ka/Ka Band RFI Scenario Preliminary System Dimensioning (sensors diameter 6 λ) 71

Table 4-8: Ka/Ka Band RFI Scenario Preliminary System Dimensioning (sensors diameter 13 λ) 72

Table 5-1: Single-Shot Performances of Phase and Gain Calibration.....93

Table 7-1: Classification of super-resolution algorithms.....111

1 RESEARCH ACTIVITY SUMMARY

L'attività di ricerca svolta nel triennio di dottorato si è articolata intorno al tema delle interferenze che impattano sulle telecomunicazioni da satelliti geostazionari principalmente in ambito commerciale e istituzionale. L'attività è stata sviluppata secondo le seguenti fasi:

1. In una prima fase si è fatta un'analisi delle soluzioni per identificare gli episodi d'interferenza e caratterizzarli.

2. A seguire si sono proposte e analizzate delle tecniche per individuare e localizzare le sorgenti d'interferenza. In questa fase si è identificata una soluzione opportuna per soddisfare sia i requisiti funzionali e prestazionali che quelli legati all'ambito in cui la soluzione è proposta (ambito commerciale SATCOM).

L'attività di dottorato è stata impostata partendo dall'esperienza di ricerca già maturata dal dottorando in ambito industriale in cui lavora (Thales Alenia Space Italia o TAS-I). Egli, infatti, ha gestito e gestisce tecnicamente e in qualità di Responsabile Tecnico di attività di Ricerca e Sviluppo (R&D), studi finanziate dall'Agenzia Spaziale Europea (European Space Agency nel seguito indicata come ESA) e dall'Agenzia Spaziale Italiana (in seguito indicata con ASI), in collaborazione con Operatori Satellitari quali EUTELSAT S.A., lo sviluppo di tecnologie satellitari per contrastare fenomeni d'interferenza che impattano soprattutto su satelliti ad uso commerciale.

Per inquadrare il tema della ricerca, è necessario partire dalla situazione in cui la tecnologia proposta e studiata si colloca.

In questo periodo il mondo delle telecomunicazioni satellitari sta conoscendo un nuovo sviluppo, in vista della possibilità di poter effettivamente consentire un accesso ai dati più efficiente in modo paritario con quanto già accade con le infrastrutture di accesso terrestri sia wired sia wireless (reti DSL, in fibra, Wi-Fi, WiMAX ecc.). Tale sviluppo è molto sti-

molato e favorito dalle istituzioni europee (Commissione Europea ed ESA) e nazionali (ASI, Comitato delle Regioni Italiane, Governo Italiano) perché consentirebbe di ridurre se non abbattere definitivamente il problema del Digital Divide in Europa e nel bacino del Mediterraneo. Con la frase Digital Divide s'intende che gran parte di un territorio non è servita da opportune infrastrutture di telecomunicazioni (TLC), non consentendo ai cittadini di accedere ai relativi servizi come invece avviene per altri (tipicamente chi vice in zone molto urbanizzate).

Tale nuovo sviluppo è favorito dalle tecnologie che si stanno studiando e proponendo per quanto alle TLC satellitari (in seguito indicate come SATCOM ovvero Satellite Communication) e che contribuiscono allo sviluppo di sistemi definiti High Throughput Satellite (HTS) o anche Terabit Satellite. Questo consentirà a breve di poter disporre in orbita di satelliti molto più potenti di quelli attuali, in grado di garantire coperture e prestazioni simili se non migliori a quelle fornite dalle infrastrutture terrestri più evolute.

Anche nell'ambito dei servizi satellitari per la televisione (Broadcast Satellite Service o BSS) tradizionali e, in generale, per i servizi multimediali (video e suono), tale sviluppo tecnologico sta favorendone una maggior diffusione.

2 MOTIVATION: RADIO FREQUENCY INTERFERENCE CONTEXT DEFINITION (CONTEXT OF THE RESEARCH)

The subject of the research activity has been stimulated by actual requests coming from the Satellite Communication (SATCOM) commercial context. In this business area constituting one of the more growing markets in the worldwide telecommunication one, the radio frequency interference phenomena are becoming very critical. The technology growing in the SATCOMs is opening new perspectives for the future telecommunication market inducing the operators and, in general, the stakeholders to consider very seriously the impact of the RFI in order to stimulate the research of suitable and affective solutions taking into account the costs.

In this paragraph the preliminary analysis of the SATCOM context towards the RFI phenomenon carried out in the first phase of the research is described, providing the suitable references and defining the requirements introduce definition, analysis and design of the proposed and studied technical solution.

2.1 RFI ANALYSIS IN THE SATCOM CONTEXT

Nowadays the satellite communication (SATCOM) can bridge the digital gap across European and, in a larger view, worldwide regions and deliver broadband and telecommunications services to under-served areas and populations, reducing in this way the so called "Digital Divide".

Another stimulus for the SATCOM growth and, in general, for the space technologies (for Navigation, for Earth Observation and so on) comes from the improvement of the competitiveness of the space sector technologies and service offers supporting the European Union (EU) policies. This is notably the Digital Single Market also supported by the continuous seamless integration of SATCOM technologies and networks with terrestrial ones, offering a more effective, performing and extended services to the European population and follow-

ing to the worldwide one. For the SATCOM currently this objective is favoured and supported by the implementation of the High Throughput Satellite (HTS) or Terabit systems and by the improvement of the classical SATCOM broadband services (video broadcasting, multimedia services etc.).

Growing satellite telecommunications and related technologies in the commercial space industry and the ever-increasing revenues that are produced, the necessity for developing space secure conditions and solutions are justified and required by the stakeholders. The security discipline is already applied in the Military Satellite Communication (MILSATCOM) where customised solutions and technologies have been developed and actually implemented.

On the other side for what concerns commercial SATCOM operators, value for money has to be carefully considered thinking that possible customised AI/AJ functions/solutions have to be an asset that is worth procuring and selling as an added feature, contributing in increasing their revenues [RD 1]. To approach this objective, for commercial SATCOM applications the operators have to assess the level of the risk (probability of interference per gravity of the effects) with respect to the costs of mitigating the impacts of interferences. For these reasons Radio Frequency Interference (RFI) issues represent a serious threat for the commercial and military SATCOM systems.

The importance of controlling and mitigating RFI is well-known among the satellite community and several stakeholders (including satellite operators, manufacturers and international organisations - such as, for SATCOM satellites, IRG and GVF) have been actively contributing to raise awareness on interference, coordinating among key players, proposing and promoting technical solutions.

To be aware on the criticality of the RFI impact on the SATCOM, understanding the right approach to face the problem, it is useful to take in mind the target services impacted or can be impacted by the RFI. Currently the SATCOMs provide services for:

- content distribution, such as the broadcasting of sport, news or entertainment channels, either for direct reception or as a contribution link to terrestrial (cable or wireless) distribution network
- backhauling of terrestrial networks, such as mobile cellular networks

- military communications, e.g. for reach back communications, tactical headquarters, military navy ships, command control and transmission of payload data of Remotely Piloted Aircraft Systems (RPAS).

In a pictorial way, Figure 2-1 shows the main commercial satellite services can be impacted by RFIs.

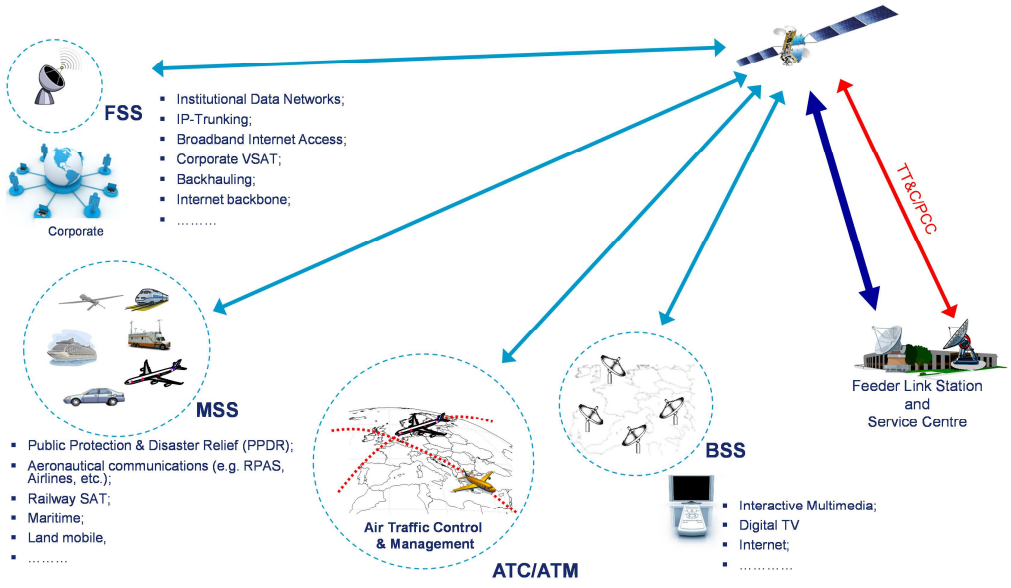

Figure 2-1: SATCOM Service Mission Scenarios

In the future, SATCOMs could also be used for Air Traffic Management (ATM) applications (already several initiatives are in progress by European Space Agency and the European Union).

In all these cases, the availability of the satellite network, as part of a wider information system, is critical to guarantee the satisfaction of the customers in terms of:

- distribution of the final of the football world cup cannot suffer of being interrupted, with the potential of creating billions of unsatisfied supporters;
- Mobile communication network service providers cannot accept service disruptions for certain part of their coverage areas, since they would suffer from commercial effects;

- The command and control links of RPAS, as well as payload data, cannot be disrupted during mission critical phases;
- Communication links contributing to the safety of human personal are also critical.

As a matter of illustration, up link interferences into satellite receivers may have the following impacts, as a function of the actual RFI power:

- Disruption of telecommand (TC) link of the satellite, which effects may vary according to the Fault Detection (FD), Identification and Recovery (FDIR) implemented on board the satellite;
- Increase of the noise floor in the satellite payload receivers, RF power stealing (and capacity reduction in terms of power robbing), partial or total disruption of user or network signalling channels, and physical destruction of the receivers.

While modern and dedicated communication satellite systems procured for the dedicated use by military forces may offer significant protection features against jamming, the corresponding on board hardware, on ground equipment and system architecture are quite complex to handle, and may be subject to export control constraints (being ultimately banned from export). The implementing and operating costs of such a function can be significant with respect to the total cost of the system. However, information assurance being a must for world leading military forces, even under heavy threats, the costs of this anti-jamming function for this type of users is accepted.

In the commercial SATCOM, RFI (both unintentional or intentional) phenomena are generating concerns and are worrying the satellite operators, mainly for what concern the Broadcasting (and broadband) Satellite Services (BSS) and Fixed Satellite Services (FSS). This is also a large risk for the emerging and growing Mobile Satellite Services (MSS) typically operating in L band (frequency range 1,0 – 2,0 GHz) and today addressed also towards other frequency ranges as the K/Ka band (frequency range 18,0 – 27,0 GHz for the K band and 27,0 – 40,0 GHz for the Ka) and to expand the band capabilities. From the point of view of risk management, it is mandatory to assess the level of the risk (probabil-

ity per gravity) with respect to the costs of mitigating the impacts of interferences.

Despite the great number of interfering signal types, a preliminary classification of RFI has been carried out according to the nature of interfering sources [RD 1]:

- Intentional RFI. The transmitting events are deliberately performed in order to attack other systems (e.g., jamming, spoofing, etc…) and it consists typically in in-band emissions;
- Unintentional RFI. The inference events are caused by signals of space/ground systems other than the interfered system or by signals intended for the interfered systems but transmitted with characteristics (e.g., frequency, polarisation, etc…) not compliant with the system requirements. Unintentional RFI may be both in-band or excessive out-of-band emissions from services in adjacent bands.

Currently possible anti interference methodologies and techniques are available mainly in the military SATCOM area and, some time, these are described or reported in literature. These techniques can be considered as applicable at antenna/RF level and/or at base-band level in the SATCOM payload combined with the ground segment where typically the management software runs. The techniques developed at antenna/RF level are more effective and well experienced. Today it is possible to choice between several approaches in this sense, depending on the correlation between effectiveness, impact on the traffic, complexity and cost to be taken into account.

Taking into account the above scenario description and the role of RFI in the SATCOM, the study activity has been modulated on three main phases: (i) a first one concerning the analysis on the status–of-the-art (SotA) related to the RFI events impacting on the commercial SATCOM. A second phase concentrated on the geo-localisation techniques and methodologies to localise the position at the ground of the RFI sources. A final phase targeted on the definition and analysis of anti-interference techniques suitable for the implementation on SATCOM commercial satellites highlighting their effectiveness in terms of performances and cost implementation.

Due to complexity of the subject as above summarised, in the present only the results of the first activity phase is described, giving some preview on the second phase.

3 BACKGROUND: RADIO FREQUENCY INTERFERENCE CHARACTERISATION AND QUANTIFICATION

Currently the majority of the commercial communication satellites are not hardened to protect against unintentional (true interference) and intentional (jamming) interferences. At the same time the growing request of services and application field (not only commercial ones but institutional and military well represented by dual-use payload technique) is increasing the exigency by the operator to guaranty a high level and constant quality-of-service (QoS) to the final users.

Due to the above mentioned situation it is mandatory to provide also for the commercial SATCOM market anti-interference/anti-jamming (AI/AJ) technical solutions as in the military context, but having a view on the suitable ratio between effectiveness (performances) and implementation costs intended.

In SATCOM, it is reported that only a small percentage of overall satellite capacity is affected by RFI (around 1-2%) [RD 5], yet RFI represents the single most important operational problem affecting customer services main on geostationary satellites causing the satellite industry to lose millions of euros per year due to their detrimental effects, ranging from a degradation in the QoS to the completely outage of service.

Additional RFI impacts that could be mentioned include also power robbing effects for traditional bent-pipe transponders, generation of (additional) intermodulation products and spurious in the satellite analogue front ends, blinding/saturation of satellite payload receiving chains. RFIs are also responsible for operational problems (such as the time and resources required in order to properly detect and resolve the interference events) and aspects not easily quantifiable but of paramount importance, such as SATCOM operators' image damages.

For SATCOM the most important contributor to all interference events is due to unintentional interferences, while intentional interferences typically represent only around 7%

[RD 5]of all interference events. However, it is also well known that these percentages may largely vary. For instance, intentional interferences up to (and, in some cases, over) 20% are reported in critical geographical areas such as North Africa and Middle-East [RD 1].

Unintentional RFI may be classified in terms of the service the interfering signals belong to (e.g. BSS, FSS, occasional use, SCPC/MCPC, VSAT, etc…), with the VSAT RFIs typically representing the major contribution and being the most critical and time consuming RFI to detect and resolve [RD 1]. This is due, among other aspects, to the intrinsic characteristics of VSAT signals (based on MF-TDMA according to DVB-S/S2-RCS/RCS2 standards), the nature of RFI, which typically results from aggregated interfering signals generated by emitters spread over the service coverage, the difficult identification of faulty or misspointed user terminals and unreliable remote terminals installation and products. RFI in lowest frequency bands (e.g., VHF, UHF, L/S bands) used for MSS and/or maritime communications is also an important issue to be considered.

Effectively tackling interference is a complex task to be performed at multiple levels, i.e.:

a. At Technical Level
   - ✓ Proactive Solutions (e.g., Training and Certification, Type Approvals, Network Validation)
   - ✓ Reactive Solutions (e.g., Carrier Identification or ID, RFI Geo-location, etc…)
b. At Regulatory Level (e.g., International Telecommunication Union or ITU)

With respect to above point "a", Table 3-1 reports the preliminary reviewed guidelines to be applied for the definition of the RFI scenarios.

Scenario Parameter	Aspects to be Defined
Interference Emitters	• Classification of static and dynamic ground emitters; • Estimated contribution of each interfering emitter type to the overall RFI events; • Expected interferer locations/regions; • Statistics of the RFI.
Interfering Signals	• Type and characteristics of intentional and/or unintentional interference • Detailed characterization of interfering signals in terms of, at least, type of interfering signals (e.g. modulated signals, CW, chirp signals, bursty signals, radar like burst signals), typical power levels, signal bandwidths and centre frequencies, etc.; • For intentional interference, jamming signals such as noise interfering (including broadband noise, partial band noise, narrowband noise); • Type of service the interferer belongs to (e.g. BSS, FSS, MSS, occasional use, SCPC/MCPC, C&R, etc.); • Effects of both single and aggregate interfering signals received by the telecom satellite.
Impact of Interfering Signals on SATCOM Services	• The identified signals will be classified, at least, according to the following KPIs: o Expected relative occurrence of interfering event; o Expected impact on telecom services(s) in terms of degradation of QoS and /or service outage; o Estimated time/difficulty required for RFI geo-location; o (Impacted Bandwidth)*(time to Resolve RFI).

Table 3-1: RFI Scenarios Definition Preliminary Guidelines [RD 6]

3.1 RADIO FREQUENCY INTERFERENCE IMPACT AND CHARACTERISATION

It has been demonstrated and quantified the risk of financial losses by the SATCOM Operators simply considering the already available data on Internet [RD 1], and in general in

literature [RD 2] the losses caused by interferences and mainly by jammer signals, as described in Table 3-2 and graphically shown in Figure 3-1 where the statistical occurrence of interference events per month is reported. Due to the intrinsic nature of the wanted interference (jammer, i.e. a voluntary attack towards the satellite operativeness) for the Operators it represents a difficult problem to solve, more difficult than the unwanted interference, where suitable procedures and protocols have been implemented and effectively used.

Starting from the above described situation, currently the implementation in the SATCOM commercial context of suitable and effective anti-interference techniques, embedded into the payload, it is becoming an important asset to add in the satellite order commitments but with attention in the final costs.

To define and propose suitable solutions it is useful to start from the military SATCOM technology. In this context, indeed, the anti-interference/anti-jamming (AI/AJ) techniques have already been developed and implemented from long time. To identify a suitable technical solution it is necessary to start from the identification of the differences between the requirements on the commercial and military SATCOM contexts.

Most Relevant Interference Event (EI) Typology		*Numb. of EI per month*	*Occurrence percentage*	*Total Percent.*
Total Interference Event per month		*303*	*100,0%*	
Unwanted	Adjacent Satellite Interference	57	18,8%	**82,7%**
	Cross-polarization Interference	72	23,8%	
	Co-Polarization Interference	93	30,7%	
	Intermodulation Interference	27	8,9%	
Wanted	Raised Floor Noise	3	*1,0%*	*16,3%*
	Continuous Wave Jamming	21	*6,9%*	
	Re-transmit/Re-Broadcast (FM/Radar)	12	*4,0%*	
	Sweeper Jamming	12	*4,0%*	
Unknown		3	1,0%	

Table 3-2: Statistical Analysis of the Interference Events per Month

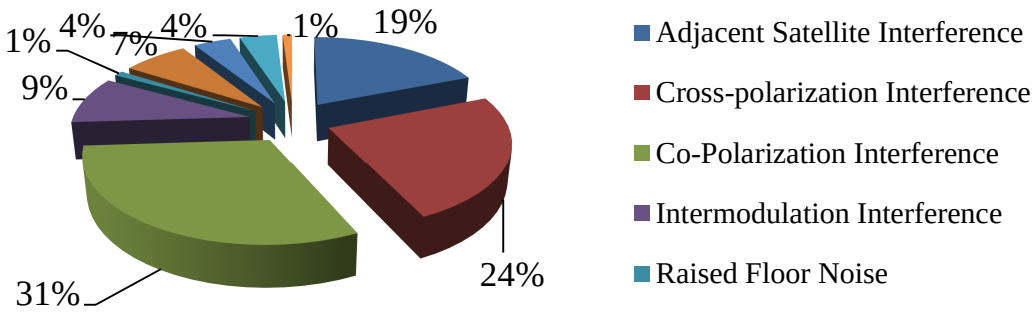

Figure 3-1: Graphic Representation of the Statistical Analysis of the Interference Occurrence per Mont Percentage, [RD 5]

The military market requires more preforming and robust AI/AJ solutions for their pay-loads, but typically applied on a reduced number of transponders operating in the typical military frequency ranges as the UHF (240 – 320 MHz) and SHF (7 – 8 GHz) [RD 7].

The commercial market requires a more extended solution covering all the available band-width on board the satellite (about 500 MHz) on all the polarisation modes (linear vertical and horizontal or circular left and right) and in the frequency ranges they utilise, i.e. C (3,6 – 6,4 GHz), Ku (10,7 – 14,5 GHz), K/Ka (17,7 – 20,2 GHz/27,5 – 30,0 GHz) [RD 8] and upper bands. In addition, they want to optimise the cost of the investment, synergising it with the revenue forecasts due to the reduction of the interference losses risks. As it is clear, the implementable technical solution has to be tailored to this market target trying to propose a smart technology in terms of performances and costs.

Starting from the above description of the RFI impact, clarifying the market reason in de-fining a suitable technological solution for the commercial SATCOM, the scenarios con-sidered in the research activity have been targeted on the three typical satellite service cat-egories, i.e.:

1. the Broadcast Satellite Services (BSS) that constitutes the main impacted service typology;
2. the Fixed Satellite Services (FSS), very critical in terms of consequences when im-pacted by the RFI;
3. the Mobile Satellite Services (MSS) typically stronger than the others, due to the nature of the provided service (the mobile TLCs have an intrinsic robustness to-wards the interference phenomena).

Table 3-3 lists the experienced unintentional and intentional RFI by the SATCOM Operators. In the common experience of the operators, the highest percentage of the interferences detected during the operations on their space capacity can be classified as unintentional (about the 93% of the total interference events per year[1]). This kind of interference is mainly due to poorly trained personnel and faulty equipment.

Unintentional	Intentional
when interference occur mainly as result of defective equipment, operator error or propagation effects. Typologies are:	when we refer to on purpose generated signals as defensive or offensive interference. Typologies are:
■ Frequency modulation interference ■ Cross Polarization ■ Digital Channel Overriding ■ Intermodulation ■ Raised Noise Floor ■ Spike Interference ■ Ionosphere scintillation ■ Co-channel Interference ■ Adjacent transponder Interference ■ Adjacent Satellite Interference	■ Noise Jamming ■ Tone Jamming ■ Multi- Tone Jamming ■ Sweep Jamming ■ Barrage Jamming ■ Pulse Jamming ■ Deceptive Jamming ■ Reactive Jamming

Table 3-3: Interference classification and typology

In Table 3-4 the main typologies of unintentional interference sources are reported providing a summary on their characteristics.

Two interference types can be included in this category. They differ from each other in their purpose, i.e.: Jamming and Pirates attacks.

"Jamming" consists of transmitting a carrier on top of the legal traffic present on the victim satellite. The interfering carrier is transmitted from an Earth Station within the Uplink footprint of the victim satellite. It is typically a high power clean carrier, within the frequency band of the target carrier. When a carrier is jammed, a geo-location process is launched in order to establish if possible a target geographical area where the interference should be transmitted from.

The "Pirate Attack" is a voluntary act aiming to use the space capacity without any legal or commercial agreement. Pirates normally access the space capacity in order to transmit con-

1 *October 25th, 2011, Martin Coleman, WBU-ISOG 2011-Zagreb, "Satellite Interference...The Carrier ID Process."*

tributions without being noticed. A pirate carrier is considered as interference since it occupies available capacity but it is quite different from the previous cases here defined. Since the carrier is very often transmitted on the guard bands of the affected transponder or on any available frequency gap on the victim satellite, it "steals" a certain amount of the overall available power of the transponder and can degrade the performance of legitimate services. This degradation does not necessarily happen. The service disruption can be an unwanted side effect. Those carriers are usually detected upon transponder watch activities and look like any other modulated standard DVB carrier.

Interference Typology	Occurrence	Sources	Causes	Preventions
Cross Polarization	When cross-polarization due to its lack of purity or lack of polarization plan induces fluctuations in intended carrier. Cross polarization will interfere with existing carrier.	Uplink antenna, when XPD is less than 30 dB due to it can be considered, antenna to transmit both polarizations.	Poor Antenna Pointing; Poor Cross Polarization Isolation; Sudden changes in antenna pointing due to mistake or storm; Carrier uplink assignation without proper User Acceptance Test with S-PCNS Cross Polarizations Interference.	Do not uplink the carrier without performing User Acceptance Test with S-PCNS; Do not uplink un-modulated carrier for UAT before S-PCNS's directions; Perform Regular Preventive maintenance.
Intermodulation	More than one carrier is transmitted by a single HPA or is mixed intermodulation processes take place; Other carrier displacement at multiple frequencies of the two involved frequencies difference.	Ground Station and Earth Station.	Equipment non linearity generates spurious frequencies, due to Intermodulation products at: • $f_{IM1}=2(f_1-f_2)$; • $f_{IM2}=2(f_2-f_1)$. (where f_1 is the frequency of carrier #1 and f_2 is the frequency of carrier #2); As the amplification power increases, superior order of modulation products becomes relevant.	Avoiding amplifier to work in saturation zone, if it's not specifically needed; Correct setting of Output Back-off power in order to force amplifier to work in linear zone.
Raised Noise Floor	Some kind of energy source makes raising of the noise floor.	Earth Station Equipment Ground Station Equipment Satellite	Wrong Earth Station Equipment Configuration Gain of Up-Converter or HPA is not set suitably Excess in Up-Link Power Wrong or Not performer UAT, especially for coding multiple access strategies	Use good ES setup Set suitable gain of ES equipment Do not increase the Uplink power without informing S-SPCN Verify uplink noise level at the output of HPA before transponder access.
Radar Interference	When civil or military Radar System have commence service following deployment of the satellite. This situation is usually time consuming and difficult to resolve, especially in the military arena.	Ground Control Station and User Earth Station	Spurious emission interference Receiver Preamplifier Overload	Robust Filtering Spurious Frequency; Avoiding amplifier work in saturation zone; Correct setting of Output Back-off power in order to force amplifier to work in linear zone; New method ought to be investigated.
Adjacent Satellite	Two satellite operators due to lack of coordination or errors involuntary disturb each other transmissions	Authorized Satellite broadcast	Lack of cooperation between operators; Operator errors.	Properly set frequency channel assignment Properly set transmission power level Better operators coordination

Table 3-4: Unintentional Interferences [RD 6]

An exhaustive literature and press overview suggested that intentional interference is a small but significant subset of all types of satellite communications problems experienced. Within this subset, it has been observed that the cause of the most part of interference events was determined to be non-hostile. However, there are some interference events, for which the cause could not be defined. These events often have a similar "profile" and make communication to be disrupted forcing operator to relocate transmissions to another satellite, another transponder or another band of the same transponder (this is deleterious due to the cost of each MHz of bandwidth on-board the satellite!). When it happens, it is reasonable to deduce that at least some of these interferences have a hostile matrix. It can be called: "denial of service" or DoS attack provided that jammers tent to compromise service provision. DoS attack is conducted by hostile radio frequency interference (RFI) that can impact on:

- the Ground Segment (GS), even called "downlink jamming", directed at local receivers;
- the Space Segment (SpS), even called "uplink jamming", presented at the satellite, affecting by mixing or overriding the intended carrier.

By means of algorithms of direction finding, pointing and triangulation techniques, downlink jamming source position can be easily detected and coped with. On the contrary, the vulnerability of commercial satellites to uplink jamming lies within its own structure and operational mode: a bent-pipe satellite transponder is designed to accept microwave energy over a certain band and to re-transmit it at the downlink frequency after appropriate amplification. So that the presence of a hostile signal, if it reaches satellite with a sufficient power level, could result in:

- a mixing with the intended signals making reception of the legitimate signal unable;
- raise the noise floor of the electronic equipment, like transponders, reducing carrier to noise ratio;
- degradation or severing of all transponder's communications, by inducted satura-

tion, if satellite receiver has limitation in terms of received power.

It must be pointed out that due to the significant encoding gain employed in current commercial satellite communication modulation protocols, even a small decrease of carrier-to-noise-ratio (SNR), can force communication to go out of service [RD 9].

Intrinsic geosynchronous satellite vulnerability is that, due to their orbital position, they can be targeted very easily. There is no need to use tracking equipment: it is sufficient to set the intended satellite reference elevation and azimuth and transmit a continuous wave at the desired carrier frequency.

In terms of power needed to sever or disrupt commercial communications must be underlined that typical broadcast carrier to noise ratio are at least 20 dB or more, so that in order to induce degradations of these carriers, it would be required large aperture antenna (9 m or more) and powerful amplifiers rated in thousands of watts [RD 9]. According to what has been noticed, many documented cases of interference against commercial broadcast satellite have involved another commercial broadcast site.

In the case, ground segment is operated using a Very Small Aperture Terminals (VSATs), as it happens, for example, when commercial satellites lease some of their transponders, during wartime, to provide communications over a specific battlefield, equipment needed to implement uplink jamming becomes more affordable.

VSATs generally use dish antennas with dimension up to 4 m paired with power limited transceiver developing carrier to noise ratio varying between 6 to 10 dB above noise floor. Depending on the bandwidth of intended signal, interference signals one-half powerful as target signal can sever communications. Due to extensive use of advanced coding techniques a relatively slight decrease of the C/N can put communication channel down. This aim can be accomplished with VSATs using a few watt power amplifiers.

Another major issue connected to uplink jamming is the coverage of geostationary satellite. When a jammer tries to attack a satellite, it might be in two different scenarios:

- **Around the Edge of Coverage** (see Figure 3-2): the jammer station is located in the outer nearby of the victim satellite feeder footprint. In this case the jammer

would aim to gain his way toward satellite transponders through satellite antenna side lobes or lateral side of main lobe. This scenario requires a huge amount of power for the attack to be effective.

- **Inside Coverage** (see Figure 3-3): the jammer station is located within the victim satellite feeder footprint. As far as this scenario is concerned, jammer can reach transponders directly toward satellite antenna main lobe with required levels of power far lower than the previous case.

Either the jammer lies within the footprint contour or around its outer border, it has to be noticed that the jammer may be anywhere throughout a geographical area of thousands of square kilometres, making localization very hard to pursue. Even if the satellite was endowed with a secondary antenna system for jammer localization, in order to implement some algorithm of direction finding to locate interference transmitter angular position, jammer might be able to move or to operate only on a limited duty-cycle, or both. Moreover a jammer geo-location on air is made even more difficult due to the high directivity antenna pattern used for uplink transmissions. Energy will be not broadcasted over a wide radiation pattern but concentred in a focused, quasi-pencil beam, making *de facto* threat signals very hard to triangulate.

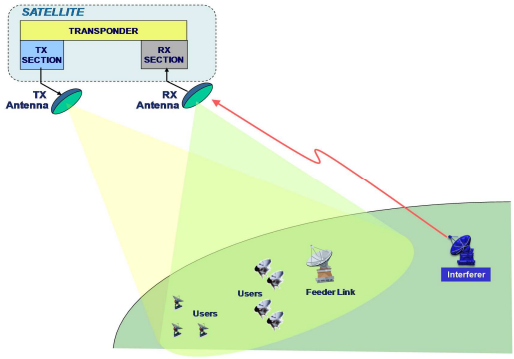

Figure 3-2: Around the Edge of Coverage

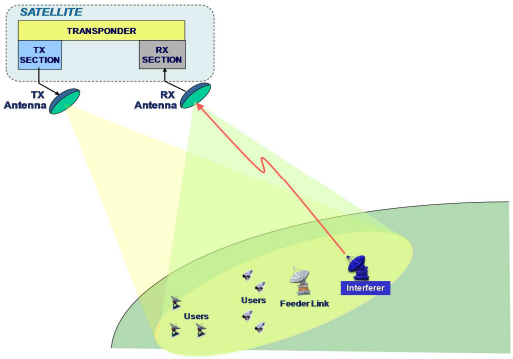

Figure 3-3: Inside Coverage

In Table 3-5 a summary of the typical intentional interference attack typologies are provided.

Interference Typology	Attack Strategy	Interferer Characteristics	Final Effect
Single and Multi Tone Jamming (CW Tone)	One or more un-modulated carrier Continuous wave	Single Tone Jamming, if it is radiated just one carrier; Multi Tone Jamming, if more than one carrier is transmitted. Major drawbacks: • Its ease of detection • Its great power consumption	Keep medium always busy
Sweep Jamming	Like Noise jamming Signal scanned in time across frequency band of interest	Transmitted Power level; Bandwidth of swept signals; Victim portions of the spectrum swept Number of hops	Against FHSS target system To jam signals, whose carrier frequency is not known
Deception Jamming	Under coverage jamming Receive intended signal and then re-transmit it Lower detection probability respect to constant jammer	Spectral power density mask; Transmitted power level; Bandwidth; Time Delay for re-transmission.	Against singular satellite channel

Table 3-5: Intentional RFI Scenarios Definition

3.2 SATCOM RADIO FREQUENCY INTERFERENCE SCENARIO ANALYSIS AND QUANTIFICATION

In this second frame of the research activity starting from the direct experience of the Commercial SATCOM Operators, in the specific case Eutelsat S.A. (France) and Telespazio S.p.A. (Italy), and analysing the related literature, two reference SATCOM scenarios have been considered, i.e.:

1. **Scenario 1**: that is targeted on the feeder-link gateway side working in the C or Ku band and devoting to feed Broadcasting Satellite Service (BSS) mission. The interference has been considered affecting this side of the up-link spectrum. This scenario represents the principal one taken into account in the research activity. It is highlighted in Figure 3-4.
2. **Scenario 2:** that is targeted on the user segment sides working at the Ka band still for BSS mission. The interference has been considered affecting the user up-link spectrum in one or several beams composing the coverage. Currently this scenario

is one of the more challenging (see Figure 3-5) but in a future perspective and in the research activity it has not overriding as the scenario 1.

The characterising parameters of the two scenarios are summarised in the Table 3-6.

Mission/System Parameters	Scenario 1 C or Ku-band BSS/FSS	Scenario 2 Ka-band BSS/FSS Mission
Orbit	GEO	GEO
Service Area	Continental	Continental
Coverage Type	Single shaped beam	Multi-beam
C band option feeder-link up-link frequency ranges (GHz):	5,850 - 7,075[1]	Not applicable
Ku band option feeder-link up-link frequency ranges (GHz):	12,500 - 12,750[2]	Not applicable
Ka band user segment up-link frequency ranges (GHz):	Not applicable	28,450 - 28,940 29,460 - 30,000
Payload Specifications:		
Repeater Type	Bent-pipe	Bent-pipe
Antenna sub-system	Passive Antenna (Reflector) Single Feed	Option a: Passive Antenna *(Single Feed Per Beam or Multiple Feed Per Beam)* Option b: Active/Semi-Active Antennas *(Direct Radiating Array or Array-Fed Reflector)*

Table 3-6: Reference Scenario Parameters

From these scenarios the requirements for the study of the RFI management solution have been defined. Starting from the experience of the CSO, to quantify the RFI impact on the

[1] *Ref.: ITU Radio Regulations, Appendix 30B, Edition of 2012*
[2] *Ref.: ITU Radio Regulations, Appendix 30B, Edition of 2012*

satellite service the following Key Performance Indicators (KPI) have been considered:

1. expected relative occurrence of the interfering events (Occurrence);
2. expected impact on SATCOM service(s) in terms of degradation of the QoS and/or service outage (Impact);
3. estimated time/difficulty required for RFI geo-location (Estimation);
4. and by the factor defined as:

$$Impacted\ Bandwidth\ \times Time\ to\ Solve\ the\ RFI.$$

The victim SATCOM scenario taken into account has been the Broadband Satellite Service/Fixed Satellite Service (BBS/FSS) operating at Ku band for the up and down link as described in Figure 3-5. The approach is applicable also for the next generation broadband satellite system as the High Throughput Satellite (HTS) or Terabit systems, as in Figure 3-5, a) and for the mobile satellite service (MSS) as depicted in Figure 3-5, b).

Currently the considered scenario constitutes one of the more popular satellite systems providing essentially digital television (Digital TV) and data traffic services.

The actual reference scenario has been based on the satellite HotBird of the Eutelsat's fleet positioned on the geo-stationary orbit at 13°E (this is one of the better orbital positions to cover the centre of Europe). The satellite system provides services in the Ku band frequency range, with regional antenna coverage for both user segment and feeder links for Fixed-Satellite Services (FSS) and Broadcasting-Satellite Services (BSS).

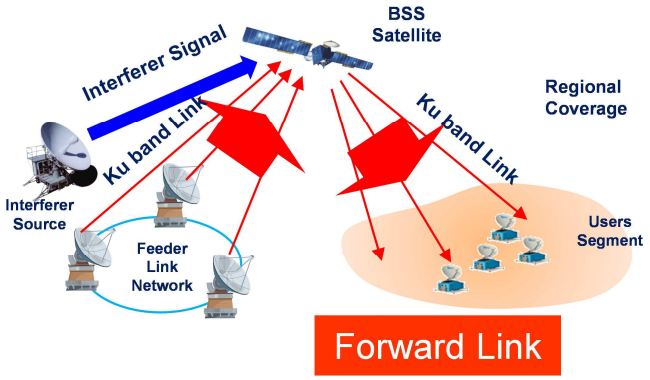

Figure 3-4: BSS/FSS Commercial SATCOM Scenario Victim Scenario

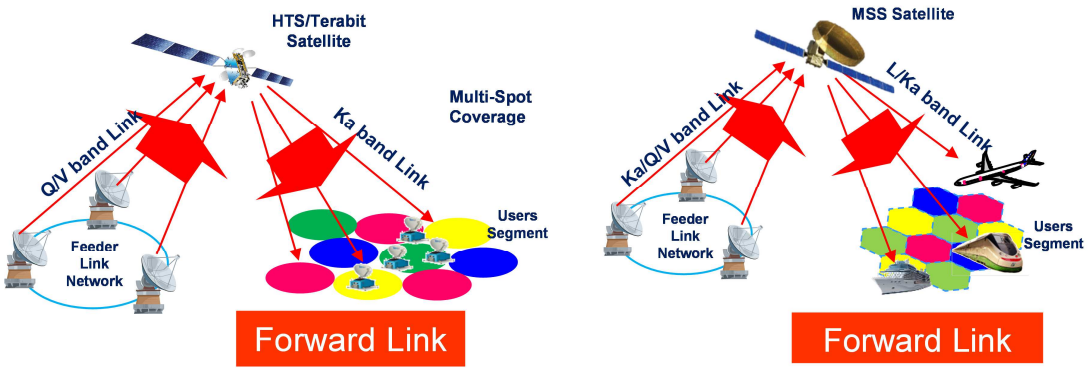

a) HTS Scenario ***b) MSS Scenario***

Figure 3-5: NTS and MSS SATCOM Victim Scenario

The main parameters characterizing the scenario and useful for the RFI analysis activity, are:

1. the feeder link service area (antenna coverage);
2. the G/T performance;
3. the Effective Isotropic Radiated Power (EIRP) performance;
4. the frequency plan mainly on the feeder link side
5. the polarisation plan.

Figure 3-6 shows the antenna up-link footprint (G/T) while Figure 3-7 shows the down-link antenna footprint (EIRP).

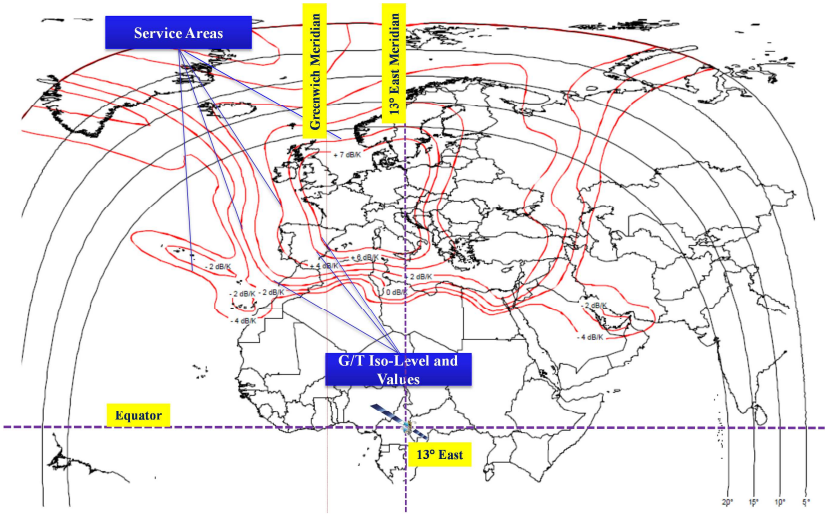

Figure 3-6: G/T Performance on the HB6 coverage [RD 14]

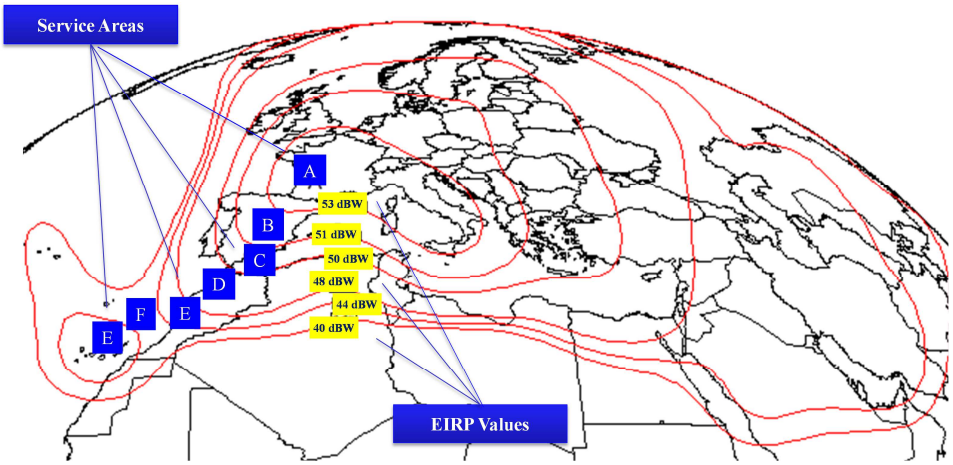

Figure 3-7: EIRP Performances on the HB6 Coverage [RD 14]

Table 3-7 lists the G/T and EIRP in the service area detailing the values for each sub-area indicated by capital letter contoured by the isolevel lines.

Uplink Service Area	Minimum G/T (dB/K)	Minimum EIRP (dBW)
Area A	7,0	53,0
Area B	5,0	51,0
Area C	3,0	49,0
Area D	-2,0	44,0
Area E	-4,0	42,0
Area F	-6,0	40,0

Table 3-7: Service Area G/T and EIRP

The reference Ku-band scenario operates between 10.7-11.2 GHz and 11.45-12.75GHz on the downlink and between 13.75 GHz and 14.5 GHz in the uplink. A typical 36 MHz transponder channelization is provided and in Table 3-8 the frequency plan is detailed (X means linear horizontal polarisation and Y linear vertical polarisation).

A minimum cross-polar performance of 27 dB of Cross Polar Discrimination (XPD) has been assumed for all the Service Areas in both uplink and downlink.

The abovementioned data coming from the SATCOM Operator allow defining a target iso-

lation required as starting point in comparing the effect of the interference towards the wanted signal. This gives the right quantification elements to lead to the definition of required isolation at the satellite antenna level.

Channel Number	Uplink Frequency (MHz)	Downlink Frequency (MHz)	Channel Bandwidth (MHz)	Uplink Polarisation	Downlink Polarisation
C1	14271,25	10971,25	36	Y	X
C2	14292,00	10971,25	36	X	Y
C3	14312,75	11012,75	36	Y	X
C4	14333,50	11012,75	36	X	Y
C5	14354,25	11054,25	36	Y	X
C6	14333,50	11054,25	36	X	Y
C7	14395,75	11095,75	36	Y	X
C8	14333,50	11095,75	36	X	Y
C9	14437,25	11137,25	36	Y	X
C10	14333,50	11137,25	36	X	Y
C11	14478,75	11178,75	36	Y	X
C12	14333,50	11178,75	36	X	Y

Table 3-8: Frequency Plan and Channelization

The fundamental parameters characterising the link environment are reported as "I" that represents the time-averaged interference power and "C" that represents the time-averaged useful signal power, the ratio I/S defines how much the interfering power is greater than the useful signal. Regardless of the signal and interferer waveforms, in a digital context, it is possible to define the equivalent bit energy-to-jammer noise ratio as [RD 12]:

$$\frac{E_b}{N_I} = \frac{B \cdot C}{R_b \cdot I} \qquad \text{Eq. 3-1}$$

In the reference scenario, the RFI physical analysis has been carried out assessing the $\frac{C}{N}$ under no interference (*uni*) situation applying the calculation steps in following reported.

1. First of all the $(C/N_0)_{uni}$ has been calculated by the Eq. 3-2 [RD 10]:

$$\left(\frac{C}{N_0}\right)_{uni} = \frac{P_r \cdot G_r}{k \cdot T_0 \cdot NF \cdot L} \qquad \text{Eq. 3-2}$$

where:

C is the received carrier power density;

N_0 is the noise power density per Hz at the input of the receiver;

P_r is the received signal power level measured in Watt and calculated through the link budget analysis;

G_r is the receiver antenna gain;

k is the Boltzmann's Constant i.e. $1{,}38 \cdot 10^{-23}$ (J/K) or -228,6 dBW/K/Hz);

T_0 is the reference temperature usually 290 K;

NF is the receiver noise figure including antenna and cable loss;

L is the implementation loss comprising the analog-to-digital (A/D) conversion loss in case of digital system.

$(C/N)_{uni}$ calculation has been carried out for both the clear sky and rain conditions.

2. The calculation of the maximum critical interference-to-signal power ratio $(I/C)_{max}$ value has been performed, giving the estimation of the loss with respect to the desired performance level. This parameter is given by Eq. 3-3:

$$\left(\frac{I}{C}\right)_{\max} = \left\{ \cdot \frac{B \cdot Q_p}{\left[\left(\frac{C}{N_0}\right)_{uni} - \left(\frac{C}{N_0}\right)_{req}\right]} \right\} \qquad \text{Eq. 3-3}$$

where:

I is the received interference power density;

B is the bandwidth (in Hz) of the signal;

Q_p is a dimensionless adjustment factor that depends on the interference bandwidth occupation $\rho_I = \frac{B_I}{B}$, i.e. the fraction of the total band affected by the interference.

3. The calculation of the received interference power corresponding to the critical interference level has been done by Eq. 3-4:

$$I_{r\max} = \left(\frac{I}{C}\right)_{\max} \cdot C_r \qquad \text{Eq. 3-4}$$

where the subscript *r* means "received".

Once the maximum critical received interference signal power has been calculated, the total interference signal level can be derived for a given amplitude spectrum density, as far as unintentional interference is concerned, or for a given jammer's Equivalent Isotropic Radiated Power, in case of intentional interference. Generally, the received interference signal level can be written as:

$$C_r = \frac{EIRP_I \cdot G_r(\vartheta_{doa}, \varphi_{doa})}{L_p L_i} \qquad \text{Eq. 3-5}$$

where:

$EIRP_I$: is the interference equivalent isotropic radiated power derived from the source of the interference;

$G_r(\vartheta_{doa}, \varphi_{doa})$ in the receiver antenna gain in the direction of arrival of interference signal;

L_p : is a cumulative figure that takes into account all the propagation losses;

L_i : is a cumulative figure that takes into account other impairments may occur in the transceiver chain.

4. The interference spectral density has been evaluated by Eq. 3-6:

$$N_I = \frac{I_r}{B_I} = \frac{I_r}{B}\frac{B}{B_I} = \frac{N_{I_{bb}}}{\rho_I} \qquad \text{Eq. 3-6}$$

where:

N_I is the interference power spectral density in the link band;

B_I is the portion of total available signal bandwidth superimposed with a partial band interference signal;

B is the total available signal bandwidth;

$N_{I_{bb}} = \frac{I_r}{B}$ is the equivalent interference noise single-sided power spectral density;

$\rho_I = \frac{B_I}{B}$ is the fraction of the total band affected by interference.

5. The signal-to-interference-plus-noise ratio (SINR) has been calculated considering the C/N already calculated obtaining:

$$\left(\frac{C}{N+I}\right)_{tot} = \frac{E_b \cdot R_b}{N_0 + N_{I_{bb}}} \qquad \text{Eq. 3-7}$$

Table 3-9 reports the C/N and C/(N+I) values obtained with the above described theory. The last column, labelled "Remarks", reports the assumptions on the interference characteristics (i.e. EIRP level, bandwidth, etc.), taken into account for the following of the activity.

Figure 3-8 describes the SATCOM feeder link side of the considered system scenario. The assumption for the feeder link and the space segment receiving section (RX) are:

- Feeder link Gateway (Ground Station):
  - ✓ Antenna diameter: 3.7 m;
  - ✓ HPA power: 750 W;
  - ✓ Maximum uplink EIRP: 76 dBW
- RX Space Segment
  - ✓ Satellite G/T on the feeder link coverage: 7 dB/K;
  - ✓ Transponder bandwidth: 36 MHz.

The ground station is assumed to work at 4 dB Output Back-Off (OBO), in order to improve linearity performance in case of transmission of multiple carriers.

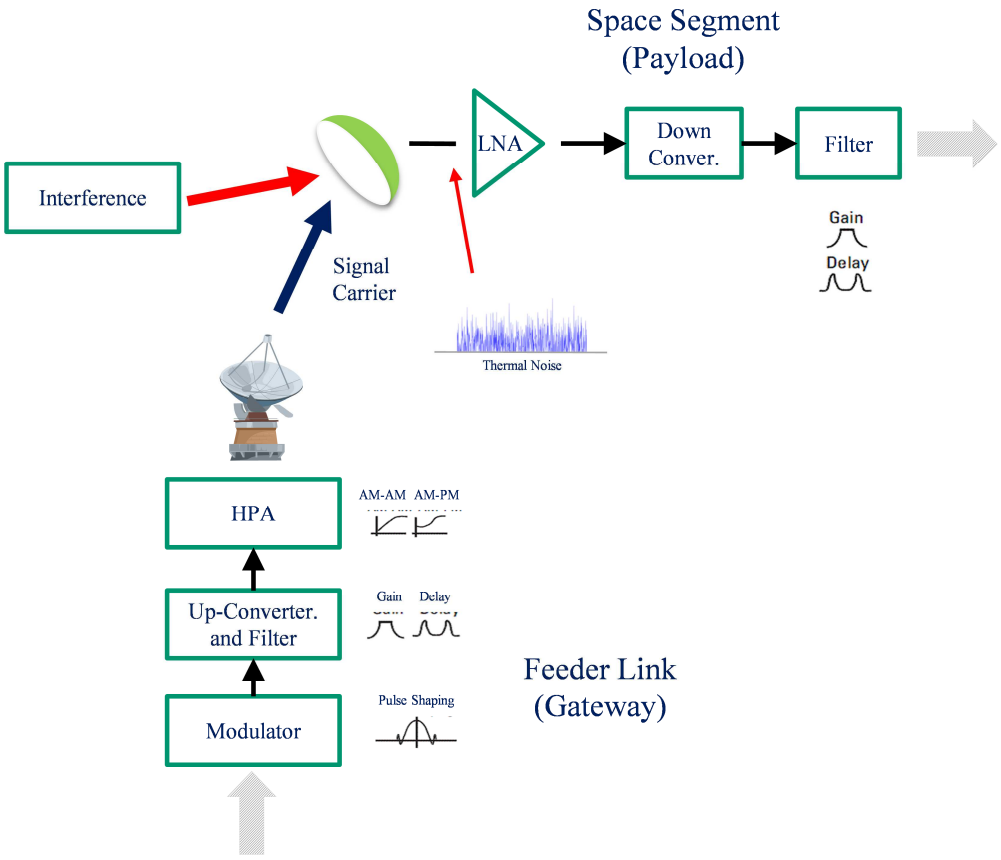

Figure 3-8: SATCOM Feeder Link Chain Details

Interference Typology	Nominal C/N (FL)	C/(N+I) (FL)	E2E Nominal C/N	E2E C/(N+I)	C/(N+I) degradation (FL)	Remarks
	[dB]	[dB]	[dB]	[dB]	[dB]	
No Interference	26,3	NA	11,9	NA	NA	
Adjacent Satellite Interference	26,3	24	11,9	11,8	-2,3	Assuming two adjacent satellites with comparable uplink power spectral density at 3° orbital separation each
Cross-Polarisation Interference	26,3	22,6	11,9	11,7	-3,7	Due to typical nominal TX terminal cross-polarisation isolation
Adjacent Channel/Transponder Interference	26,3	21,2	11,9	11,6	-5,1	Assuming TX OBO set in order to guarantee at least 25 dB between peak and frequency side-lobes
Intermodulation	26,3	(Intermodulation Effect can be avoided by setting HPAs at a suitable OBO level)	11,9	(Intermodulation Effect can be avoided by setting HPAs at a suitable OBO level)		
Digital Channel Overriding	26,3	0	11,9	-0,3	-26,3	Assuming a signal of equal power spectral density transmitting over the used frequency)
Noise Jamming	26,3	-4,5	11,9	-4,5	-30,8	Assuming a Jammer with 80 dBW EIRP spread over an entire channel of 36 MHz bandwidth)
Tone Jamming or Continuous Wave	26,3	-4,5	11,9	-4,5	-30,8	Assuming a Jammer with 80 dBW EIRP spread over the useful carrier bandwidth)

Interference Typology	Nominal C/N (FL)	C/(N+I) (FL)	E2E Nominal C/N	E2E C/(N+I)	C/(N+I) degradation (FL)	Remarks
	[dB]	[dB]	[dB]	[dB]	[dB]	
Barrage Jamming	26,3	-4,5	11,9	-4,5	-30,8	Assuming a Jammer with 80 dBW EIRP spread over an entire channel of 250 MHz bandwidth

Table 3-9: Ku/Ku Band Scenario Preliminary C/(N+I) evaluation

4 METHODOLOGY: THE GEO-LOCALISATION TECHNIQUE FOR RFI MITIGATION

As already motivated in the previous chapter, the importance for effective solutions and strategies aiming at reducing the impact of RFIs is universally acknowledged by all the key SATCOM players operating at all levels of the value chain, ranging from equipment manufacturers to SATCOM operators. In particular, several heterogeneous international organisations (e.g., IRG, GVF, ETSI, DVB, ITU, SDA, etc.) are actively working on this challenging subject. This conditions future products' definition on which the outcome of the present research activity is contributing.

Despite the efforts of all key players in the areas of SATCOMs, there are still major technological gaps to be filled in order to derive viable solutions aiming at meeting current application needs. The relative limited knowledge and early status of interference countermeasures in institutional and commercial applications contrasts with the level of maturity reached in military and security applications. However, restricted access and confidentiality issues greatly limit information flow from military to civil community, making the need for pushing developments in civil and commercial applications of paramount importance [RD 11].

Effectively tackling interference is a complex task to be performed at multiple levels. These levels can be summarised as in following:

- Technical Level
  - Proactive Solutions (e.g., Training & Certification, Type Approvals, Network Validation)
  - Reactive Solutions (e.g., Carrier ID/Geo-location, Data Sharing/SDA, Statistics)
- Regulatory Level (e.g., ITU)

In this phase of the research activity, indeed, taken into account the motivation and the

background on the incidence and characterization of the interference events and considering the defined reference scenario, the methodology to define, to perform the analysis on the problem parameters and to find a consistent RFI mitigation technique for commercial SATCOM satellites has been carried out.

Focusing on the actual experience reported by the spectrum monitoring at the operator side, the right interference management strategy has been defined. It is summarised by the following items:

1. Spectrum/Interference Monitoring: consisting in monitoring emissions over an identified frequency range;
2. Interference Detection and Isolation: including all steps required to extract the interfering signals;
3. Interference Classification: Estimation of main characteristics of interfering signals;
4. Interference Localisation: i.e. estimation of geographic location of interfering sources;
5. Interference Mitigation: i.e. all steps to counteract the interfering signal (e.g., interference nulling).

The above sequence of operations is schematically reported in the Figure 4-1. It, as already written, represents also the methodological approach followed during the research activity.

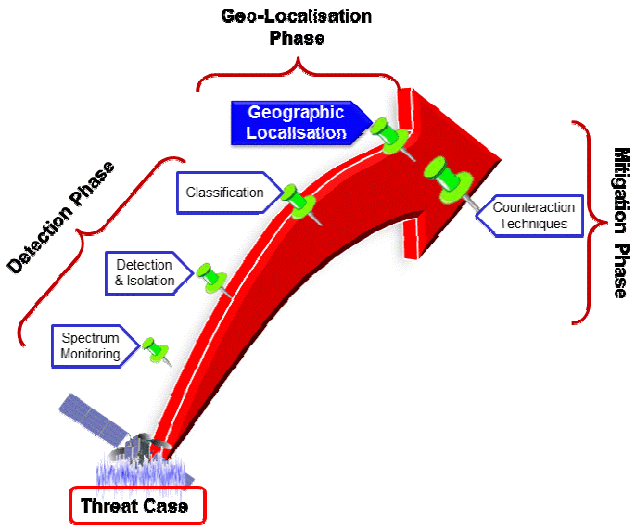

Figure 4-1: RFI Management Strategy

Considering the above listed items, the methodology approach has been grouped and de-

veloped in two phases:

Phase 1. At the Satellite Service Centre (SSC) the understanding of the approach adopted by the SATCOM Operator for carrying out the Spectrum Monitoring Operation (SMO) to intercept interference events impacting the provided services, followed by the RFI detection/isolation and classification;

Phase 2. The definition of Geographic Localization Technique (GLT) to be considered as suitable and acceptable by commercial SATCOM Operators, satisfying the requirements defined by them and in general by the related context/market;

Practically speaking the above listed phases are useful as operational methodology and procedure in managing the AI system in an actual situation applicable at the Satellite Service Centre (SSC) or at the Network Service Centre (NSC) that in the overall SATCOM system constitute the two main entities to manage the service delivery towards the User Segment or Final Customers.

4.1 PHASE 1 - SPECTRUM MONITORING OPERATION APPROACH FOR INTERFERENCE INTERCEPTION

In the first phase of the methodology approach, the research activity has been devoted on the spectrum monitoring operation. Principally this operation is performed on the receiving section of the satellite on the side of the feeder link due to the fact that the interferences have a critical impact on this satellite access point side where the service contents are provided.

In a SATCOM system at the feeder link side, it is mandatory to be aware in time when an interference phenomenon appears. Typically this is done in two sequential steps: (i) a qualitative one strictly related to the impact on the QoS of the provided service and (ii) a quantitative one represented by the interception on the satellite transponder spectrum where and how the interferer is impacting.

When an interfering event is detected (qualitative step) the first action performed at the

service centre by the operator is to move the service on a not impacted frequency sub-band or on another transponder and, sometime, if possible, on another satellite present on the orbital position and constituting one of the element of the satellite fleet.

As consecutive action a systematic scan of the allocated spectrum is performed (quantitative step). On this item information provided by the commercial SATCOM Operators confirm that currently this action is performed inevitably at the service centre side, i.e. at the ground segment!

Currently some supported studies by ESA are in progress to develop suitable and effective solutions to be integrated on the SATCOM payload on-board the satellite: in this way it will fastened the detection phase providing, at the same time, the capability to monitor all the transponder spectrum independently by the service centre, optimising at the source the frequency utilisation.

The spectrum monitoring approach, as reported by the actual operators (Eutelsat and Telespazio) as in [RD 2] and [RD 3], have been focused on the capability and way to proceed to intercept anomalies in the link data traffic due to the impact of interferers. The monitoring action is performed at the feeder link side monitoring with suitable instruments (typically spectrum analysers) the RX section of the satellite.

For the research activity, actual interference situations have considered. They have been provided by the SATCOM Operator on an actual commercial satellite, i.e. HOT BIRD™ 6 (HB6) at 13° East orbital position and providing Ku band broadband and fixed satellite services. In following the intercepted typologies of interferences are described reporting the link configuration and a brief description of the event typology.

Piracy Interference

In Figure 4-2 the spectrum monitoring result of piracy interference is shown. It is a voluntary act aiming to use the space capacity without any legal or commercial agreement and possibly without being noticed.

This definition implies that the interfering carrier does not necessarily have a "commercial" impact on the traffic since a pirate normally transmits on the guard bands of the affected transponder or on any available frequency gap on the victim satellite.
A pirate carrier is considered to be interference since it uses a certain amount of the overall

transponder available bandwidth but does not necessarily implies a degradation of the legitimate services.

The service disruption can be an unwanted side effect. Those carriers are usually detected upon transponder watch activities and look like any other modulated standard DVB carrier.

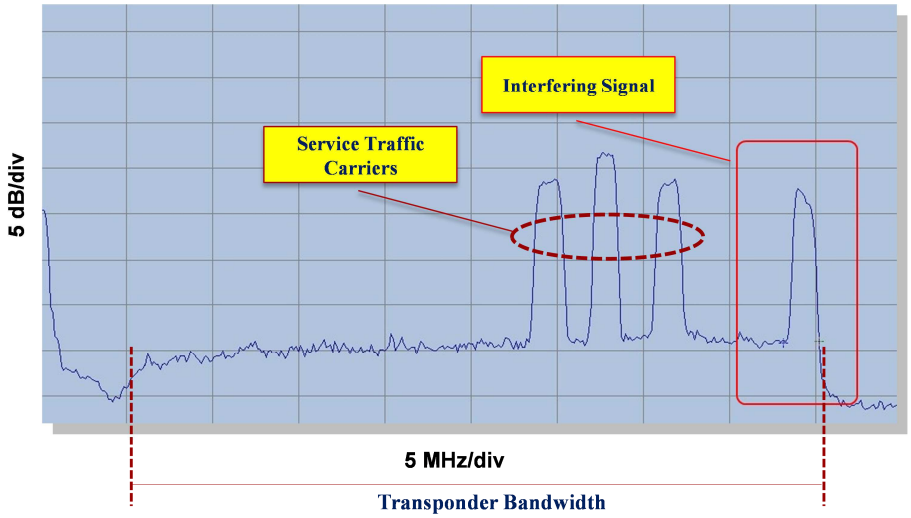

Figure 4-2: Pirate Interference [RD 4]

The parameters of the pirate source are in following listed:

1. Source Service Area: D
2. Up-Link Frequency: 13996,5 MHz
3. Down-Link Frequency: 11696,5 MHz
4. Modulation and Coding (MODCOD): QPSK; FEC 3/4; 2,9 MSym/s
5. Up-Link EIRP: 63 dBW
6. Geographic Location: Beirut (Lebanon);
7. Antenna Diameter: 2,4 m

Continuous Wave Interference (Jamming)

The strategy of the jamming interferes consists of permanently transmitting the continuous wave (CW) signal on top of the legitimate carrier, not necessarily depending on the content carried by the victim carrier. A continuous wave interference can be present on the victim channel indefinitely.

The smart jamming technique instead implies that the interferer signal is generally transmitted only when the victim carrier is diffusing some controversial content. Due to its nature, the interfering signal is extremely difficult to identify at first sight, and this gives the interferer entity an advantage in time.

In the actual considered scenario the victim service is a 33 MHz DVB S2 carrier transmitted on channel C1 (see Table 3-8) of the reference victim satellite scenario (Vertical Uplink polarization/Horizontal downlink polarization). Table 4-1 lists the link parameters of the victim transponder and the interferer signal, while Figure 4-2 plotting the spectrum monitoring result. The transponder sensitivity is set to - 80 dBW/m^2.

For this scenario, the interfering Earth Station dimension is assumed to be 9 m. The choice is due to the fact that the antenna size has a strong impact on the chances to obtain reliable geo-localisation results. Currently when running a geo-localisation process, an indispensable condition consists of the possibility to receive a contribution of the interferer signal transmitted towards an adjacent satellite. The bigger the interferer antenna is the smaller is the side-lobe contribution thus leading to unreliable results. This scenario is becoming more and more common and often leads to the impossibility to obtain a geographic localization of the interference (this has been one of the motivation for the described research activity).

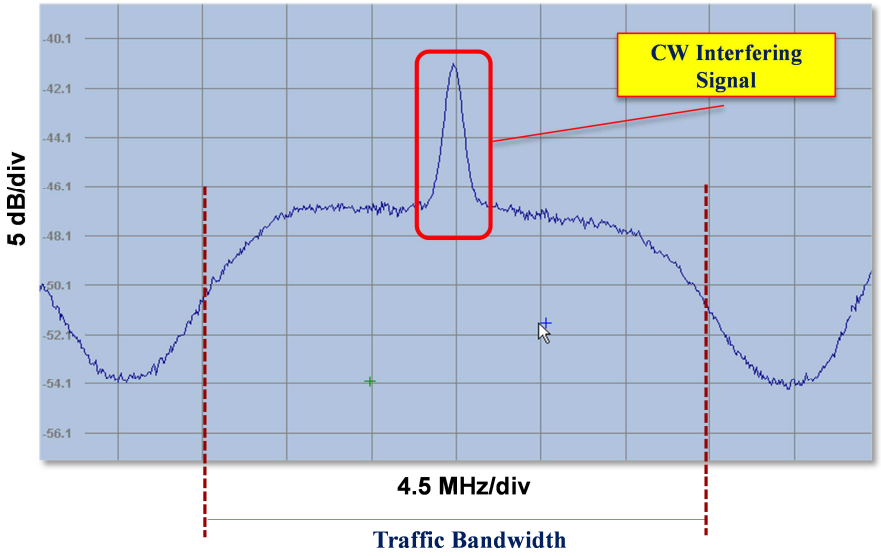

Figure 4-3: CW Interference [RD 4]

The parameters of the CW interference scenario are reported in Table 4-1.

Parameter	Victim	Interferer
Service Area:	A	E
Up-Link Frequency:	14271,25 MHz	14271,25 MHz
Down-Link Frequency:	10971,25 MHz	10971,25 MHz
MODCOD:	8PSK; FEC 2/3; 29,7 Msym/s	CW
Up-Link EIRP:	72 dBW	80 dBW
Geographic Location:	Lyion (FR)	Teheran (Iran)
Antenna Diameter:	9 m	9 m

Table 4-1: Victim/Interferer Parameters

In Figure 4-4 the case of sweep CW interferences is shown, while in Figure 4-5 that of multi-tone is reported. They are managed in the same way of the CW interference as above described.

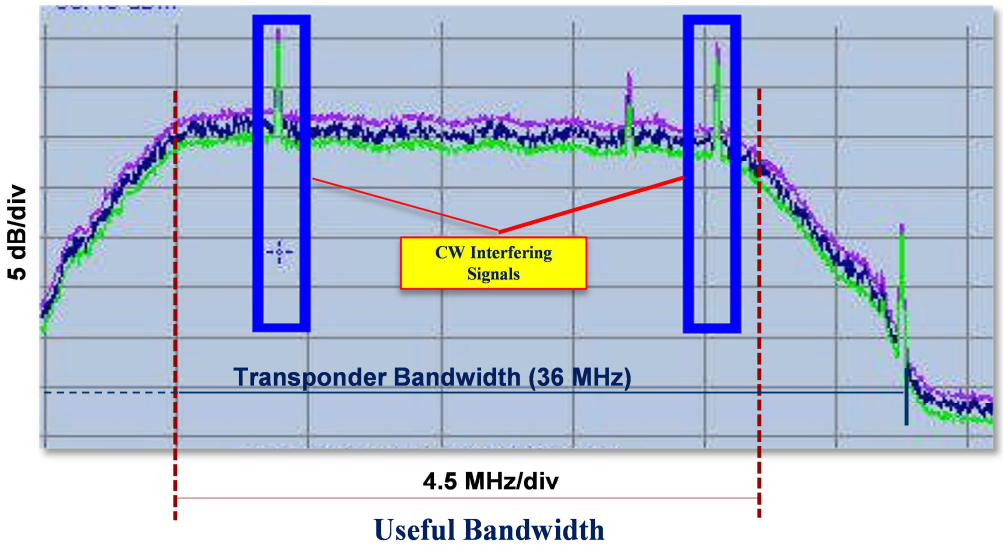

Figure 4-4: Sweep CW Interference (Jammer) Spectrum Plot [RD 4]

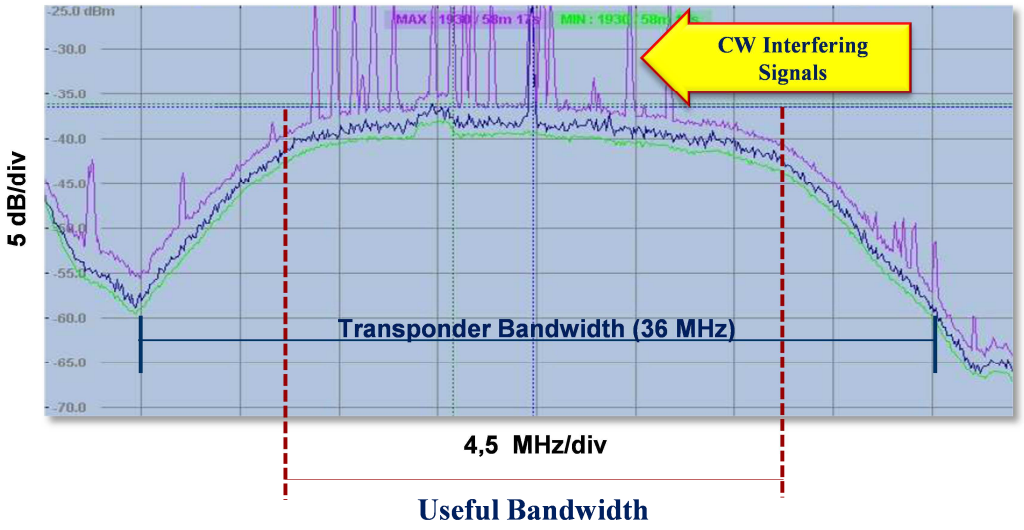

Figure 4-5: Multi-Tone CW Interference (Jammer) Spectrum Plot [RD 4]

The parameters of the sweep and multi-tone interference scenarios, common to the case of CW interference, are listed in Table 4-2.

Parameter	Victim	Interferer
Service Area:	A	E
Up-Link Frequency:	14271,25 MHz	14271,25 MHz
Down-Link Frequency:	10971,25 MHz	10971,25 MHz
MODCOD:	8PSK; FEC 2/3; 29,7 Msym/s	CW
Up-Link EIRP:	72 dBW	80 dBW
Geographic Location:	Lyion (FR)	Baghdad (Iraq)
Antenna Diameter:	9 m	9 m

Table 4-2: Victim/Interferer Parameters

Smart or Deception Interference

The deception jamming scenario represents one of the most difficult interference to identi-

fy. In the actual scenario, the victim service is a 33 MHz DVB S2 carrier transmitted on channel C5 (see Table 3-8) of the reference victim satellite scenario (Vertical Uplink polarization/Horizontal downlink polarization). The uplink frequency is 14354,25 MHz, downlink 11054,25 MHz.

The victim service is a QPSK 3/4 carrier, carrying 27,5 MSym/s, transmitted from Milan, Italy with a 7 meter antenna. The uplink station is located within uplink service are A (see Table 3-7) and downlink service area A. The uplink power is 68 dBW.

The interferer signal is a carrier equivalent in bandwidth to the legitimate one. The uplink earth station is located within the +2 dB/K satellite contour, in Nicosia, Cyprus. The uplink power is supposed to be 75 dBW. The transponder sensitivity is set to - 80 dBW/m2.

Smart jamming is impossible to detect RF wise since the two carriers are absolutely similar in shape and power. The interference nevertheless causes a drastic drop of the legitimate carrier E_b/N_0. If the nominal E_b/N_0 of the victim carrier above described is about 12-13 dB with a 1,8 m receive antenna within the downlink service area A, the interference can drop it down to 5 dB or lower.

The conclusion is that to detect the deception interferences it is necessary to monitor the signal level through a test receiver at the feeder link side, comparing the received signal spectrum with the foreseen one to intercept anomalies.

4.2 PHASE 2 – RFI GEO-LOCATION CONCEPTS AND TECHNIQUES, DEFINITION AND DESIGN

The activity of the second phase of the methodology approach has been concentrated on the core subject of the research activity, i.e. the RFI signal source geo-localisation technique definition and design.

In principle three technological approaches have been considered and analysed for the architectural for the implementation of a RFI system, i.e.: the On-Ground Solution, the On-Board Solution and the Shared On-Ground/On-Board Solution.

These three technological approaches are described as in following:

- In the On-Ground Solution or Implementation approach the RFI management sub-system is located at the ground segment, typically at the Satellite Operation Centre (SOC) strictly connected with the Network Operation Centre (NCC) (these two centres can be located in the same place also connected with the feeder link gate-way) In this case the satellite acts as transparent transponder managed through a satellite TT&C (Telemetry, Tracking and Control) or/and a satellite PCC (Payload Control and Configuration) links. Possible implementations include professional equipment/products specifically developed for being used in on-ground stations typically owned by satellite system Operators;
- The On-Board Solutions consists in implementing at the satellite payload the sub-system to manage the active operations for the RFI management as the monitoring, the geo-localisation and the counteracting procedures. This is especially useful when the main payload does not re-transmit the received frequency spectrum on-ground (meaning that no alternative on-ground implementations may be adopted), or when an On-Board Processor (OBP) is available [RD 1].
- The Shared On-Ground/On-Board Solution consists in a sort of hybrid approach between the two previous ones. Indeed the solution is based on a shared architecture where a minimal hardware sub-system is integrated at satellite payload and the algorithm and management part is located at ground, taking advantage from the utilisation of suitable and performing calculation capabilities. The link between the on-board and on-ground section is guaranteed by a PCC link or, due to the current evolution of the TT&C channel performance (up to 1 Mbps of rate), it can be performed through this last.

Potential advantages of the on-board implementation solutions w.r.t. the on-ground one include:

- Potential increase in the number of detected and geo-localised RFI events. In this respect, it should be noted that a major challenge for geo-location systems consists in the capability of geo-locating RFI signals by making use of a single satellite (i.e., the satellite affected by the RFI). Indeed, most of the commercial on-ground products relies on a minimum of 2 satellites (the one affected by RFI plus an adjacent satellite) located close enough to be able to receive the same RFI signals. This ap-

proach, even though effective, presents significant limitations:

- ✓ Even though more than 200 geo-stationary satellites are in operation from the main satellite operators, some of them occupy an orbital slot not close enough to any other satellite orbital slot in order the geo-location technique to work (i.e., typically orbital slots separation > 8-10 degrees);
- ✓ The adjacent satellites need to have the same up-link (at least) frequency bandwidth and the same service areas;
- ✓ Even in case an adjacent satellite is available, the accurate knowledge of satellite ephemerides of both the adjacent satellites is required. Indeed, the ephemerides have a significant impact on the accuracy of geo-location systems. It shall be also noted that, in case the adjacent satellite belongs to a different operator, its ephemerides are often not known or known with a degraded accuracy;
- ✓ In principle, the ephemerides may be also derived from tracking techniques. However, one of the preconditions of successful tracking is the availability of enough reference stations. A reference station is a known station in terms of its localization (Latitude. Longitude), which transmits a known (reference) signal to the satellite to be tracked. It is reported that a number of reference station greater than 5-6 are necessary in order to calculate the ephemeris data with sufficient accuracy.

- Avoidance of downlink impairments potentially affecting the frequency spectrum observed on ground. For instance, in case of telecom multi-beam satellites, the on-board RFI geo-location sub-system may be programmed in such a way to analyse the uplink of a single specific beam, instead of monitoring the Earth-to-Space and Space-to-Earth aggregated traffic of multiple beams managed by a gateway on-ground;
- Simplification of Ground Segment by avoiding equipment replication in multiple Earth stations as what would happen in telecom multi-beam satellites;
- Operational network flexibility (especially related to telecom satellites equipped with transparent transponders): it should be noted that this aspect is not strictly related to the interference topic but may offer a significant advantage for satellite Operators. For instance, an on-board sub-system could offer the capability of monitoring the downlink transmission quality without the need to deploy on-ground moni-

toring stations within the satellite coverage. This is particularly convenient in case of remote coverage or steerable beams;

- Solutions may be tailored to the specific SATCOM satellite systems the RFI geo-location sub-system will be embarked on, with proper definition of RFI geo-location sub-system interfaces and equipment shared with the main telecom payload.

It is clear that the capability to implement an On-Board Solution system is more performing to respect an On-Ground Solution. On the other side the current technology in implementing performing OBP to manage all the digital operations and processing on-board is not enough mature (up to now the technology is targeting the TRL 6) to propose a time-to-market product to the operators. For this reason, in the research activity the third approach has been considered, i.e. the Shared On-Ground/On-Board Solution. This solution represents a good compromise to match performance, easy integration on-board, product time-to-market and costs.

Starting from the information provided by the SATCOM Operator the Figure of Merits (FoM) reported in Table 4-3 have been considered for the geo-localisation technique.

Figure of Merit	Value	Comments
RFI geo-location accuracy	less than 3 km (in a future evolution the goal is be less than 1 km)	RFI geo-location accuracy depends on a wide range of factors, including: I. accuracy in the knowledge of satellite ephemerides, II. type of interfering signal, III. SNR of interfering signals, IV. continuous/burst transmission of interfering signals, etc. These aspects shall be clearly defined and used as inputs for carrying out the RFI geo-location trade-off and performance assessment to be performed in tasks 2 and 3 of the activity.
Time required to geo-localise the RFI sources	less than 10 minutes	

Table 4-3: Preliminary RFI Geo-Location Figure-of -Merit

To define the geo-localisation technique suitable to the considered reference scenario and

in compliance with the objectives of the activity, taken into account the FoM parameters expressed in Table 4-3, a review of the state-of-the art of the RFI geo-location concepts, technologies, techniques and algorithms, also revising the current commercial products, has been carried out.

During the research activity, each considered technology has been critically analysed to identify the suitable technique that is based on the requested performances and on their effective applicability to the identified SATCOM scenario.

In the literature and also in the technical heritage of the Company (Thales Alenia Space Italia or TAS-I) where the doctoral candidate works, several RFI geo-location techniques and methodologies are described, analysed and some of them already experienced. Some of them, indeed, have been successfully implemented in flying Italian military satellites (SICRAL).

Table 4-4 reports the candidate techniques considered in the research activity and in compliance with the above sentence. The table reports a brief description on the technique and the favourable (PROS) and unfavourable (CONS) factors to respect the target application.

RFI Geo-location Concept/Algorithm	Description	PROS	CONS
Ra.F.I.S.S. **Radio Frequency Interferometer Sensor System**	Phase comparison between two signals picked-up by two adjacent antenna elements	It requires very few sensors, at least five to resolve the ambiguity and obtain the required resolution.	Capability to resolve one single signal for frequency bin
MU.SI.C. **(MUltiple SIgnal Classification)**	Based on spatial covariance matrix elaboration and decomposition in noise and signal subspaces	Generality and versatility, which allows the application to any type of array, performance in terms of resolution not closely linked to the size of the array	Number of signals to be estimated linked to the number of array elements. When the interference sources are coherent MUSIC algorithms have problems. Performance of the MUSIC algorithm declines for low SNR
S.M.L. **(Stochastic Max-**	Based on spatial covariance matrix elaboration and maximum likelihood concept	It can be applied without problems also in presence of coherent signals	High computational cost

RFI Geo-location Concept/Algorithm	Description	PROS	CONS
Likelihood)			
Capon **(or Minimum Variance Distortionless Response)**	Based on spatial covariance matrix elaboration and spatial spectrum calculation	Better performance than the conventional, and makes it possible to resolve signals even very close	Resolution capacity linked closely to the size of the antenna
Conical scan	Conical scan of the antenna beam around the searching direction	Mechanical technique that allows to reach high accuracy, but with narrow angular sector	Long time for scan when the service area is large. High gain antenna is needed to reach high accuracy. Not negligible impacts on mass and power consumption budget
Monopulse	Simultaneous amplitude comparison of the received signals from different beam of the same antenna	Mechanical technique that allows to reach high accuracy, but with narrow angular sector	Long time for scan when the service area is large. High gain antenna is needed to reach high accuracy. Not negligible impacts on mass and power consumption budget

Table 4-4: RFI Geo-Location Concepts and algorithms characteristics

After the analysis summarised in Table 4-4, taking into account the implementation context as described in the previous chapter and considering the constrains of the possible design and implementation of the solution, the **Radio Frequency Interferometer Sensor System (RaFISS)** technique has been taken into account for the study.

The RaFISS represent a relative simple but effective technique in term of integrability and installability on board of a conventional SATCOM satellite used for BSS and FSS applications and services. Indirectly on the other hand it is a more consolidated and already studied technique because applied in the context of the multi-feed or array antenna systems.

In a simple configuration, RaFISS is based on the principle of the phase comparison between two signals picked-up by two and suitably spaced adjacent antenna elements from an incoming plane wave-front.

If the line jointing the two antenna elements is orthogonal to the propagation path, the sign is received with the same phase by both the antennas.

Any inclination of the plane wave-front from the normal direction will however induce a phase difference between the two received signals proportional to the inclination.

In order to achieve the resolution required in [AD 1], the two sensors should have a high baseline length to wavelength ratio, and this introduced ambiguity. In order to solve the ambiguity, a second short baseline is required. In order to achieve the accuracy and resolve the ambiguity in three dimensions, at least five sensors are required. The main disadvantage of this technique is the capability to resolve one single signal for frequency "Bin" (To remember that: $Bin=f_{sample}/N_{record}$) and in the other hand its main advantage is in a simple implementation and low cost.

The **MUltiple SIgnal Classification (MUSIC)** is in the group of super-resolution algorithms for the DoA detection also considered during the activity because already applied in other project and, for this, useful for performances comparison with the RaFISS.

The algorithm is based on the elaboration of a "spatial covariance matrix" (SCM). The SCM is calculated on board of the satellite then the data are forwarded to the ground elaboration centre in order to define the "spatial spectrum" that gives information about the DoA of the received signals in the coverage area. In the algorithm, the received SCM is decomposed in noise and signal-sub-spaces.

MUSIC algorithm's performances in terms of resolution are not closely linked to the size of the array, but mainly to the SNR and the number of samples used for the SCM calculation. The main disadvantage of this method is that the maximum number of signals to be estimated is linked to the number of array elements and that when the interference sources are coherent the algorithms do not work well.

The **Stochastic Max-Likelihood (SML)** algorithm is still based on SCM elaboration. Starting from the SCM and from the knowledge of the array response, the estimation of the DoA is obtained by solving a complex minimization problem.

This algorithm allows solving also coherent signals, but it has the drawback in the very high computational cost. In order to obtain a solution of the minimization problems in a reasonable time, sub-optimal solutions can be applied to the algorithm.

The **Capon (or Minimum Variance Distortionless Response)** algorithm is once again based on "spatial covariance matrix" elaboration in order to obtain the spatial spectrum that gives information about the direction of arrival of the received signals present in the scenario. This algorithm makes it possible to resolve signals even very close, but the resolution capacity is linked closely to the size of the antenna. For a comparison among the methods, see ANNEX 1.

The **Conical Scan and Amplitude-Comparison Monopulse** methods are mechanical techniques that allow to reach high accuracy if the antenna is large enough, but with narrow angular sector and thus with long time for scan when the service area is large. In addiction these two methods have not negligible impacts on mass and power consumption budget.

4.3 RFI GEO-LOCATION TECHNIQUE AND ALGORITHM: INTERFEROMETER GEO-LOCALISATION TECHNIQUE

In this phase the activities have been focused mainly in the identification of the most promising RFI-geo-localisation technique applicable to the considered scenario. The identification and definition work has been supported by the large experience acquired in several years of research activity preliminary to the doctoral period ([RD 1], [RD 7] and [RD 15]).

As already stated the objective of the research and its focus is the definition of a geo-localisation technique suitable for the commercial telecommunication satellite context and market where the solution performances and low cost are the two main challenging requirements.

The cost reduction is favoured mainly by the low impact on the overall design of the SATCOM payload in implementing the geo-localisation solution "option". This means that the integration of the solution into the overall SATCOM payload architecture has to be less invasive and well combined with the overall system. This objective is reached through a more compact and flexible layout that the geo-localisation sub-system has to guarantee.

In the research activity to reach the objective of defining and preliminary design a suitable geo-localisation technique suitable for the integration on-board of a commercial SATCOM satellite and, at the same time, satisfying the performances, flexibility and low impact/cost requirements an interferometer concept based on an array of sensors associated with super-resolution algorithms (in the research case based on MUSIC algorithm) has been considered.

In the following part the evaluations bringing to the solution definition, dimensioning and preliminary design is reported.

To arrive to choose the mentioned interferometer technique, the status-of-the-art of the direction-of-arrive (DoA) techniques and technologies have been investigated, analysed and traded-off.

The basic configuration of the interferometer radio frequency (RF) array sensor technique is based on the principle of phase comparison between two signals picked-up by two adjacent antenna elements (horn antenna, patch antennas or other sensors) from an incoming plane wavefront as sketched in Figure 4-6.

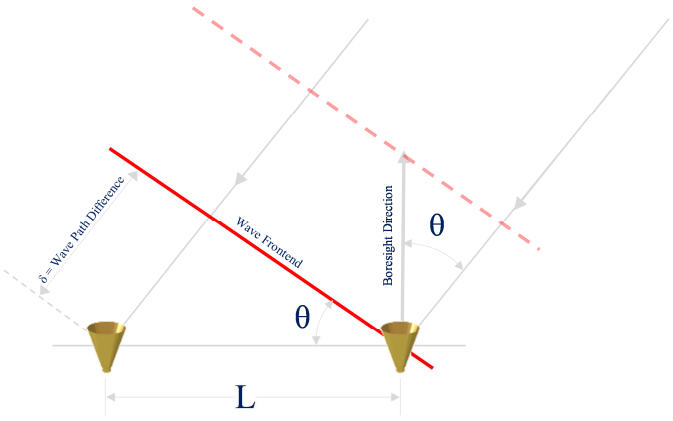

Figure 4-6: Radio Interferometer Principle Scheme

As in the figure, the phase angle is given by: $\varphi = 2\pi \cdot \frac{L}{\lambda} \cdot \sin\theta$, with $\varphi = \varphi + 2n\pi$ and n integer.

If the line joining the two antenna elements is orthogonal to the propagation path, the signal is received with the same phase by both antennas. Any inclination of the plane wave front from the normal will however induce a phase difference between the two received signals proportional to the inclination.

Measuring the phase difference, it is possible to derive the offset angle between the line-of-sight (LoS) or direction of arrival (DoA) of the signals and the normal to the baseline length.

The system performance is constrained by the antenna physical layout as well as by the receiver characteristics. Since the error angle is proportional to the detected phase difference and to the distance (in wavelength) between the two antenna elements, the angular sensitivity of such a sensor is greater, the greater is the distance between the antenna elements. Consequently, the field of view of such systems is larger; the shorter is the distance between the antenna elements, because ambiguity occurs for more than one wavelength path difference (360 degrees phase difference). The antenna layout has thus to be optimized for any actual requirement.

In some cases a switchable system connecting the receiver to a multiple antenna systems could be advantageously implemented, thus providing two basic configurations:

- short baseline configuration providing a large field of view (FoV) but poor sensitivity;
- long baseline configuration providing narrow FoV but high sensitivity for fine error measurements.

To understand how this technique can be used for the purpose of geo-localisation on SATCOM satellite, the phase attitude re1ationshipa need to be described.

The interferometer receiver measures the relative phase of signal pairs received from couples of antenna elements on orthogonal baselines as in Figure 4-7 schematically reported.

As in Figure 4-7, the measurements at the receivers are converted to direction cosines of the LoS to the ground beacon according to the relation:

$$sin\,\theta_{ij} = \frac{\varphi_{ij}\cdot\lambda_i}{2\cdot\pi\cdot L_j}; \quad i=1..n;\ j=1,2 \qquad \text{Eq. 4-1}$$

where:

θ_{ij} is the angle from arm j (in our case j represent the two arms concerning the two couple of antennas 1-1 and 2-2) to LoS vector to the signal source *i* of a group of n-sources;

L_j is the electrical separation of the antenna elements' phase centres on arm *j*;

λ_i is the wavelength of the signal from station *i*;

$\varphi_{ij} = \varphi_{ij} + 2n\pi$ is the phase angle measured with ambiguities resolved by the integer n.

Eq. 4-1 and its counterpart:

$$\varphi_{ij} = \frac{2 \cdot \pi \cdot L_j}{\lambda_i} \cdot \sin\theta \approx \frac{2 \cdot \pi \cdot L_j}{\lambda_i} \cdot \theta \qquad \text{Eq. 4-2}$$

where for low values of θ it is possible to approximate $sin\ \theta \approx \theta$ that is the last member of the equations.

As shown in Figure 4-8, the Eq. 4-2 implies that for a high accurate system the baseline length to wavelength ratio should be as high as possible (long base line interferometer) in order to have high slope sensitivities (i.e. degrees per degree off-boresight) and this can be done or lengthening the arm fixing the wavelength or decreasing the wavelength i.e. increasing the considered frequency. This is a critical question impacting on the final design and implementation of the solution in term of sizing on-board the satellite.

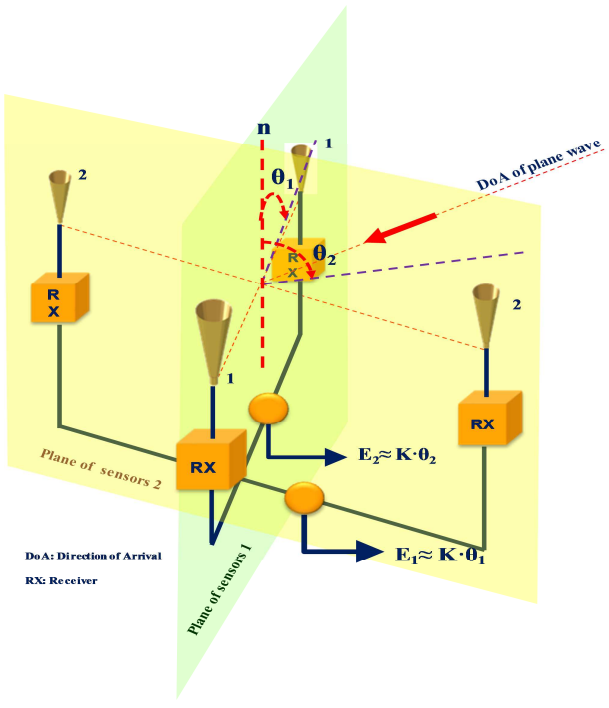

Figure 4-7: Interferometer Implementation Scheme

However, since the electrical phase angles measured may vary through several $2 \cdot \pi$ radiant, ambiguities will exist. In the study case this has been solved directly on board with the use of a suitable configuration using a baseline interferometer, supported by the ground con-

figuration and management algorithm. For this reason, one of the major items considered in designing and implementing the final interferometer sub-system on the target satellite payload layout, has been the above described ambiguity solution considering, at the same time, the required accuracy as reported in Table 4-3 that impacts on the FoV evaluation described in Figure 4-8.

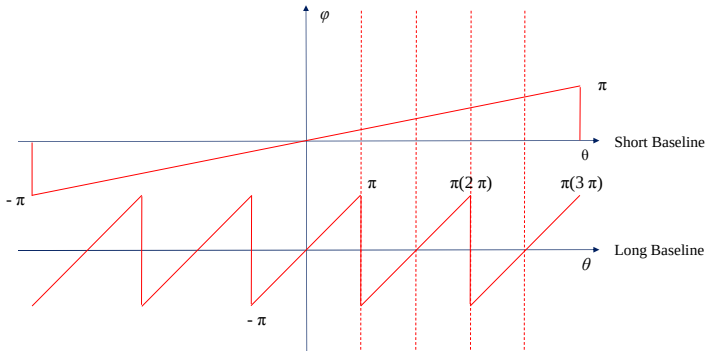

Figure 4-8: Ambiguity Resolution, Accuracy and FoV

As in Figure 4-9 and Figure 4-10, the FoV is defined as the angular extension over which the interferometer can measure with a predetermined accuracy (see above) the direction of cosine directors[1] to one or more ground signal sources.

The FoV is in principle only determined by the antenna element patterns, while in. practice the linearization errors in the determination of the offset will further limit the measurement FoV.

It can be assumed that the element pattern beamwidth is such to cover the angle subtended by the earth from geosynchronous orbit (about 17°), plus an amount depending on (if desirable) the acquisition range (say + 20° - 30°) therefore an element 3 dB beamwidth of about 60° - 80° may be considered satisfactory.

As in Table 4-3, the accuracy taken in to account has been 1 Km and the requirement is translated into angular accuracy requirement for the FoV.

In Figure 4-10 considering the arc at ground, centred in the satellite orbital position the value of θ is done by:

$$\theta \approx \frac{B}{A} = 0{,}000028\, rad = 0{,}0016^{\circ} \qquad \text{Eq. 4-3}$$

[1] *In a Cartesian reference system, the direction cosines (or directional cosines) of a vector are the cosines of the angles between the vector and the three coordinate axes.*

approximating the length of the arc with the chord at the ground (swath). The ambiguity arises from the fact that a given phase out put φ_{ij} corresponds to more than one angle between the boresight and the line-of-sight (LoS) to the reference signal (beacon), as in Eq. 4-2 and schematically described in Figure 4-8.

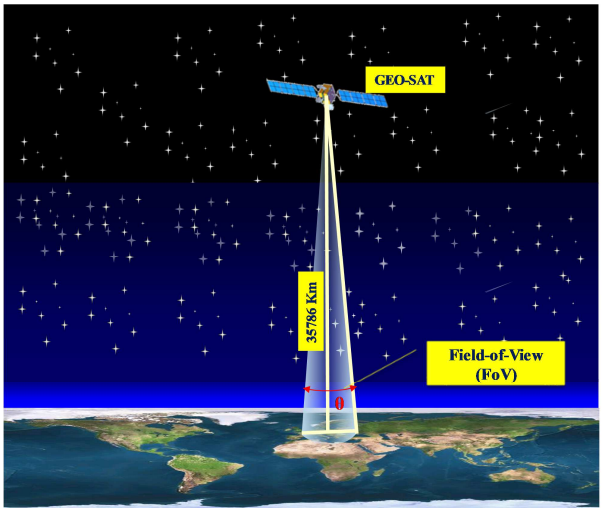

Figure 4-9: Geo-Satellite Field-of-View

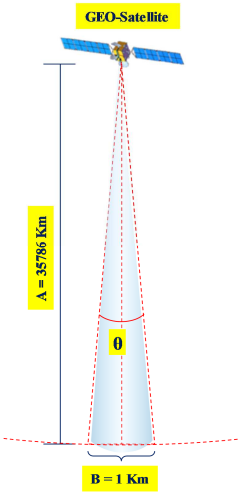

Figure 4-10: Link Geometry

The lowest practical "n" may lie between 2 and 3: the maximum unambiguous acquisition angular extent achievable with a short baseline interferometer is therefore between 10 and 18 degrees, which is sufficient.

On the other side the maximum "n" value for a long baseline interferometer is only dictated by technological reasons (not to increase too much the baseline length with a possible increase of the bias error).

A "11" value between 15 and 25 seems preliminary a good compromise between system sensitivity, bias error susceptibility and compactness.

The spacing among the elements of the array of sensors is defined on the basis of this required angular accuracy.

The proposed solution is based on an array of sensors with minimum impact at satellite level, in terms of complexity, size and mass. This shall, at the same time, attenuate the levels of other communication signals outside the service area (wanted, i.e. coming from another regional service area of the considered network, or coming from other satellite communication networks working in geographic separation on the same frequency bands), in order to obtain a better geo-location performance of RFI.

4.3.1 SYSTEM DIMENSIONING FOR KU BAND SCENARIO

The proposed interferometer solution is based on a geometry derived from the scheme as in Figure 4-7 applied for the Ku band reference scenario. As in Figure 4-11 five antenna sensors with a diameter of 6 λ, a short baseline of 6 λ and a long baseline of 100 λ.

The value of 100 λ for the long baseline is derived from maximum size constraints of a typical small platform top floor (2 ÷ 2.5 m), like a SpaceBus 4000 B2 (see in the Figure 4-12 the standard set of satellite platform currently utilised). The sensors' diameter of 6 λ is derived from the objective of minimizing the mass impact of the proposed system.

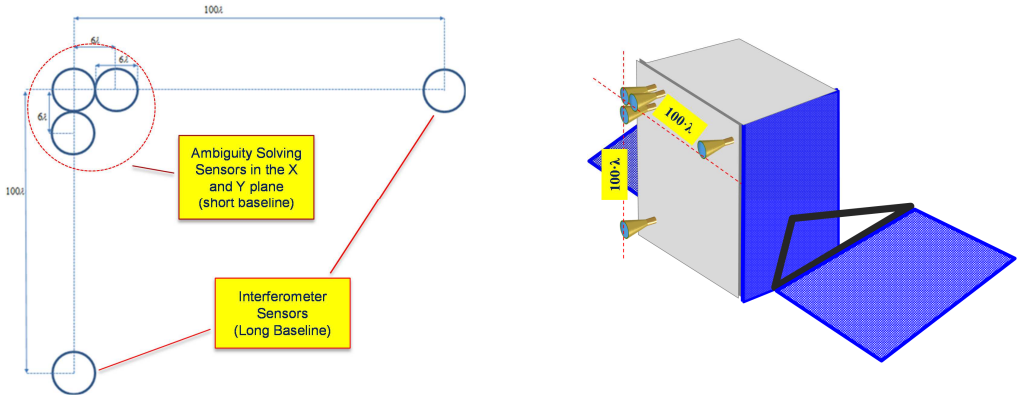

Figure 4-11: Sensor Antenna Spatial Configuration and Possible Installation Layout on the Satellite

The communication signals coming from other regional coverage areas of the intended satellite network are to be considered as disturbs to the RFI measurement. For this reason, the feeds of the array shall be opportunely oriented in order to optimize the gain, and then the interference detection capability, on the service area.

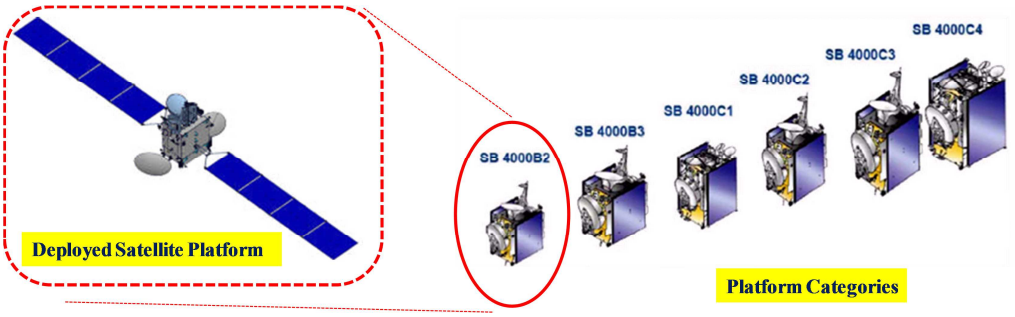

Figure 4-12: SpaceBus B2 and Related Deployed Satellite

It is possible to consider other possible geometrical configurations of the sensors of the ar-

ray, depending from the available room on the satellite top-floor also the combinations of long and short baselines and different sensors dimensions can be taken into account (e.g. 9 or 13 λ).

In the chosen layout, the performance analysis for the case of sensors' diameter of 13 λ (or 9 λ) has been done. This could lead to a better directivity on the service area, improving the RFI detection and the elimination (or better attenuation) of communication signals coming from outside the service area. Furthermore, this could solve the issue of ambiguity, allowing to geo-locate RFI over the entire visible Earth.

The super-resolution algorithms described in the Annex 1 allow to apply the proposed solution to any geometry of the array of sensors. The constraint of maximum envelope for accommodation on a top floor of a small platform shall be respected in any case.

In the proposed system, each receiving sub-system is able to detect two polarisations (Vertical V and Horizontal H). In the research activity, the possibility to simplify the system and reduce its impact in terms of mass and power has been considered taking into account the current available and future technologies (frequency increase, photonic technology etc.) and the heritage coming from the large experience acquired in several year of activities. This implies the reception of a single polarization at a time, switching the received polarization alternatively from V to H (or vice versa).

The detection of RFI in circular polarisations LHCP/RHCP is also possible by means of on ground processing of the FFT samples in V and H polarisation.

Preliminary System sizing for Ku scenario

Suppose a first sizing that provides a long baseline of 2 m, with wavelength of 2 cm, and thus a baseline length to wavelength ratio of around 100.

Applying the Eq. 4-3, the physical angle that subtends a radius of 1 Km to the sub-satellite point, at the distance of 35786 Km (slant range), is 0,0016° or $0{,}000028^{rad}$.

Applying the Eq. 4-2, the corresponding phase angle considering a long baseline of 2 m, is 1°.

The short baseline length should be chosen according to two conditions:

- to have a FoV large enough to cover the service area;
- to have an accuracy solving the ambiguity of the long baseline.

It has been supposed a short baseline length of 12 cm, with a baseline length to wavelength ratio around 6. The corresponding field of view is 4.78°, which corresponds to slightly more than half the earth visibility from the geostationary satellite.

The long baseline, with baseline length to wavelength ratio of 100, has an ambiguity physical angle with period of $\theta = 0.573°$. In order to resolve this ambiguity, the short baseline should have a resolution physical angle much smaller than 0.573°. It corresponds, with a baseline length to wavelength ratio around 6, to a phase angle much smaller than 21.6°. Graphically Figure 4-13 shows these last results.

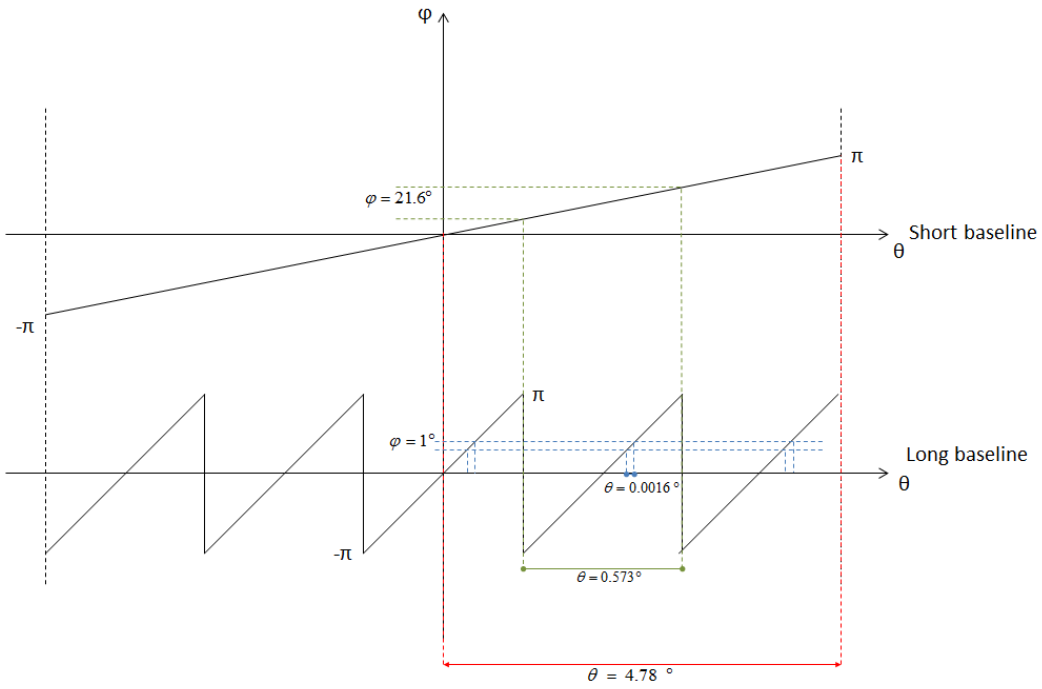

Figure 4-13: Ambiguity Resolution, Accuracy and FoV

Preliminary System sizing for Ka scenario

In this scenario the considered frequency range is the Ka band (27,0 GHz – 40,0 GHz), considering a reference frequency of 29,0 GHz.

Also in this case, suppose a first sizing that provides a long baseline of 2 m, with wave-

length of around 1 cm, and thus a baseline length to wavelength ratio of around 200.

The physical angle that subtends a radius of 1 Km to the sub-satellite point, at the distance of 35786 Km, is provided by Eq. 4-3, i.e. 0.0016° or 0,000028^{rad}. Applying the Eq. 4-2, the corresponding phase angle considering a long baseline (L) of 2 m referred to a wavelength (λ) of 1 cm, is 2°.

Suppose a short baseline length of 6 cm, with a baseline length to wavelength ratio around 6.

The corresponding field of view is 4.78°, which corresponds to slightly more than half the earth visibility from the geostationary satellite.

The long baseline, with baseline length to wavelength ratio of 200, has an ambiguity physical angle with period of $\theta = 0.2865°$. In order to resolve this ambiguity, the short baseline should have a resolution physical angle much smaller than 0.2865°. It corresponds, with a baseline length to wavelength ratio around 6, to an electrical angle much smaller than 10.8°.

Coherent integration gain is the increase in SNR obtained by coherently integrating multiple measurements of signal in additive noise. The integration is considered "coherent" when performed on the complex data, so that both the amplitude and the phase of the data are utilized. Consider complex data x[n] comprised of a complex constant signal $s[n] = Ae^{j\varphi}$ (independent of the index n) and additive zero complex white Gaussian noise w[n] of variance σ_w^2:

$$x[n] = s[n] + w[n] = Ae^{j\varphi} + w[n] \qquad \text{Eq. 4-4}$$

The SNR of a single sample of x, denoted χ_1, is

$$\chi_1 = \frac{A^2}{\sigma_w^2} \qquad \text{Eq. 4-5}$$

Consider the sum of N such samples:

$$z = \sum_{n=0}^{N-1} x[n] = \sum_{n=0}^{N-1} \left(s[n] + w[n]\right) = \sum_{n=0}^{N-1} \left(Ae^{j\varphi} + w[n]\right) = NAe^{j\varphi} + \sum_{n=0}^{N-1} w[n] \qquad \text{Eq. 4-6}$$

The sum z is still in the form of the sum of a signal component $NAe^{j\varphi}$ and a noise compo-

nent that is the sum of N noise samples. The power in the signal component is clearly $(NA)^2$. The power in the noise component is:

$$E\left\{\left|\sum_{n=0}^{N-1} w[n]\right|^2\right\} = E\left\{\left(\sum_{n=0}^{N-1} w[n]\right)\left(\sum_{l=0}^{N-1} w^*[l]\right)\right\} = \sum_{n=0}^{N-1}\sum_{l=0}^{N-1} E\{w[n]w^*[l]\} = N\sigma_w^2 \quad \text{Eq. 4-7}$$

The SNR of **z**, χ_N, is

$$\chi_N = \frac{(NA)^2}{N\sigma_w^2} = \frac{NA^2}{\sigma_w^2} = N\chi_1 \quad \text{Eq. 4-8}$$

The SNR, obtained downstream of N coherent integration as defined above shall be high enough to guarantee the required accuracy in terms of electrical angle estimation.

The total vector x, obtained downstream of N coherent integration, is sum of the signal s and the Gaussian noise w:

$$x = s + w = Ae^{j\varphi} + w = A'e^{j\varphi'} \quad \text{Eq. 4-9}$$

The worst case in terms of angular error of the resulting vector $x = A'e^{j\varphi'}$ is obtained when φ'- φ is maximum, that is when the noise vector w is orthogonal to the signal vector s, as shown in Figure 4-14.

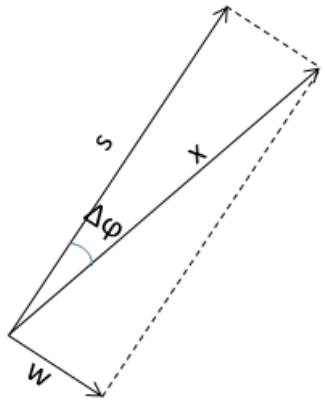

Figure 4-14: Electrical Angle Error Introduced by the Noise

The error angle $\Delta\varphi = \varphi' - \varphi$, for small angle $\Delta\varphi$, is given by:

$$\Delta\varphi = arctg\left(\frac{|w|}{|s|}\right) \approx \frac{|w|}{|s|} \qquad \text{Eq. 4-10}$$

it can be written:

$$\frac{|w|^2}{|s|^2} = \frac{1}{SNR} \approx \Delta\varphi^2 \qquad \text{Eq. 4-11}$$

the required SNR, that guarantees an error angle $\Delta\varphi = 0.33° < 1°$ as required for the Ku scenario with the proposed preliminary system sizing, is given by:

$$SNR \approx \frac{1}{\Delta\varphi^2} = 44.70dB \qquad \text{Eq. 4-12}$$

In the same way, for the Ka scenario, where the required $\Delta\varphi$ is $\Delta\varphi = 0.66° < 2°$, the required SNR is:

$$SNR \approx \frac{1}{\Delta\varphi^2} = 38.68dB \qquad \text{Eq. 4-13}$$

Based on the system description provided above, the J/N and C/J performance is evaluated for the Ku and Ka band mission scenarios.

The number of coherent integrations (see previous section …) necessary to achieve the required J/N that allows to detect the interfering signal above the thermal noise floor is evaluated. This J/N requirement depends on the electric angle Δφ required in order to achieve the geo-location accuracy provided in the SOW (see computation in section…).

Several EIRP levels of the RFI are assumed and, for each of them, the following parameters are evaluated:

- Achievable J/N ratio without coherent integration gain;
- Number ("M") of coherent integrations necessary to achieve the required J/N ("J/N_req");
- C/J ratio: for each scenario (Ku or Ka) the C/J threshold below which the RFI causes detrimental interference with QoS reduction is evaluated and indicated. It is not necessary to detect and geo-localise RFI that do not cause significant (i.e. impact-

ing QoS) C/(N+I) reduction.

Ku/Ku Band Scenario

For the Ku band reference scenario the evaluation of the J/N and C/J ratios has been performed through analysis assuming that:

- Ground station:
  - ✓ Antenna diameter: 3.7 m;
  - ✓ HPA power: 750 W;
  - ✓ Maximum uplink EIRP: 76 dBW
  - ✓ The ground station is assumed to work at 4 dB Output Back-Off (OBO), in order to improve linearity performance in case of transmission of multiple carriers.
- Satellite G/T on feeder link coverage: 7 dB/K;
- Transponder bandwidth: 36 MHz;
- Interferer (J)
  - ✓ EIRP range: 0 ÷ 100 dBW
  - ✓ Bandwidth: 0.5 ÷ 36 MHz
- Geo-location system
  - ✓ Frequency bin: 0.5 MHz
  - ✓ Sensors antennae diameter: 6 λ or 13 λ

Table 4-5 and Table 4-6 report the J/N and C/J evaluation for the short baseline and sensors dimensions 6 λ and 13 λ, respectively.

The number "M" of coherent integrations necessary to achieve the required J/N ("J/N_req") is shown for all the combinations of Interferer's EIRP and bandwidth and geo-location system's frequency bin and sensors antennae diameter.

	Parameters	Units	Radio Frequency Interfernce (RFI) Radiated Power per Bandwidth									
RFI Scenario	**Interference EIRP (Jammer)**	**dBW**	**40,00**	**50,00**	**60,00**	**80,00**	**100,00**	**40,00**	**50,00**	**60,00**	**80,00**	**100,00**
	RFI BW	**MHz**	**36,00**	**36,00**	**36,00**	**36,00**	**36,00**	**0,50**	**0,50**	**0,50**	**0,50**	**0,50**
Payload Receiver Parameters	Frequency	Hz	1,40E+10	1,40E+10	1,40E+10	1,40E+10	1,40E+10	1,40E+10	1,40E+10	1,40E+10	1,40E+10	1,40E+10
		GHz	14,00	14,00	14,00	14,00	14,00	14,00	14,00	14,00	14,00	14,00
	Wavelength (λ)	m	0,02	0,02	0,02	0,02	0,02	0,02	0,02	0,02	0,02	0,02
	Slant Range	Km	35.786,00	35.786,00	35.786,00	35.786,00	35.786,00	35.786,00	35.786,00	35.786,00	35.786,00	35.786,00
	Sensors' Displacement (Equ. Dish Diam. D): 6 λ	m	0,13	0,13	0,13	0,13	0,13	0,13	0,13	0,13	0,13	0,13
	Antenna efficiency		0,55	0,55	0,55	0,55	0,55	0,55	0,55	0,55	0,55	0,55
	Antenna Reception Gain @ EoC	dBi	19,91	19,91	19,91	19,91	19,91	19,91	19,91	19,91	19,91	19,91
	System Temperature (Ts)	dBK	30,00	30,00	30,00	30,00	30,00	30,00	30,00	30,00	30,00	30,00
	Figure of Merit (G/T)	dB/K	-10,09	-10,09	-10,09	-10,09	-10,09	-10,09	-10,09	-10,09	-10,09	-10,09
RFI/Noise Ratio Evaluation	**Frequency bin**	**MHz**	**0,50**	**0,50**	**0,50**	**0,50**	**0,50**	**0,50**	**0,50**	**0,50**	**0,50**	**0,50**
	RFI IPFD	dBW/m2	-122,07	-112,07	-102,07	-82,07	-62,07	-122,07	-112,07	-102,07	-82,07	-62,07
	RFI IPFD0	**dBW/m^2*Hz**	**-197,63**	**-187,63**	**-177,63**	**-157,63**	**-137,63**	**-179,06**	**-169,06**	**-159,06**	**-139,06**	**-119,06**
	Noise IPFD	**dBW/m^2*Hz**	**-174,14**	**-174,14**	**-174,14**	**-174,14**	**-174,14**	**-174,14**	**-174,14**	**-174,14**	**-174,14**	**-174,14**
	Noise IPFD per channel	dBW/m2	-117,15	-117,15	-117,15	-117,15	-117,15	-117,15	-117,15	-117,15	-117,15	-117,15
	RFI IPFD0/Noise IPFD0 Ratio (i.e. J/N)	**dB**	**-23,49**	**-13,49**	**-3,49**	**16,51**	**36,51**	**-4,92**	**5,08**	**15,08**	**35,08**	**55,08**
	REQUIRED J/N (for φ = 1°/3)	**dB**	**44,70**	**44,70**	**44,70**	**44,70**	**44,70**	**44,70**	**44,70**	**44,70**	**44,70**	**44,70**
	Required number of integrations (M)		**6.602.143,27**	**660.214,33**	**66.021,43**	**660,21**	**6,60**	**91.696,43**	**9.169,64**	**916,96**	**9,17**	**1,00**
	Final J/N	**dB**	**44,70**	**44,70**	**44,70**	**44,70**	**44,70**	**44,70**	**44,70**	**44,70**	**44,70**	**55,08**
C/RFI Evaluation	EIRP useful signal (user uplink)	dBW	75,50	75,50	75,50	75,50	75,50	75,50	75,50	75,50	75,50	75,50
	IPFD useful signal	dBW/m^2	-86,57	-86,57	-86,57	-86,57	-86,57	-86,57	-86,57	-86,57	-86,57	-86,57
	Useful Signal Bandwidth	MHz	36,00	36,00	36,00	36,00	36,00	36,00	36,00	36,00	36,00	36,00
	IPFDo useful signal	dBW/m^2*Hz	-162,13	-162,13	-162,13	-162,13	-162,13	-162,13	-162,13	-162,13	-162,13	-162,13
	C/J	**dB**	**35,50**	**25,50**	**15,50**	**-4,50**	**-24,50**	**16,93**	**6,93**	**-3,07**	**-23,07**	**-43,07**

Table 4-5: Ku/Ku Band RFI Scenario Preliminary System Dimensioning (sensors diameter 6 λ)

	Parameters	Units	Radio Frequency Interfernce (RFI) Radiated Power per Bandwidth									
RFI Scenario	**Interference EIRP (Jammer)**	**dBW**	**40,00**	**50,00**	**60,00**	**80,00**	**100,00**	**40,00**	**50,00**	**60,00**	**80,00**	**100,00**
	RFI BW	**MHz**	**36,00**	**36,00**	**36,00**	**36,00**	**36,00**	**0,50**	**0,50**	**0,50**	**0,50**	**0,50**
Payload Receiver Parameters	Frequency	Hz	1,40E+10	1,40E+10	1,40E+10	1,40E+10	1,40E+10	1,40E+10	1,40E+10	1,40E+10	1,40E+10	1,40E+10
		GHz	14,00	14,00	14,00	14,00	14,00	14,00	14,00	14,00	14,00	14,00
	Wavelength (λ)	m	0,02	0,02	0,02	0,02	0,02	0,02	0,02	0,02	0,02	0,02
	Slant Range	Km	35.786,00	35.786,00	35.786,00	35.786,00	35.786,00	35.786,00	35.786,00	35.786,00	35.786,00	35.786,00
	Sensors' Displacement (Equ. Dish Diam. D): 13 λ	m	0,28	0,28	0,28	0,28	0,28	0,28	0,28	0,28	0,28	0,28
	Antenna efficiency		0,55	0,55	0,55	0,55	0,55	0,55	0,55	0,55	0,55	0,55
	Antenna Reception Gain @ EoC	dBi	26,63	26,63	26,63	26,63	26,63	26,63	26,63	26,63	26,63	26,63
	System Temperature (Ts)	dBK	30,00	30,00	30,00	30,00	30,00	30,00	30,00	30,00	30,00	30,00
	Figure of Merit (G/T)	dB/K	-3,37	-3,37	-3,37	-3,37	-3,37	-3,37	-3,37	-3,37	-3,37	-3,37
RFI/Noise Ratio Evaluation	**Frequency bin**	**MHz**	**0,50**	**0,50**	**0,50**	**0,50**	**0,50**	**0,50**	**0,50**	**0,50**	**0,50**	**0,50**
	RFI IPFD	dBW/m2	-122,07	-112,07	-102,07	-82,07	-62,07	-122,07	-112,07	-102,07	-82,07	-62,07
	RFI IPFD0	**dBW/m^2*Hz**	**-197,63**	**-187,63**	**-177,63**	**-157,63**	**-137,63**	**-179,06**	**-169,06**	**-159,06**	**-139,06**	**-119,06**
	Noise IPFD	**dBW/m^2*Hz**	**-180,85**	**-180,85**	**-180,85**	**-180,85**	**-180,85**	**-180,85**	**-180,85**	**-180,85**	**-180,85**	**-180,85**
	Noise IPFD per channel	dBW/m2	-123,86	-123,86	-123,86	-123,86	-123,86	-123,86	-123,86	-123,86	-123,86	-123,86
	RFI IPFD0/Noise IPFD0 Ratio (i.e. J/N)	**dB**	**-16,78**	**-6,78**	**3,22**	**23,22**	**43,22**	**1,80**	**11,80**	**21,80**	**41,80**	**61,80**
	REQUIRED J/N (for φ = 1°/3)	**dB**	**44,70**	**44,70**	**44,70**	**44,70**	**44,70**	**44,70**	**44,70**	**44,70**	**44,70**	**44,70**
	Required number of integrations (M)		**1.406.373,71**	**140.637,37**	**14.063,74**	**140,64**	**1,41**	**19.532,97**	**1.953,30**	**195,33**	**1,95**	**1,00**
	Final J/N	**dB**	**44,70**	**44,70**	**44,70**	**44,70**	**44,70**	**44,70**	**44,70**	**44,70**	**44,70**	**61,80**
C/RFI Evaluation	EIRP useful signal (user uplink)	dBW	75,50	75,50	75,50	75,50	75,50	75,50	75,50	75,50	75,50	75,50
	IPFD useful signal	dBW/m^2	-86,57	-86,57	-86,57	-86,57	-86,57	-86,57	-86,57	-86,57	-86,57	-86,57
	Useful Signal Bandwidth	MHz	36,00	36,00	36,00	36,00	36,00	36,00	36,00	36,00	36,00	36,00
	IPFDo useful signal	dBW/m^2*Hz	-162,13	-162,13	-162,13	-162,13	-162,13	-162,13	-162,13	-162,13	-162,13	-162,13
	C/J	**dB**	**35,50**	**25,50**	**15,50**	**-4,50**	**-24,50**	**16,93**	**6,93**	**-3,07**	**-23,07**	**-43,07**

Table 4-6: Ku/Ku Band RFI Scenario Preliminary System Dimensioning (sensors diameter 13 λ)

Ka/Ka Band Scenario

This section reports the evaluation of the J/N and C/J ratios for the Ka band scenario.

The assumptions for the analyses are:

- User terminal:
  - ✓ Antenna diameter: 0.7 m;
  - ✓ HPA power: 3W;
- Satellite G/T on user link multi-spot coverage: 16 dB/K at Edge of Coverage (EOC) of each beam;
- Target data rate per user terminal: 2 Mbps.
- Interferer (J)
  - ✓ EIRP range: 30 ÷ 100 dBW
  - ✓ Bandwidth: 0.5 ÷ 50 MHz
- Geo-location system
  - ✓ Frequency bin: 0.5 MHz
  - ✓ Sensors antennae diameter: 6 λ or 13 λ as reference examples for this proposal.

The user terminal is assumed to work at 1 dB Output Back-Off (OBO), in order to reduce spectral regrowth phenomenon.

Table 4-7 and Table 4-8 report the J/N and C/J evaluation for the short baseline and sensors dimensions 6 λ and 13 λ, respectively.

The number "M" of coherent integrations necessary to achieve the required J/N ("J/N_req") is shown for all the combinations of Interferer's EIRP and bandwidth and geo-location system's frequency bin and sensors antennae diameter.

	Parameters	Units	Radio Frequency Interference (RFI) Radiated Power per Bandwidth													
RFI Scenario	**Interference EIRP (Jammer)**	**dBW**	**0,00**	**20,00**	**40,00**	**50,00**	**60,00**	**80,00**	**100,00**	**0,00**	**30,00**	**40,00**	**50,00**	**60,00**	**80,00**	**100,00**
	RFI BW	**MHz**	**50,00**	**50,00**	**50,00**	**50,00**	**50,00**	**50,00**	**50,00**	**0,50**	**0,50**	**0,50**	**0,50**	**0,50**	**0,50**	**0,50**
Payload Receiver Parameters	Frequency	Hz	2,90E+10	2,90E+10	2,90E+10	2,90E+10	2,90E+10	2,90E+10	2,90E+10	2,90E+10	2,90E+10	2,90E+10	2,90E+10	2,90E+10	2,90E+10	2,90E+10
		GHz	29,00	29,00	29,00	29,00	29,00	29,00	29,00	29,00	29,00	29,00	29,00	29,00	29,00	29,00
	Wavelength (λ)	m	0,01	0,01	0,01	0,01	0,01	0,01	0,01	0,01	0,01	0,01	0,01	0,01	0,01	0,01
	Slant Range	Km	35786,00	35786,00	35786,00	35786,00	35786,00	35786,00	35786,00	35786,00	35786,00	35786,00	35786,00	35786,00	35786,00	35786,00
	Sensors' Displacement (Equ. Dish Diam. D): 6 λ	m	0,06	0,06	0,06	0,06	0,06	0,06	0,06	0,06	0,06	0,06	0,06	0,06	0,06	0,06
	Antenna efficiency		0,55	0,55	0,55	0,55	0,55	0,55	0,55	0,55	0,55	0,55	0,55	0,55	0,55	0,55
	Antenna Reception Gain @ EoC	dBi	**19,91**	19,91	19,91	19,91	19,91	19,91	19,91	19,91	19,91	19,91	19,91	19,91	19,91	19,91
	System Temperature (T_s)	dBK	30,00	30,00	30,00	30,00	30,00	30,00	30,00	30,00	30,00	30,00	30,00	30,00	30,00	30,00
	Figure of Merit (G/T)	dB/K	-10,09	-10,09	-10,09	-10,09	-10,09	-10,09	-10,09	-10,09	-10,09	-10,09	-10,09	-10,09	-10,09	-10,09
RFI/N Ratio Evaluation	**Frequency bin**	**MHz**	**0,50**	**0,50**	**0,50**	**0,50**	**0,50**	**0,50**	**0,50**	**0,50**	**0,50**	**0,50**	**0,50**	**0,50**	**0,50**	**0,50**
	RFI IPFD	dBW/m^2	-162,07	-142,07	-122,07	-112,07	-102,07	-82,07	-62,07	-162,07	-132,07	-122,07	-112,07	-102,07	-82,07	-62,07
	RFI $IPFD_0$	**dBW/m^2*Hz**	**-239,06**	**-219,06**	**-199,06**	**-189,06**	**-179,06**	**-159,06**	**-139,06**	**-219,06**	**-189,06**	**-179,06**	**-169,06**	**-159,06**	**-139,06**	**-119,06**
	Noise IPFD	**dBW/m^2*Hz**	**-167,81**	**-167,81**	**-167,81**	**-167,81**	**-167,81**	**-167,81**	**-167,81**	**-167,81**	**-167,81**	**-167,81**	**-167,81**	**-167,81**	**-167,81**	**-167,81**
	Noise IPFD per channel	dBW/m2	-110,82	-110,82	-110,82	-110,82	-110,82	-110,82	-110,82	-110,82	-110,82	-110,82	-110,82	-110,82	-110,82	-110,82
	RFI $IPFD_0$/Noise $IPFD_0$ Ratio (i.e. J/N)	**dB**	**-71,24**	**-51,24**	**-31,24**	**-21,24**	**-11,24**	**8,76**	**28,76**	**-51,24**	**-21,24**	**-11,24**	**-1,24**	**8,76**	**28,76**	**48,76**
	REQUIRED J/N (for φ = 1°/3)	**dB**	**38,68**	**38,68**	**38,68**	**38,68**	**38,68**	**38,68**	**38,68**	**38,68**	**38,68**	**38,68**	**38,68**	**38,68**	**38,68**	**38,68**
	Required number of integrations (M)		**98363139354**	**983631394**	**9836314**	**983631**	**98363**	**984**	**10**	**983631394**	**983631**	**98363**	**9836**	**984**	**10**	**1**
	Final J/N	**dB**	**38,68**	**38,68**	**38,68**	**38,68**	**38,68**	**38,68**	**38,68**	**38,68**	**38,68**	**38,68**	**38,68**	**38,68**	**38,68**	**48,76**
C/RFI Evaluation	EIRP useful signal (user uplink)	dBW	47,50	47,50	47,50	47,50	47,50	47,50	47,50	47,50	47,50	47,50	47,50	47,50	47,50	47,50
	IPFD useful signal	dBW/m^2	-114,57	-114,57	-114,57	-114,57	-114,57	-114,57	-114,57	-114,57	-114,57	-114,57	-114,57	-114,57	-114,57	-114,57
	Useful Signal Bandwidth	MHz	1,50	1,50	1,50	1,50	1,50	1,50	1,50	1,50	1,50	1,50	1,50	1,50	1,50	1,50
	IPFDo useful signal	dBW/m^2*Hz	-176,33	-176,33	-176,33	-176,33	-176,33	-176,33	-176,33	-176,33	-176,33	-176,33	-176,33	-176,33	-176,33	-176,33
	C/J	**dB**	**62,73**	**42,73**	**22,73**	**12,73**	**2,73**	**-17,27**	**-37,27**	**42,73**	**12,73**	**2,73**	**-7,27**	**-17,27**	**-37,27**	**-57,27**

Table 4-7: Ka/Ka Band RFI Scenario Preliminary System Dimensioning (sensors diameter 6 λ)

	Parameters	Units	Radio Frequency Interference (RFI) Radiated Power per Bandwidth													
RFI Scenario	**Interference EIRP (Jammer)**	**dBW**	**0,00**	**20,00**	**40,00**	**50,00**	**60,00**	**80,00**	**100,00**	**0,00**	**30,00**	**40,00**	**50,00**	**60,00**	**80,00**	**100,00**
	RFI BW	**MHz**	**50,00**	**50,00**	**50,00**	**50,00**	**50,00**	**50,00**	**50,00**	**0,50**	**0,50**	**0,50**	**0,50**	**0,50**	**0,50**	**0,50**
Payload Receiver Parameters	Frequency	Hz	2,90E+10	2,90E+10	2,90E+10	2,90E+10	2,90E+10	2,90E+10	2,90E+10	2,90E+10	2,90E+10	2,90E+10	2,90E+10	2,90E+10	2,90E+10	2,90E+10
		GHz	29,00	29,00	29,00	29,00	29,00	29,00	29,00	29,00	29,00	29,00	29,00	29,00	29,00	29,00
	Wavelength (λ)	m	0,01	0,01	0,01	0,01	0,01	0,01	0,01	0,01	0,01	0,01	0,01	0,01	0,01	0,01
	Slant Range	Km	35786,00	35786,00	35786,00	35786,00	35786,00	35786,00	35786,00	35786,00	35786,00	35786,00	35786,00	35786,00	35786,00	35786,00
	Sensors' Displacement (Equ. Dish Diam. D): 13 λ	m	0,13	0,13	0,13	0,13	0,13	0,13	0,13	0,13	0,13	0,13	0,13	0,13	0,13	0,13
	Antenna efficiency		0,55	0,55	0,55	0,55	0,55	0,55	0,55	0,55	0,55	0,55	0,55	0,55	0,55	0,55
	Antenna Reception Gain @ EoC	dBi	**26,63**	26,63	26,63	26,63	26,63	26,63	26,63	26,63	26,63	26,63	26,63	26,63	26,63	26,63
	System Temperature (T_s)	dBK	30,00	30,00	30,00	30,00	30,00	30,00	30,00	30,00	30,00	30,00	30,00	30,00	30,00	30,00
	Figure of Merit (G/T)	dB/K	-3,37	-3,37	-3,37	-3,37	-3,37	-3,37	-3,37	-3,37	-3,37	-3,37	-3,37	-3,37	-3,37	-3,37
RFI/N Ratio Evaluation	**Frequency bin**	**MHz**	**0,50**	**0,50**	**0,50**	**0,50**	**0,50**	**0,50**	**0,50**	**0,50**	**0,50**	**0,50**	**0,50**	**0,50**	**0,50**	**0,50**
	RFI IPFD	dBW/m^2	-162,07	-142,07	-122,07	-112,07	-102,07	-82,07	-62,07	-162,07	-132,07	-122,07	-112,07	-102,07	-82,07	-62,07
	RFI $IPFD_0$	**dBW/m^2*Hz**	**-239,06**	**-219,06**	**-199,06**	**-189,06**	**-179,06**	**-159,06**	**-139,06**	**-219,06**	**-189,06**	**-179,06**	**-169,06**	**-159,06**	**-139,06**	**-119,06**
	Noise IPFD	**dBW/m^2*Hz**	**-174,53**	**-174,53**	**-174,53**	**-174,53**	**-174,53**	**-174,53**	**-174,53**	**-174,53**	**-174,53**	**-174,53**	**-174,53**	**-174,53**	**-174,53**	**-174,53**
	Noise IPFD per channel	dBW/m2	-117,54	-117,54	-117,54	-117,54	-117,54	-117,54	-117,54	-117,54	-117,54	-117,54	-117,54	-117,54	-117,54	-117,54
	RFI $IPFD_0$/Noise $IPFD_0$ Ratio (i.e. J/N)	**dB**	**-64,53**	**-44,53**	**-24,53**	**-14,53**	**-4,53**	**15,47**	**35,47**	**-44,53**	**-14,53**	**-4,53**	**5,47**	**15,47**	**35,47**	**55,47**
	REQUIRED J/N (for φ = 1°/3)	**dB**	**38,68**	**38,68**	**38,68**	**38,68**	**38,68**	**38,68**	**38,68**	**38,68**	**38,68**	**38,68**	**38,68**	**38,68**	**38,68**	**38,68**
	Required number of integrations (M)		**20953094774**	**209530948**	**2095309**	**209531**	**20953**	**210**	**2**	**209530948**	**209531**	**20953**	**2095**	**210**	**2**	**1**
	Final J/N	**dB**	**38,68**	**38,68**	**38,68**	**38,68**	**38,68**	**38,68**	**38,68**	**38,68**	**38,68**	**38,68**	**38,68**	**38,68**	**38,68**	**55,47**
C/RFI Evaluation	EIRP useful signal (user uplink)	dBW	47,50	47,50	47,50	47,50	47,50	47,50	47,50	47,50	47,50	47,50	47,50	47,50	47,50	47,50
	IPFD useful signal	dBW/m^2	-114,57	-114,57	-114,57	-114,57	-114,57	-114,57	-114,57	-114,57	-114,57	-114,57	-114,57	-114,57	-114,57	-114,57
	Useful Signal Bandwidth	MHz	1,50	1,50	1,50	1,50	1,50	1,50	1,50	1,50	1,50	1,50	1,50	1,50	1,50	1,50
	IPFDo useful signal	dBW/m^2*Hz	-176,33	-176,33	-176,33	-176,33	-176,33	-176,33	-176,33	-176,33	-176,33	-176,33	-176,33	-176,33	-176,33	-176,33
	C/J	**dB**	**62,73**	**42,73**	**22,73**	**12,73**	**2,73**	**-17,27**	**-37,27**	**42,73**	**12,73**	**2,73**	**-7,27**	**-17,27**	**-37,27**	**-57,27**

Table 4-8: Ka/Ka Band RFI Scenario Preliminary System Dimensioning (sensors diameter 13 λ)

5 PRELIMINARY ARCHITECTURAL DESIGN

As already described, to manage the geo-localisation solution a complex algorithm need to be implemented but today this cannot be done on-board of the satellite payload due to the no more mature on-board processing (OBP) technology. For this reason, a hybrid on-board/on-ground technological approach has been considered and analysed.

As example, this methodology has been already successfully applied for the implementation of complex on-board phased array antennas based on the Ground Beam Former Network (GBFN) technology [RD 16]. For a GBFN all the algorithm section runs at the ground segment side driving a more compact hardware integrated (composed by the feed section, by the phase shifter, by the combiners etc.) on-board the satellite. A performing link connection joins the on-board/on-ground sides composing the entire system; this is based on an advance TM/TC connectivity guaranteeing a bitrate up to 100 Kbps (typically a TT&C bitrate for the satellite management ranges between few bps up to few Kbps). Currently suitable solutions are studied having the objective to arrive at a bitrate of some Mbps protecting the link through a spread spectrum (SS) technology approach (Secure TT&C).

In Figure 5-1 the architecture layout of the chosen approach is depicted.

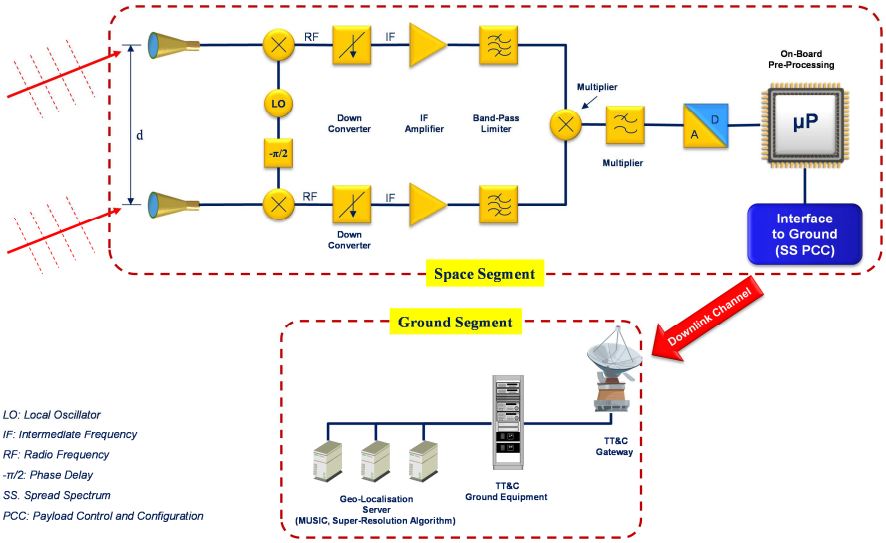

Figure 5-1: Geo-Localisation Hybrid Technology Architecture

In following the description of the preliminary design of the proposed technical solution is provided.

5.1 RAFISS ON-BOARD RFI GEO-LOCALISATION SYSTEM INTEGRATION

As already described the RFI geo-localisation system (Radio Frequency Interferometer Sensor System or RaFISS) front-end is based on the utilisation of with five receiving sensor antennas (see Figure 4-11) and a dedicated transponder integrated into the satellite payload. The sensor front-end is integrated on the Earth Face Panel (EFP) of the satellite as in Figure 5-2 and Figure 5-3 drawn.

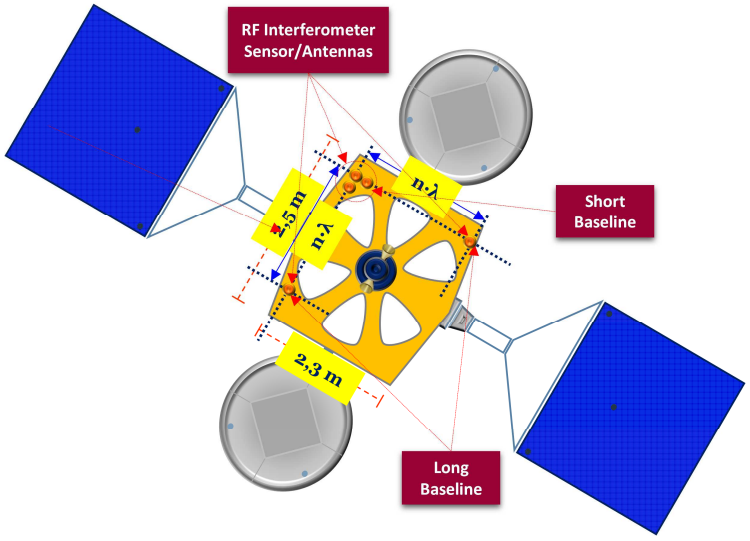

Figure 5-2: Feeds Layout on Earth Face Panel

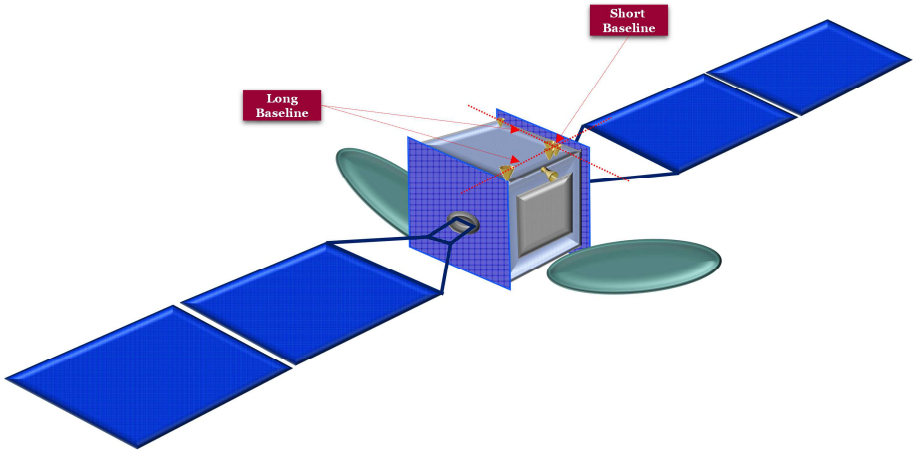

Figure 5-3: Feeds Layout on Earth Face Panel

Two sensors plus one for the calibration (reference) are devoted for the long baseline (100 λ) to achieve the required resolution in terms of direction of arrival estimation, and two sensors for the short one (6 λ), to resolve the ambiguity intrinsic with the long baseline configuration.

The received signals are then low noise amplified and down-converted at intermediate frequency (IF) and following moved into the base-band (BB) for the analog-to-digital conversion (ADC) to be feed into the digital section which performs the digital sampling and on-board pre-processing of the signals coming from the feeds.

As already written, for the practical implementation of the technique, it has been taken into account the already matured experience in the work context where the research activity has been carried out (Thales Alenia Space Italia).

For the design of the sensor section of the on-board interferometer the experience in the design of antenna feeds for Ku band satellite application has been taken into account as in Figure 5-4 shown. The feed in Figure 5-4 has been designed and developed in the frame of a Company Project and currently it is on-board of an actual operative satellite.

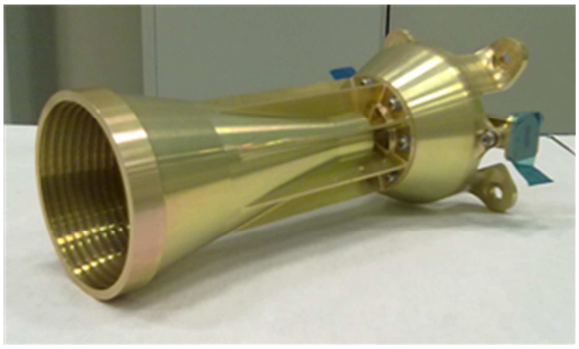

Figure 5-4: 10,00 -12,75 GHz

The receiving section box includes 10 LNA + Down-conversion chains (5 for H polarization and 5 for V polarization) and proper redundancy units. A preliminary evaluation, based on typical figure of merit (FoM), provides a redundancy scheme arranged in a 12:10 configuration.

This configuration is therefore able to process in parallel both H and V polarizations. A simplified block diagram is reported in Figure 5-5.

A reduced number of radio frequency (RF) paths (5 instead of 10) can be achieved by considering one polarization at a time in order to reduce the number of RF paths towards the

digital section. The main advantage is represented by the reduced interfaces (waveguide utilisation) but the drawback is that it is not anymore feasible the parallel H and V polarization signals processing. In this option the redundancy could be applied with a 7 : 5 scheme.

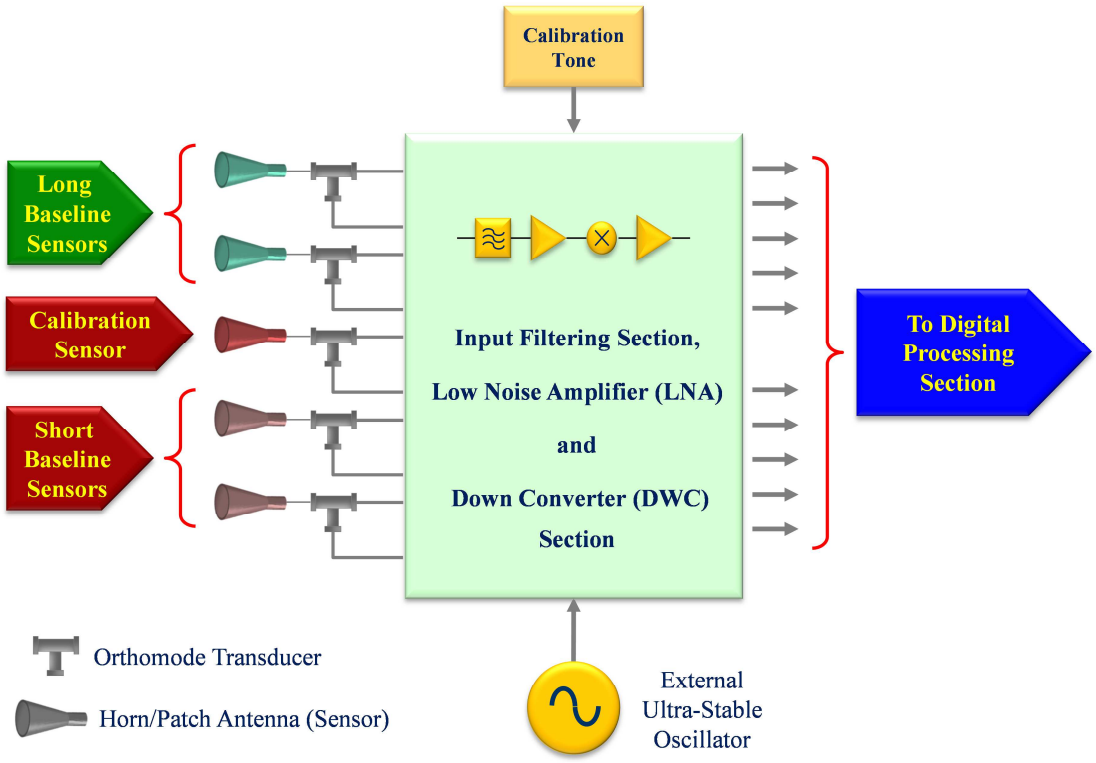

Figure 5-5: RaFISS payload RX section block diagram (baseline with H and V polarization)

After the Ortho-Mode Transducer (OMT) it is necessary to use a switch to select the H or V polarization to be processed. A simplified block diagram for this option is reported in Figure 5-6.

In order to have the phase tracked features, an external ultra-stable and low phase noise reference oscillator shall be used for the down-conversion function. If a frequency generator unit with good phase noise, stability and phase tracking performance is already available in the communication payload, some local oscillator (LO) lines can be devoted for the interferometer payload functionality.

Otherwise a dedicated Frequency Generator Unit (FGU) should be considered for the interferometer section.

The most important feature of the receive (RX) section is the phase tracking one: it is

therefore necessary to design properly all the RF routing to achieve this target and to perform unit procurement with severe phase tracking requirements in order to guarantee to achieve the required spatial resolution.

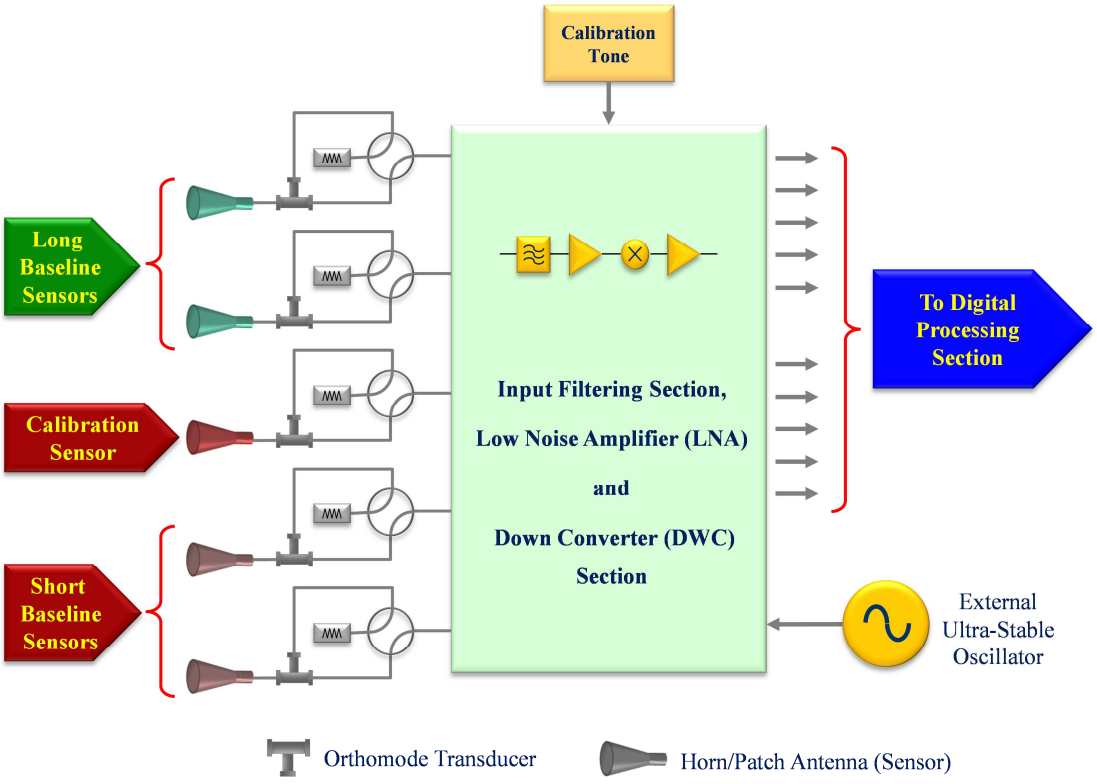

Figure 5-6: RaFISS payload PL receiving section block diagram with the H or V polarization processing option

Furthermore it is necessary to provide a Calibration Tone as close as possible to the feed interface to perform periodically the RF chain calibration and ensure the keep the phase tracking among the RF chains also in presence of RF path thermos-elastic or unit phase tracking variations.

The 10 output RF paths are then routed towards the digital section which performs the digital sampling and phase evaluation or only the digital sampling according to the selected architecture here after described.

The digital pre-processing section is interfaced to the radio frequency section through a frequency down-conversion and filtering stage as schematized in Figure 5-1. The pre-processing section provides signals analysis directly on-board the satellite mainly for what concern the real-time signal analysis and the interface to the TT/C or PCC link sub-system.

Two options could be considered for the RF section output signal type: direct IF input signal or baseband demodulated In-phase & Quadrature (I&Q) signal components.

Direct IF input signal (baseline option) relies on a less strict set of requirements for the RF sections, but imposes high clock speed on the digital processing section and requires adaptive equalisation techniques to be implemented in the DSP section making an extensive use of Digital Signal Processing (DSP) techniques to compensate the unwanted variations of RF components parameters as well as the difference among the various RF chain paths. The flexibility of direct IF sampling is suitable to allow implementation of accurate compensation techniques for electrical path difference among the different RF, IF or BB lines. RF output signal could be provided on a suitable IF frequency closed to the baseband signal bandwidth (e.g. for 1 GHz bandwidth analysis IF could be around 600 MHz).

Baseband I&Q Demodulation approach relax the requirement for conversion sample rate of the digital section but requiring the slitting of the input channels for coordinated I&Q acquisition. In this case the RF section will have in charge the analogical demodulation of the baseband I&Q components (e.g. direct Ku - baseband down conversion) provided as input to the digital section. The drawback of this solution is the increased criticality in the system calibration, indeed the unbalance and non-linearity of the used RF baseband mixer, plus the mismatch between the two I&Q input paths, represents a further addition of non-ideal contributions to be minimized.

The output coming from the Digital Section will be of three types: IF Modulated downstream; IF Calibration Signal; Digital Data Interface.

IF Modulated downstream, generated by the digital unit, will carrying on results related to the elaboration of the generic acquired scenario, in a form to be directly transmitted on ground by means of the IF injection, in the Payload transmission chains (baseline option), of an additional modulated carrier, or direct connection to a dedicated transmission (TX) section.

IF Calibration Signal generated by the digital unit for system calibration purpose. The calibration reference signal will be provided as modulated over IF signal to be up-converted and injected on the RX front-end of the Geo-localization RF section.

Digital Data Interface will be suitable for satellite TCR unit interfacing for the primary scope to handle Telecommand and Telemetry related to the Unit Monitoring/Configuration and (alternative/concurrent option) the additional task to inject the data results of the elaborated acquired scenario over a dedicated high bitrate TM channel.

RaFISS Transmitting section

In the hybrid architectural configuration, the downlink from space and ground sections has been sized to manage a bit-rate of about 576 kbps that can be easily allocated in a small portion of bandwidth. This downlink can be implemented by the following ways:

1. Via a dedicated channel, which implies the need of dedicated transmission (TX) section and antenna (additional TM/TC link);
2. Combining the sub-channel data in a telecommunication traffic channel (Payload Control and Configuration or PCC link).
3. Through conventional TT&C channel: in this case the phase estimation is provided to the TT&C section as a standard telemetry parameter.

Since standard TT&C has a limited data rate (up to 16 kbps), the new next generation performing TT&C standard system with high data rate capability shall be used. It has the capability to manage the TT&C on a bandwidth up to 1 Mbps.

The current baseline is to use one PCC link channel, i.e. the option 2. This solution derives from the Study described in [RD 20] performed with the European Space Agency in the 2009. As in Figure 5-7 sketched, in this approach the digital samples are modulated in the digital section while the up conversion is performed before combining them in the TLC channel.

The direct current (DC) power and Telemetry/Telecommand (TM/TC) interface will use

the same ones already foreseen for the telecommunication payload. This approach has been selected as baseline in order to avoid additional hardware which would have direct impact on allocation, mass and power budgets. Continuing the activity the mass and power budget can be finalised considering the current technology trend for what concern the space components.

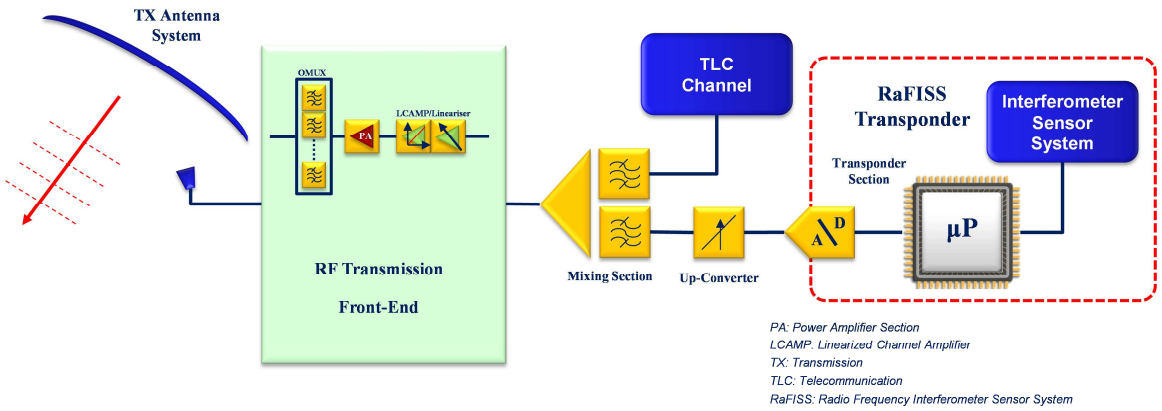

Figure 5-7: Interferometer Payload (RaFISS) transmission Section Block Diagram (PCC Link Channel Approach)

In the first analysis, the main RF interfaces, taking into account the proposed configuration as in Figure 5-7 have been defined as listed in following:

- 10 WG I/P interface with RF feed sensors
- 1 RF coax I/P interface for LO reference
- 10 or 5 RF coax O/P interface toward the digital section
- 1 coax I/P interface from digital section
- 1 coax O/P interface toward TLC high power and output section

RaFISS On-Board Transponder Architecture

Figure 5-8 describes the conceptual architecture of the RaFISS on-boarded system, dimensioned for five RX antennas in dual polarization (H and V for the linear polarisation or LHCP and RHCP for the circular one). As in Figure 5-1 schematised, the block diagram reports at high level the system components and the main components to interface the RF section with the on-board digital processor.

Designing the RF to Digital Unit interface, two approaches have been considered for the analog signal digitalisation:

1. Direct Intermediate Frequency (IF) sampling with a single Analog-to Digital Converter (ADC);
2. Analog quadrature mixer, followed by a double ADC.

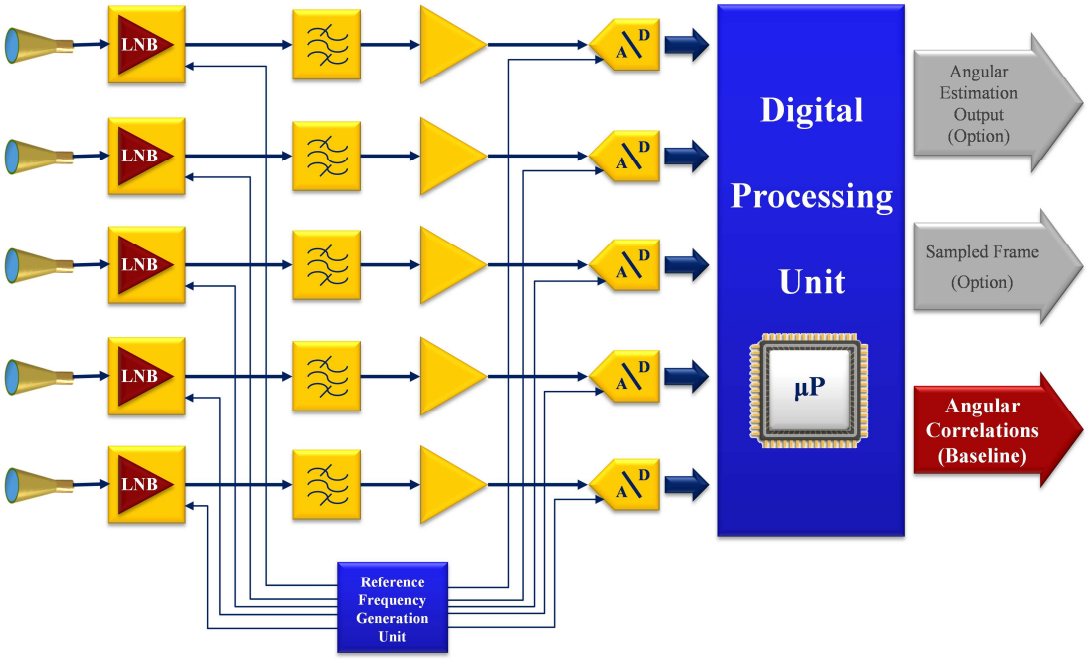

Figure 5-8: Block Diagram of signal acquisition chains of Digital Processor Operating in Single Polarisation

Typically, an IF sampling operated via a single ADC allows digital extraction of the In-Phase (I) and In-Quadrature (Q) signal components with an ADC sampling frequency roughly ranging from a theoretical minimum of 2 – 3 time of the bandwidth of the signal. On the other hand, a zero IF solution, based on a quadrature mixer (i.e. analogue extraction of the components of the complex envelope), allows operation of the double ADC section at a frequency ranging from an ideal minimum of 1 time up to 1,5 time of the bandwidth. This means that typically a factor of 2 on the clock rate distinguishes the two solutions.

As a matter of example, it can be introduced the hypothesis of the adoption of some optimization, oriented to reduce the demanding and complexity of the signal processing. The better way is constituted by the adoption of a technique that needs of a reduced amount of acquired data (adopting, as example, a down-sampling policy) finding a compromise to the

manifold spectral folding that, under specific hypothesis, could preserve some of the physical characteristic of the parameter to be estimated. A reasonable hypothesis can be to down-sampling the input signal, subsequently the decimated (e.g. 1/100) signal spectrum can be still suitable for the extraction of the covariance matrix under the hypothesis of unique dominant applied signal. This is possible since in current example, the pre-processing has not to preserve the full signal information but only execute estimation of some signal parameters (as is the case of system calibration support and DoA covariance matrix extraction). This kind of under-sampling policy is more efficiently implemented within a digital core exploiting the flexibility to implement fractional interpolated sample rates suitable to analyse the incoming signals using different base of decimation. During the project phases these "optimized" technique will be object of trade off for evaluation and best choice implementation.

The second solution, using an analogic quadrature mixer as front-end, have as major difference the displacement in the RF section of the base-band demodulation task of the incoming signal, using a quadrature mixer (or a quadrature down converter). The relevant benefit of this choice is the reduction of the sampling rate but, as drawback, there is also the introduction of the following reported additional impairments typical of a ZIF quadrature mixer:

- I & Q Amplitude imbalance
- Quadrature Phase error
- DC offset

These additional non-ideal behaviours of the RF chain shall be addressed by algorithms for compensation in the system calibration procedure and could be responsible, after calibration, of some residual penalty on performance. For the mentioned reasons, we consider this solution, at time of proposal, as a possible option and not the baseline.

Narrow Band Approximation

Most part of the above addressed techniques have been considered in the hypothesis of nar-

row band signals. Furthermore also most part of the searching algorithms group of DoA estimation methods based on the eigen-analysis of the correlation matrix, are validated for narrowband signals. In order to approximate the narrow band condition and, on the same time, maximize the Signal over Noise ratio (S/N), the channelization of the whole observed bandwidth is required. The analysis methods is applied on each of the coordinated sub-bands coming from different filters operating on independent sensors as in Figure 5-9 schematically reported. Typically, the channelization is implemented by means of a poliphase FFT filtering, due to the efficiency of this algorithm in term of computational performance. Recently other approaches have been evaluated to achieve frequency separation (channelizer function) based on time-frequency (TF) signal representations.

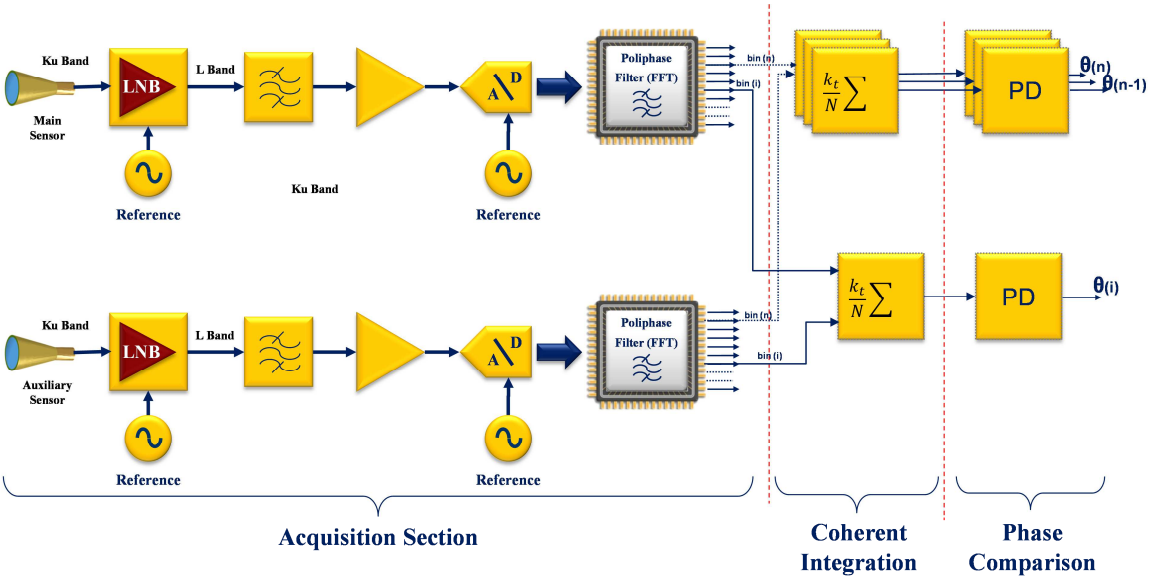

Figure 5-9: Narrow Band Analysis Approximation Concept

During the research activity a trade-off on the adoption of the two candidate techniques, hereafter reported have been taken into account.

The Poliphase FFT Filter Bank (PFFB) channelizer makes use of a poliphase filter and M-point Fast Fourier Transform (FFT) to isolate and down sampling the various channels, and then to efficiently convert each channel to baseband as depicted in the architecture described in Figure 5-10 as implementable in a Field Programmable Gate Array component. The poliphase filter is created through the decomposition of the low pass filter *p(n)* used to provide channel isolation on a per channel basis: the filter *pr(n)* is obtained from *p(n)* by considering an initial offset of r samples and then by incrementing by M. i.e.:

$$pr(n) = p(r + n \cdot M) \qquad \text{Eq. 5-1}$$

In general, in this technique the number of channels must be equal to the down-sampling rate, and the sampling rate must be a power of two times the baseband bandwidth.

It is useful to compare the conventional mixer down-converter and the poliphase down-converter.

In the mixer down-converter architecture, a separate pair of mixers and filters must be assigned to each channel of the channelizer and these mixers must operate at the high input data rate, prior to the down sampling. In the re-sampled poliphase architecture, there is only one low-pass filter required to serve all the channels of the channelizer, and this single filter allows baseband down-conversion at the low-output sample rate. Of course, the two architectures are completely equivalent, as it can be demonstrated applying the "equivalence theorem" and the "noble identity" (not recalled here).

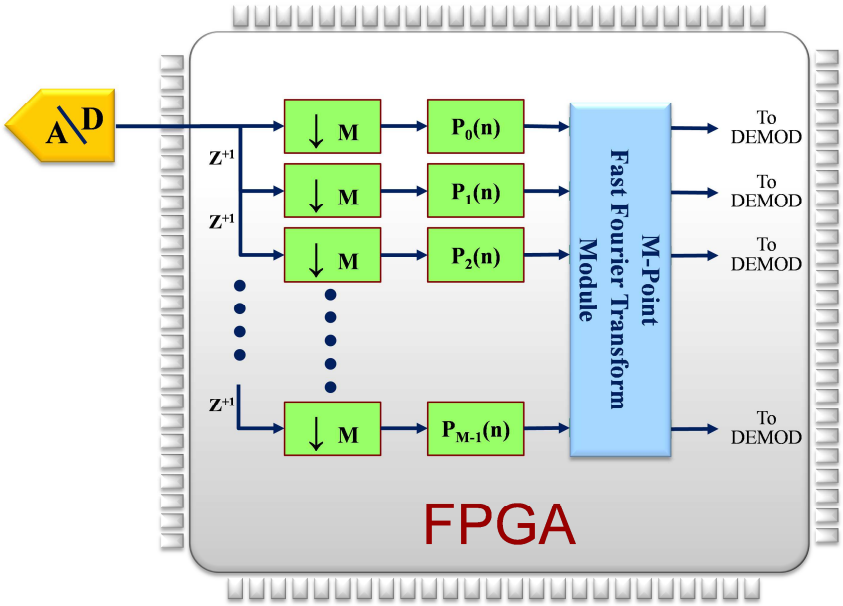

Figure 5-10: FPGA Poliphase FFT Channelizer Architecture

The Quadrature Mirror Filtering (QMF) is based on main idea to divide the total bandwidth in two halves, one high band and one low band, by using linear filters. Since the two sub bands has half the bandwidth of the input signal each filtered signal can be decimated by a factor two without violating the Nyquist criteria. The division of bandwidths can be performed repeatedly by dividing outputs from previous filtration, which will result in a tree structure, called a QMF bank. The different layers in the tree will have different properties concerning time and frequency resolution. The first layer of the tree will have the

best time resolution, while the last layer will have the best frequency resolution. In Figure 5-11 a schematic outline of a three-layer filter tree is presented.

When designing the QMF-bank one important thing is how to choose the filters in each layer.

It is possible to use *sinc* or modified *sinc* filters, allowing some degree of cross correlation between the outputs from the filter pair by using the modified *sinc* filter:

$$h(n) = \sqrt{\frac{S}{2}} \cdot sinc\left(\frac{n + 0{,}5}{C}\right) \cdot w(n)$$

By adjusting the scaling S and compression C the properties can be changed. With $S = 1$ and $C = 2$ the formula describes the *sinc* filter, but by lowering the compression parameter the energy loss, on the transition band, is reduced as an effect of that some of the energy appears in both filter outputs. The S parameter should then be modified to make the sum of squares equals one.

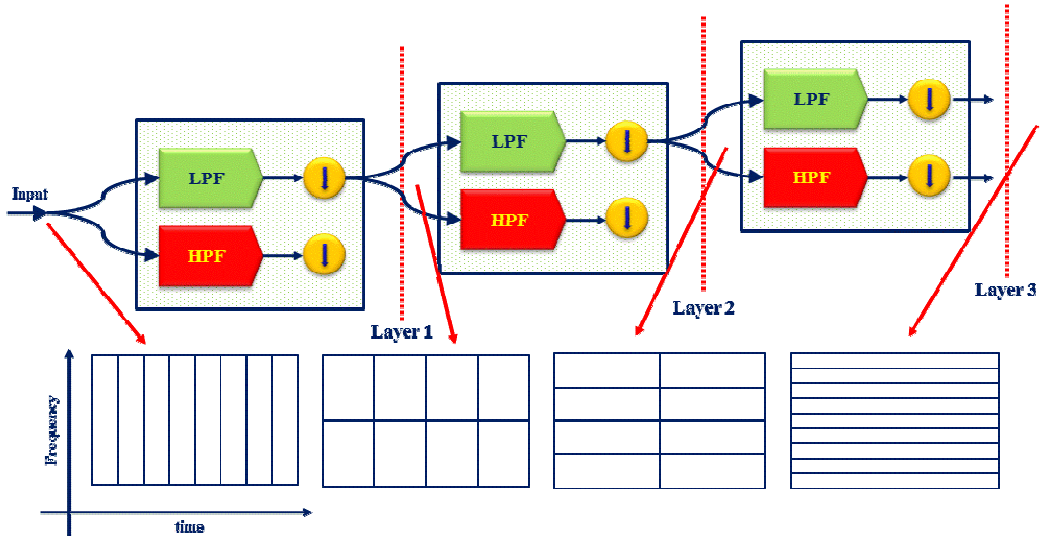

Figure 5-11: Schematic outline of a three layer QMF bank

The computational complexity of a QMF-bank depends on the length of each filter and on the number of layers in the filter bank. If each filter has N number of coefficients the filtering and decimation of one filter in the first layer takes $N/2$ multiplications. This means that the total number of multiplications in the first layer is N. For the second layer the number of filters is doubled. But since the number of samples is reduced in the second layer due to the decimation only half as many samples are produced at this level. This means

that for a fixed time only half as many multiplications have to be performed compared to the first layer. The result is that N number of multiplications is needed in the second layer as well. This can be generalized for all layers which will lead to the conclusion that $M \cdot N$ number of multiplications is needed for the entire filter bank, where M is the number of layers.

Cross-Correlation Processor

As main idea the System Flexibility should allow the selection of different methods for DoA estimation, selected on the basis of value of S/N value and the number of used sensors. On the basis of different solutions, it is allowed the possibility to perform full DSP Processing on-board e/o post processing on ground. Independent by the chosen solution method, the maximization of the parameter under estimation requires the application of specific techniques to reduce the Noise contribution or on the other word to maximize the SNR.

Hereafter will be introduced the main processing block, which have in charge of calculating the Cross-Correlation Matrix needed for Direction of Arrival estimation common in several methods based on eigenvalues solution (e.g. MUSIC algorithm).

The obtained results of the estimator accuracy can be also generalised as applicable for the estimation of such single parameters like Phase Difference used during the calibration phase and in the Interferometry based approach.

The results hereafter shown are referred to a simulation of an actual Direction of Arrival Estimator, operating in 1 MHz sub-band. As possible continuation of the research activity all the algorithms implemented in the simulation environment, can be moved in a hardware platform adopting a Software Radio Define (SRD) approach providing more compact and performing components installable on-board the satellite, contributing, in this way, to the reduce the mass and power budget. This will contribute to reduce the final impact of the proposed system solution on the overall "economy" of the satellite.

Referring to the actual in-house design, the pre-processing block capable to calculating the Cross-Correlation Matrix, works on a pre-stored block samples acquired from the feed signal, each one represented with 8 + 8 bits of precision (further bits dynamic extension is foreseen in new design).

This block has a programmable length (up to 122880 samples), and it is the input to calculate all the 136 terms of the upper half of the Correlation Matrix (which is Hermitian).

For each term, the basic operator is a complex multiplier operating on two samples to be correlated (from feed "i" and feed "j"). The completion of the matrix evaluation requires up to 122880 x 136 x 2 clock cycles.

Taking into account that the new design increases the size of samples block to improve integration performance but, on the same time the foreseen system baseline has five RX sensors, we could consider the actual design sizing, dimensioned for 16 sensors Beam Forming Network (BFN), a reliable reference for the order number handled in the new RFI Geo-Localisation project.

In new project, we could consider a processing sampling rate of 2,5 MHz for each 1 MHz channel Bandwidth under analysis. The acquisition of $10^5 \div 10^6$ samples corresponds to 40 ÷ 400 ms of duration of the observation/integration window that shall be elaborate producing the Accumulate Correlation Matrix in real-time (e.g. each 50 ÷ 500 ms).

At the end of the calculation of each matrix element it will be stored, as complex number, into a buffer to be available for next on-board elaboration or ground data delivery via proprietary link.

Telemetry Data Flow Preliminary Dimensioning

Due to the chosen architecture approach the considered solution(s) for the space and ground link connectivity has been the secure TT&C system that is a current existing space product. Another approach, similar to the TT&C, is based in the Payload Control and Configuration (PCC) spread-spectrum link approach. This last has not a dedicated channel but utilise part of border (close to the margin of the used bandwidth) frequency bandwidth in the data traffic transponder. The advantage of this last solution is the possibility to tune the bandwidth.

TT&C data flow preliminary dimensioning for super-resolution algorithms

To dimension the link channel the following analysis have been carried out, indeed suppos-

ing the proposed physical layout based on five interferometers sensor antennas and teen receiving chains (one for each sensor and polarization).

In the layout described above, there are four baselines, with two polarisations (linear horizontal "H" and vertical "V").

As first approach an FFT (Fast Fourier Transformation) with 2000 points, on a total bandwidth of 1 GHz (0.5 MHz frequency bins) has been taken into account.

For each baseline, each polarization and each frequency bin, it is produced, by comparison of the signal received by the two sensors, a vector: $A^{j\varphi} = I + jQ$ where "I" is the "in-phase" real component and "Q" is the "in-quadrature" imaginary component.

As a total 16000 vectors $A^{j\varphi} = I + jQ$ are calculated, supposing to define each vector by 17 bits.

The objective is to guarantee that the least significant bit (LSB) is small enough to resolve an angle φ smaller than 1°, e.g. 0.33°.

For I, the worst case for small angles is: $cos(\varphi=0°) - cos(\varphi=0{,}33°) = 1{,}6586 \times 10^{-5}$.

The above value represents the requirement for the LSB of I value.

The resolution of I component, obtained with 17 bit, is $\frac{2}{2^{17}-1} = 1{,}52589 \cdot 10^{-5}$, that is smaller than the required value.

The same consideration can be done for the Q component, obtaining the same values.

The total required bits are equal to:

$$vectors \times (I\ number\ of\ bits + Q\ number\ of\ bits) = 16000 \times (17 + 17) = 544\ kb$$

Supposing an integration time of one second, the total data rate is 544 kbps.

Final dimensioning with margin could foresee the use of 18 bit for each component (I or Q) of the sample. In this case, with the same assumptions, the total data rate would be 576 kbps. The data can be transmitted through a communication channel. In alternative, it can be used a dedicated antenna or the TT&C link.

TM data flow preliminary dimensioning for super-resolution algorithms

The required telemetry required in this case, consists in many spatial covariance matrixes

for the different considered frequency bins.

The covariance matrix is composed by $L \times L$ number of complex values, where L is the number of the antenna elements.

The number of bits for each complex value that composes one matrix, as well as the number of frequency bins that is the number of matrixes to be sent on ground, will be determined during the study.

TM data flow preliminary dimensioning for Sample and Dump solution

A more general solution is the "Sample and Dump", that foresees an on-board acquisition of raw signal samples and direct on ground delivery of them for any kind of off-line processing. In this case, it can be imagined that for each sensor (we can suppose as a preliminary dimensioning five sensors) a certain number of collected samples are delivered on ground. In this case, considering the large amount of data to be delivered, we can hypnotize to send on ground only once the samples, collected on a certain period of time, relative to a certain frequency bin, that is the one on which it was observed the presence of an interference.

Let's suppose 100 ms of observation time, and 1MHz output bandwidth (BW) of Poliphase Channelizing Filter (single FFT frequency bin), with 2,6 Msample/s of data rate per channel (single FFT bin). In this case the total collected data block is of 260 Ksamples. Each sample is a complex value, with I and Q components to be sent on ground only once for each sensor. Supposing 18 bit for each component and five sensors, the total data to be sent on ground is of 46,8 Mbit. In the case both polarization are acquired the double will be the data amount to be transferred. On the Raw data block to be delivered it is foreseen the application of data compression algorithms and FEC (Forwarding Error Correction) coding.

Depending by the king of in use downlink channel, the data can be sent to ground with different possible data rates, considering the lower data rates give longer transmission time.

5.2 CALIBRATION TECHNIQUES

In order to obtain a RFI geo-localisation in the required accuracy of 1 km it is important to

consider and compensate performance impairments due to:

- RF chains phase and amplitude errors;
- Satellite drift in its box and attitude pointing.

RF chains phase and amplitude error contribution can be compensated thanks to a calibration tone injected in each RF chain, for different frequencies, and elaborated on ground. This kind of calibration should be performed periodically.

The direct IF sampling solution, in the hypothesis of observed *Bandwidth (BW) = 1 GHz*, produces a required sampling rate which could be approximately: *1,3 x 2·BW = 2,6 GSample/s*.

Looking at rad-hard technology for components, there are on the market several ADC devices capable to provide these requested performance. However, this architecture allows use of adaptive equalisation in the DSP section; this implies a benefit in the relaxed required accuracy for electrical paths calibration and allows the channel equalisation versus non-linear phase behaviour.

It is possible to consider two different approaches for adaptive phase equalisation: one based on adaptive FIR filters, while the other based on transform domain equalisation, typically addressed as FFT beam-forming, enhanced by a specific state of the art technique for ADC non-linear behaviour improvement. Main advantages achieved in the last approach is the reduced penalty due to non-perfect matching between each single ADC belonging to classical pipelined architecture of the ADC devices operating beyond 250 MHz (e.g. TI ADC structure).

For the second error contribution, a dedicated solution (based on algorithms and ad hoc design) will be implemented in order to mitigate differential effects impacting the accuracy of measurements required for geo-localization application.

In addition, in order to improve geo-localization accuracy, a number of on ground reference fixed stations can be used. Each station should have known position, and transmit a predefined signal (beacon). On ground, interference position estimation shall be improved from comparison with the reference stations position estimation.

Satellite contribution to the RFI-Geo-Localisation

To enhance the overall challenging accuracy of the RFI Geo-localization system, accurate satellite ephemerides and attitude data are needed.

Based on standard performance of typical telecommunications satellites, the main contribution to geo-location accuracy is deemed the knowledge of satellite attitude. In the following, a list of the main error contributions included into the computation of a geostationary satellite pointing budget:

- *Spacecraft Structural distortion* (e.g. structure behaviour, spacecraft thermo-elastic distortion)
- *Spacecraft Body pointing Error*, due to attitude sensors accuracy, and to the precision of orbit propagator and control loop algorithm
- *Spacecraft Body Location error* (i.e. Orbital window effect on North/South and East/West position)

By way of example, assuming as reference the TAS SpaceBus platform (see Figure 4-12), the pointing error is 0,1 deg order of magnitude and the knowledge of attitude provided by sensors (i.e. gyroscopes, Star Trackers, Infra-Red Earth sensor) is 0,06 deg order of magnitude (thermal distortions included). It results that the order of magnitude of the attitude pointing error does not allow achieving the required accuracy in geo-location detection.

The proposed system for RFI geo-localization, which is based on RF chains on board, computation techniques and a suitable strategic set of known ground stations, has performance able to include and resolve the impact of ephemerides error on accuracy requirements. As a consequence, the satellite affects the RFI system measurements with second order contributions justified by the following two aspects:

a. thermo-elastic distortions of satellite structure and of all electronics and RF harness included into the RFI system;
b. high frequency disturbances due to actuators of attitude control (i.e. jitter).

Concerning the thermo-elastic differential effect, the earth facing panel (where the sensor array are installed) has an impact on the measurements, as well as electronics and RF harness of the RFI system. A mitigating action is of course a proper thermo-structural design capable of maintaining the mounting panel at a constant temperature. In addition, the components of the RFI-GL technique could be equipped with dedicated temperature sensors to compensate, via analytical models, the relevant errors.

Jitter is the most challenging disturbance to be evaluated, since it requires estimating the torque noise generated by actuators such as reaction wheels (RW), thrusters[1] and solar wing motor.

The effect induced by the thruster activation can be easily eliminated by excluding manoeuvre phases (both Station Keeping and RW desaturation) from the interference measurements periods. Appropriate design could be selected for Reaction Wheel (smoothing bearing) and solar wing motor (adequate micro-stepping).

Thanks to the capacity of the proposed RaFISS technique of achieving disturbance measurements at high frequency, once evaluated the impact of actuator torque noise at high frequency, a filtering model on board (e.g. Kalman filter) could be implemented.

Calibration tone level

Appling the analysis as in ANNEX 3, where the calibration via transfer function parameters estimation is analytically described, a calibration tone level of –15 dB w.r.t. the useful signal may be assumed as a baseline for Digital Processing operation. This level is equivalent to -35 dB_{FS} on the ADC, or -59 dBm per feed.

For this signal level, the single-shot performances of phase and gain calibration are summarized in Table 5-1 (assuming full length DFT). We have to remember that on these figures an improvement of about $\sqrt{N}$ or SQRT(N) is expected by the effect of a software moving average on N estimates.

For the BFN calibration, the calibration tone level may be as high as we want (-24 dBm, or +20dB vs. the useful signal are assumed), since this operation is performed off-line. However, the input signal to the DSPCOP (tone + noise) will be even very low because of the

[1] *A thruster is a propulsive device used by spacecraft and watercraft for station keeping, attitude control, in the reaction control system [RD 19].*

necessity of calibrating the attenuator over their full range.

Tone to Useful Signal Ratio	**FFT Length**	**I&Q Unbalance**		**Feed to Feed Unbalance**	
		Gain	Phase	Gain	Phase
-15dB	1000000	0.06 dB	0.5 deg	0.05 dB	0.5 deg

Table 5-1: Single-Shot Performances of Phase and Gain Calibration

We assume 30 dB of attenuation range, and in Table 5-2 the performances attainable for different FFT length and attenuation levels are given.

Attenuation	**FFT Length**	**I&Q Unbalance**		**Feed to Feed Unbalance**	
		Gain	Phase	Gain	Phase
-30dB	1000	0,05	0,29	0,07	0,79
	3000	0,03	0,17	0,06	0,75
	10000	0,02	0,09	0,05	0,70
	30000	0,01	0,06	0,05	0,63
	100000	0	0,02	0,04	0,63
-20dB	1000	0,05	0,29	0,05	0,36
	3000	0,03	0,17	0,03	0,27
	10000	0,02	0,09	0,03	0,23
	30000	0,01	0,06	0,02	0,22
-10dB	1000	0,05	0,29	0,05	0,28
	3000	0,03	0,17	0,03	0,17
	10000	0,02	0,09	0,02	0,12
	30000	0,01	0,06	0,02	0,09
0dB	1000	0,05	0,29	0,05	0,27
	3000	0,03	0,17	0,03	0,15
	10000	0,02	0,09	0,02	0,10
	30000	0,01	0,06	0,02	0,07

Table 5-2: Performances for Different FFT Length and Attenuation Levels

It must be noticed that in the results here summarized the I&Q unbalance estimation is

conducted each time at the same signal level of the feed to feed unbalance estimation. This is due to the structure of the simulation test bench, but it certainly isn't the best choice, since this first phase may be performed (once!) in the optimal working point of the ADC. Furthermore, higher levels of noise (i.e. lower level of calibration tone) should be explored in order to reduce quantization effects

5.3 SIMULATION ACTIVITY

Starting from the simulation activity as performed in the Lo.C.A.Te. Study [RD 1], a simulator based on MatLAB©/Simulink© environment has been designed.

The Simulink simulation block diagram is reported in Figure 5-12.

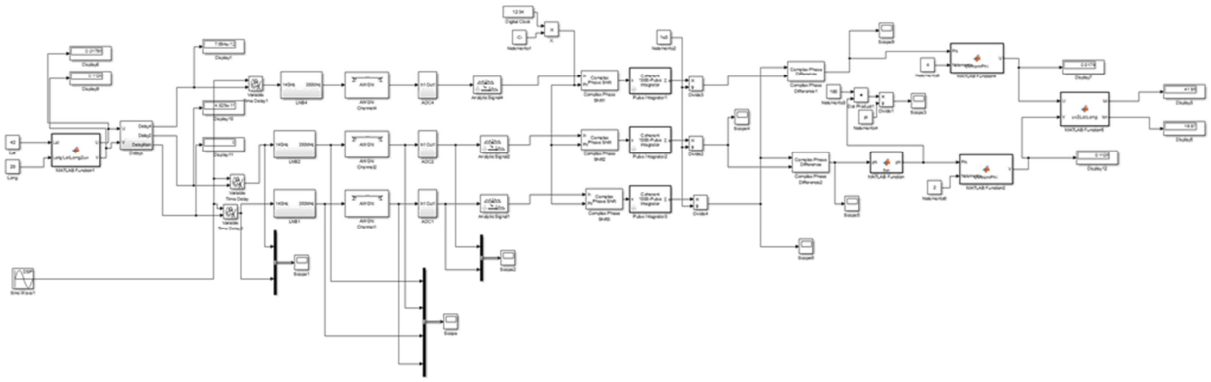

Figure 5-12: Simulator Block Diagram

The implemented modules are:

- Scenario Definition (Number and position of interferences, IPFD and SNR);
- Antenna simulation;
- Covariance Matrix calculation;
- MUSIC Direction of Arrival Elaboration (Spatial Spectrum calculation);
- Find Peaks of Spatial Spectrum:
- Zoom on Spatial Spectrum around peaks for better resolution.

The first module simulates the Scenario and the Covariance Matrix Elaboration as shown

in Figure 5-13.

In Figure 5-14 in the Spatial Spectrum the spatial resolution in localize the RFI sources is shown. The references' meaning is described in Figure 5-15 where the references are reported to respect the sensor/antennas plane. The conversion from (u; v) coordinates (linear coordinates) to the angular ones is performed at the CSS.

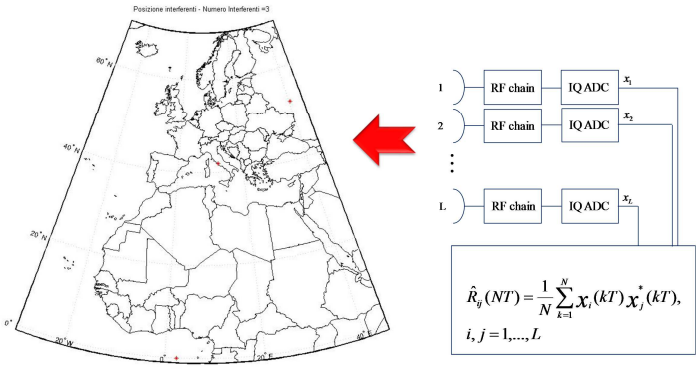

Figure 5-13: Simulation Scenario and Covariance Matrix Block Diagram

Figure 5-14 shows one of the output of the simulation where the spatial resolution of the RFI source is shown as output applying the MUSIC algorithm as in Eq. 5-2:

$$P_{MUSIC}(\theta) = \frac{\mathbf{a}^H(\theta)\mathbf{a}(\theta)}{\mathbf{a}^H(\theta)\hat{\mathbf{\Pi}}^{\perp}\mathbf{a}(\theta)} \qquad \text{Eq. 5-2}$$

The data inputs to the MUSIC algorithm are the number of the RFI signals and the covariance matrix.

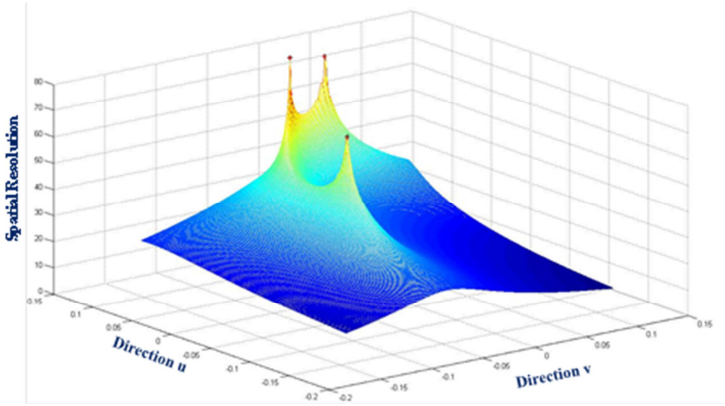

Figure 5-14: Simulation Result on the Spatial Spectrum

The spatial spectrum of the RFI sources is reported also on the geographic map as in Fig-

ure 5-17, showing through the iso-level lines the accuracy of the resolution in geo-localising the RFI sources.

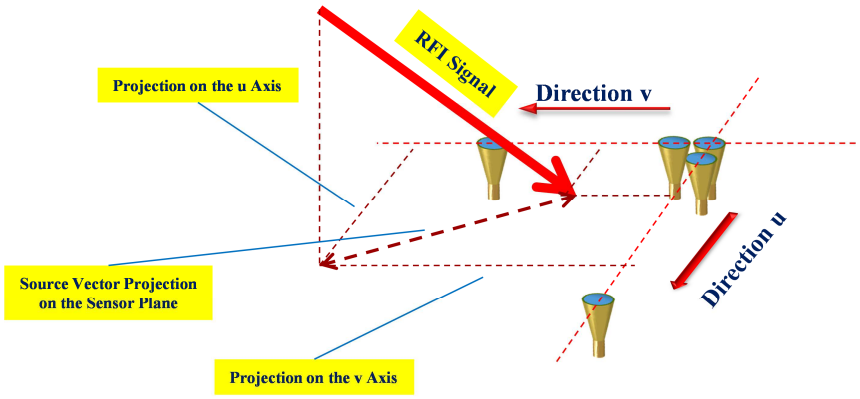

Figure 5-15: RFI signal vector referenced on the plane containing the sensors/antennas

The RFI sources are localised in geographic coordinates (latitude and longitude), with the capability to zoom around the estimated positions increasing, in this way, the information on the resolution accuracy. The procedure is summarised in the simple logic flow in Figure 5-16.

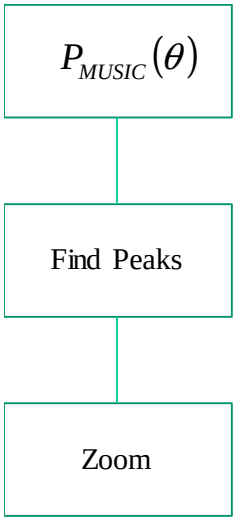

Figure 5-16: Simulation flow to find the RFI sources position improving the positioning accuracy

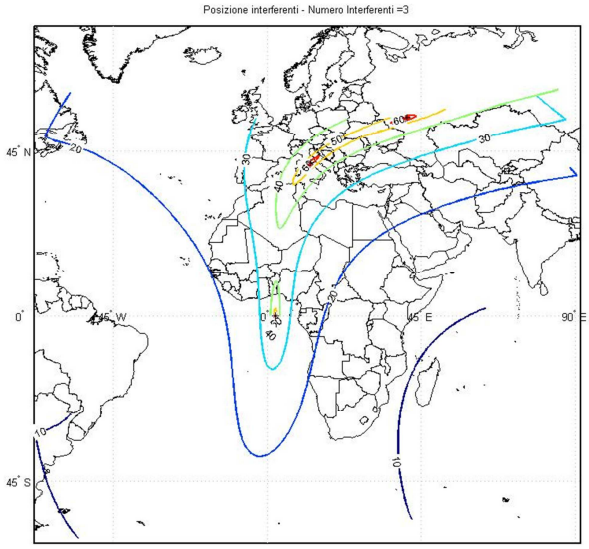

Figure 5-17: Result of the position of the RFI sources on the map

In the ANNEX 4 the MatLAB© code of the main simulation modules is listed.

6 CONCLUSIONS AND FUTURE WORK

During the doctoral period, it has been carried out a research activity already started in the context of the European industrial research supported by the European Space Agency (ESA) and answering to some specific exigency and requirements coming from the commercial satellite operators with in the front-line Eutelsat S.A. (France) that is one of the major SATCOM operator throughout the world.

The origin of the activity preceding the doctoral period has been concentrated in the definition and implementation of anti-interference/anti-jamming satellite solutions for the military satellite communication (MILSATCOM) context, confirmed by the implementation of ad-hoc solutions for the Italian satellite SICRAL (Sistema Italiano per Comunicazioni Riservate e ALlarmi) version 1B (launched in 2009) and SICRAL 2 (launched in 2015 shown in Figure 6-1).

Figure 6-1: SICRAL 2 Satellite [RD 17]

SICRAL satellites are provided of anti-interference/anti-jamming system operating only on one of the satellite transponders and utilizing a more complex antenna configuration that is not the objective of the work carried out during the study.

The results of the research have been utilised for answering to an invitation to tender published by the ESA with the title "*On-Board Interference Geo-Localisation System - GeLoSy*". It has been awarded by TAS-I on mid of 2016 and the contract (ESA contract number 4000117787/16/NL/NR) has been started end of 2016.

The technical solution for the geo-localisation defined and studied during the research activity has captured also the interest of the SATCOM operator EUTELSAT that has proposed to invest for the finalization of an in-orbit demonstrator (IoD) mission installing the prototype of the studied solution on-board of a satellite scheduled in the next years. For this reason, EUTELSAT is collaborating in the Study GeLoSy.

In the GeLoSy Study the technical solution developed during the doctoral period will be finalized and a laboratory emulator of the solution will be implemented starting and reusing the emulation set-up already implemented in the activity of the LoCATe Study and shown in Figure 6-2.

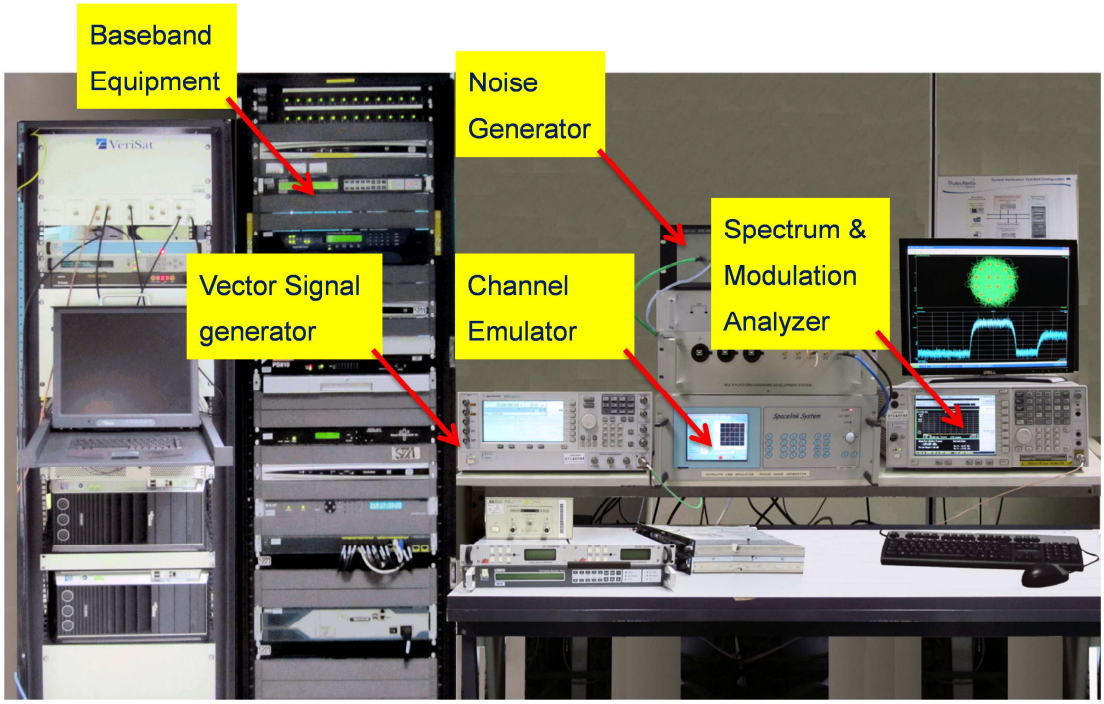

Figure 6-2: Laboratory Emulation Set-Up

As described the activity carried out during the doctoral period is continuing with the objective to verify the effectiveness of the solution in term of performance and mainly in term of compliance with the requests of the commercial SATCOM operators (represented in the case by EUTELSAT). The next step will be the design and implementation of a flying prototype to be used of an In-Orbit Demonstrator (IoD) mission starting the activities to define an effective product for the commercial SATCOM market.

Annexes

7 ANNEX 1

7.1 SUPER-RESOLUTION ALGORITHMS

The processing algorithms described can be divided into two broad categories, in relation to the approach that is used:

- Algorithms based on spectral analysis,
- Algorithms based on the method of subspace.

The first sensor array signal processing techniques date back to World War II. The first example of an algorithm based on the spectral approach is represented by conventional technique (or Bartlet). Subsequently adaptive beam-forming techniques as the Capon technique allowed to identify signals with a better spatial resolution. Algorithms based on spectral approach suffer, however, an important limitation: the performance of the algorithm, which is the spatial resolution of the signals, are directly related to the physical size of the array, regardless of ability to collect and store data.

Next sensor array signal processing techniques, using an approach based on the subspace, allowed the limit to be exceeded, marking the beginning of a new era in the literature of processing of signals. In this type of algorithms solving skills are not in theory limited by the physical size of the array.

Errore. L'origine riferimento non è stata trovata. shows the diagram of an antenna array, receiving three different signals from different directions. Appropriately combining the received signals from the various sensors, it is possible to make an accurate estimate of the direction of arrival of each signal emitted.

It is also possible to estimate other parameters, such as the polarization and the frequency of the received signals. All the information obtained can be used in order to obtain a better adaptation of the pattern to the scenario.

In this section, they are proposed three main algorithms (MUSIC, Conventional and Ca

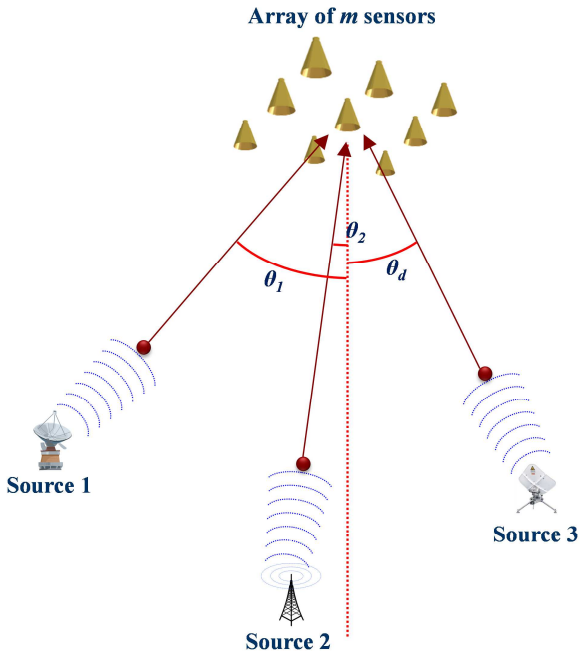

Figure 7-1: Scheme of signals which affect from different directions on a generic antenna array

pon), that, starting from the calculation of the "Spatial Covariance Matrix" **R**, allow to estimate the Direction of Arrival (DOA) of one or more signals.

Here below is the outputs of each algorithm are reported, that is the spatial spectrum. The spatial spectrum has peaks in correspondence of the Directions of Arrival of the received signals.

The MUSIC "spatial spectrum" is defined as [RD 18]:

$$P_{MUSIC}(\theta)=\frac{\mathbf{a}^{H}(\theta)\mathbf{a}(\theta)}{\mathbf{a}^{H}(\theta)\hat{\mathbf{\Pi}}^{\perp}\mathbf{a}(\theta)} \quad \text{Eq. 7-1}$$

The Conventional "spatial spectrum" is defined as [RD 18] :

$$P_{BF}(\theta)=\frac{a^{H}(\theta)\hat{R}a(\theta)}{a^{H}(\theta)a(\theta)} \quad \text{Eq. 7-2}$$

The Capon "spatial spectrum" is defined as [RD 18]:

$$P_{CAP}(\theta)=\frac{1}{\mathbf{a}^{H}(\theta)\hat{\mathbf{R}}^{-1}\mathbf{a}(\theta)} \quad \text{Eq. 7-3}$$

7.1.1 DEFINITION OF THE SPATIAL COVARIANCE MATRIX

Before describing the algorithms, it is appropriate to recall briefly the main theoretical concepts at the base of the models used, defining the concept of the Spatial Covariance Matrix.

An array is made up of two or more radiating elements, appropriately arranged in the space and electrically interconnected.

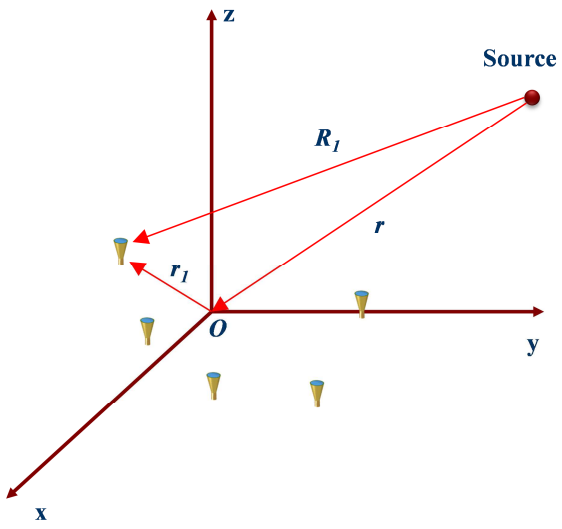

Figure 7-2: 3-dimensional array with arbitrary geometry

Figure 7-2 shows a three-dimensional array with arbitrary geometry and L receiving elements.

Let's define the vector ***x(t)***, containing the response of the L array elements for a received signal *s(t)*, coming from the direction θ:

$$\mathbf{x}(t) = \mathbf{a}(\theta)s(t) \qquad \text{Eq. 7-4}$$

where ***a***(θ) is the array manifold, $\mathbf{a}(\theta) = [a_1(\theta),..., a_L(\theta)]^T$ where $a_l(\theta)$ is the response of the l element of the array for the direction θ, and $\mathbf{x}(t) = [x_1(\theta),..., x_L(\theta)]^T$ is the vector of the received signal by the L elements of the array.

In the presence of signals coming from M different directions, the vector **x** (t) is the sum of all the contributions of the different signals, namely:

$$\mathbf{x}(t) = \mathbf{a}(\theta_1)s_1(t) + ... + \mathbf{a}(\theta_M)s_M(t) \qquad \text{Eq. 7-5}$$

More succinctly it can be written:

$$\mathbf{x}(t) = [\mathbf{a}(\theta_1) \quad ... \quad \mathbf{a}(\theta_M)]\begin{bmatrix} s_1(t) \\ ... \\ s_M(t) \end{bmatrix} = \mathbf{A}(\theta)\cdot\mathbf{s}(t) \qquad \text{Eq. 7-6}$$

where $\mathbf{A}(\theta) = [\mathbf{a}(\theta_1),...,\mathbf{a}(\theta_M)]$ is a matrix [L x M] and $\mathrm{s}(t) = [s_1(t),..., s_M(t)]^T$ is a vector.

To consider the presence of noise, it is appropriate to introduce in the model a random component to be added to the additional signal received by each array element:

$$\boldsymbol{x}(t) = \boldsymbol{A}(\boldsymbol{\theta})\boldsymbol{s}(t) + \boldsymbol{n}(t) \qquad \text{Eq. 7-7}$$

The first objective of the algorithms that are described in this chapter is to extract information about the scenario, from the signals received from the different feeds of the array. Data of interest in this context are of spatial nature. As a result, information is required about the cross-covariance between the different sensors. It is then introduced the spatial covariance matrix.

The spatial covariance matrix can be defined as:

$$\mathbf{R} \triangleq E\{\mathbf{x}(t)\mathbf{x}^H(t)\} = \mathbf{A}E\{\mathbf{s}(t)\mathbf{s}^H(t)\}\mathbf{A}^H + E\{\mathbf{n}(t)\mathbf{n}^H(t)\} \quad \text{Eq. 7-8}$$

where E{·} is the expected value.

The expected value of $\mathbf{s}(t)\mathbf{s}^H(t)$ presented in (7.5) goes under the name of the covariance matrix of the signal P:

$$E\{\mathbf{s}(t)\mathbf{s}^H(t)\} = \mathbf{P} = \begin{bmatrix} P_{1,1} & \cdots & 0 & \cdots & 0 \\ \vdots & \ddots & & \ddots & \vdots \\ 0 & & P_{i,i} & & 0 \\ \vdots & \ddots & & \ddots & \vdots \\ 0 & \cdots & 0 & \cdots & P_{M,M} \end{bmatrix} \quad \text{Eq. 7-9}$$

and under the assumption of uncorrelated signals it is a diagonal matrix. Being zero the correlation between different signals, that all the terms $P_{i,\ j}$ with $i \neq j$ are zero.

The second addend of Eq. 7-5 represents the covariance matrix of the noise. Whereas equal between all the sensors the variance of the statistical noise, equal to σ^2, and assuming that all the sensors are uncorrelated from each other, the covariance matrix of noise takes the form:

$$E\{\boldsymbol{n}(t)\boldsymbol{n}^H(t)\} = \sigma^2\boldsymbol{I} \quad \text{Eq. 7-10}$$

The matrix P is generally non-singular, until the received signals are uncorrelated. In the case of highly correlated signals the matrix P can be almost singular (is singular in the case in which the signals are coherent).

Consequently, also the matrix **R** is, in the case of uncorrelated signals, a non-singular matrix.

The covariance matrix, using the Schur decomposition can be written as follows:

$$\boldsymbol{R} = \boldsymbol{A}\boldsymbol{P}\boldsymbol{A}^H + \sigma^2\boldsymbol{I} = \boldsymbol{U}\Lambda\boldsymbol{U}^H \quad \text{Eq. 7-11}$$

Where U is a unitary matrix, whose columns are formed by L eigenvectors of R, and $\Lambda = diag\{\lambda 1, \lambda 2, \ldots, \lambda L\}$ is diagonal matrix composed by the eigenvalues of R sorted in descending order $\lambda 1 \geq \lambda 2 \geq \ldots \geq \lambda L \geq 0$.

The eigenvalues / vectors can be spit in pairs of eigenvalues / vectors of noise (corresponding to the eigenvalues $\lambda_{M+1},\ldots, \lambda_L$ all equal to each other and of value σ^2) and eigenvalues/vectors of the signal (corresponding to the eigenvalues $\lambda_1,\ldots, \lambda_M$).

It is therefore possible to decompose the covariance matrix as follows:

$$\boldsymbol{R} = \boldsymbol{U}_s \boldsymbol{\Lambda}_s \boldsymbol{U}_s^H + \boldsymbol{U}_n \boldsymbol{\Lambda}_n \boldsymbol{U}_n^H \qquad \text{Eq. 7-12}$$

where $\Lambda_n = \sigma^2 \mathrm{I}$.

7.1.2 MUSIC (MULTIPLE SIGNAL CLASSIFICATION)

Numerous methods have been developed based on spectral decomposition of the covariance matrix, but the most significant innovations have been achieved with the birth of the first so-called subspace based methods.

Among the algorithms based on subspace, the MUSIC (Multiple SIgnal Classification) is undoubtedly the most studied. The main reasons of the great popularity of MUSIC are its generality and versatility, which allows the application to any type of array, and the ability to achieve excellent performance in terms of resolution regardless of the size of the array.

As explained in the previous paragraphs, the structure of the covariance matrix exact, with assumption of Gaussian white noise implies that the spectral decomposition of the same can be written separately considering the contribution of noise and signal. The covariance matrix therefore takes the form:

$$\boldsymbol{R} = \boldsymbol{APA}^H + \sigma^2 \boldsymbol{I} = \boldsymbol{U} \boldsymbol{\Lambda} \boldsymbol{U}^H = \boldsymbol{U}_s \boldsymbol{\Lambda}_s \boldsymbol{U}_s^H + \sigma^2 \boldsymbol{U}_n \boldsymbol{U}_n^H \qquad \text{Eq. 7-13}$$

Where, assuming that $\mathbf{APA}^{\mathrm{H}}$ has full rank (ie in the presence of signals uncorrelated) the diagonal matrix Λ_S contains the M largest eigenvalues, namely those related to the signal. Since the eigenvectors of the noise that constitute the columns of $\mathbf{U_n}$ are all orthogonal to the array manifold **A**, we have:

$$\boldsymbol{U}_n^{\boldsymbol{H}} \boldsymbol{a}(\theta) = 0, \qquad \theta \in \{\theta_1, \ldots, \theta_M\}. \qquad \text{Eq. 7-14}$$

In practice, we do not have the exact covariance matrix, but only the matrix of estimated. Also for the estimated matrix is possible to separate the eigenvectors in eigenvectors of the signal and the noise eigenvectors:

$$\hat{\mathbf{R}} = \hat{\mathbf{U}}_s \hat{\mathbf{\Lambda}}_s \hat{\mathbf{U}}_s^H + \hat{\mathbf{U}}_n \hat{\mathbf{\Lambda}}_n \hat{\mathbf{U}}_n^H \qquad \text{Eq. 7-15}$$

The operator of orthogonal projection on the subspace noise is:

$$\hat{\mathbf{\Pi}}^{\perp} = \hat{\mathbf{U}}_n \hat{\mathbf{U}}_n^H \qquad \text{Eq. 7-16}$$

The MUSIC "spatial spectrum" is then defined as:

$$P_{MUSIC}(\theta) = \frac{\mathbf{a}^H(\theta)\mathbf{a}(\theta)}{\mathbf{a}^H(\theta)\hat{\mathbf{\Pi}}^{\perp}\mathbf{a}(\theta)} \qquad \text{Eq. 7-17}$$

Although $P_{MUSIC}(\theta)$ is not a spatial spectrum in the strict sense (it is rather the distance between two subspaces, the noise and signal), it shows peaks at the arrival directions of the signals, thanks to the property exposed in the Eq. 7-14.

The great advantage of MUSIC that is based on the spectral analysis, is that its performances in terms of resolution are not dependent by the antenna beamwidth or dimensions. Independently from the dimensions of the antenna, using MUSIC it is possible to obtain estimates of accuracy and high resolution, having high number of samples and a signal-noise ratio values.

It is important to notice that MUSIC algorithm foresees the knowledge of the number of signals.

For the estimation of the number of signals other algorithms can be considered, such as:

- AIC (Akaike Information-theoretic Criterion),
- MDL (Minimum Description Length).

The MUSIC, however, has a limitation: it fails in the presence of coherent signals. This limitation is overcome by a new category of methods, said parametric methods, such as the method of maximum likelihood. This method has however the drawback to have a high computational cost. In Figure 7-3 the performance of MUSIC algorithm is graphically shown and in Figure 7-4 the comparison among the Classical Method, CAPON and MUSIC algorithms is shown.

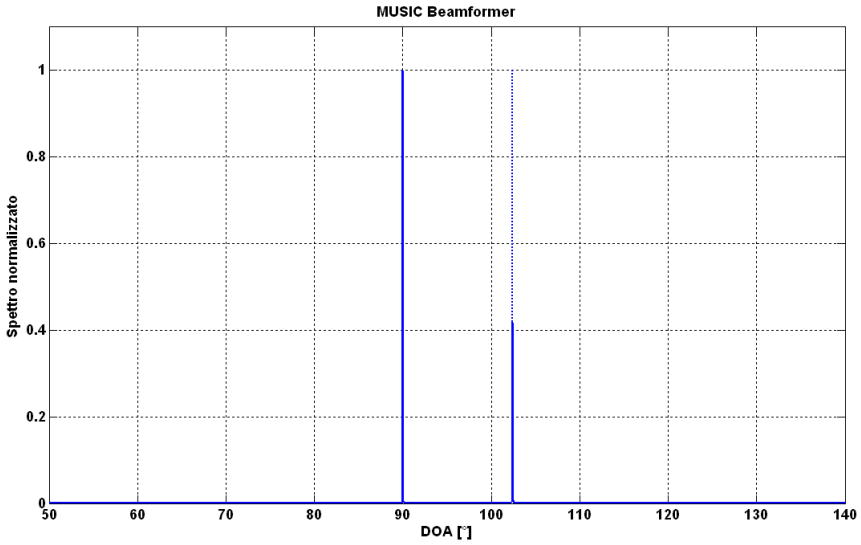

Figure 7-3 Performance of MUSIC

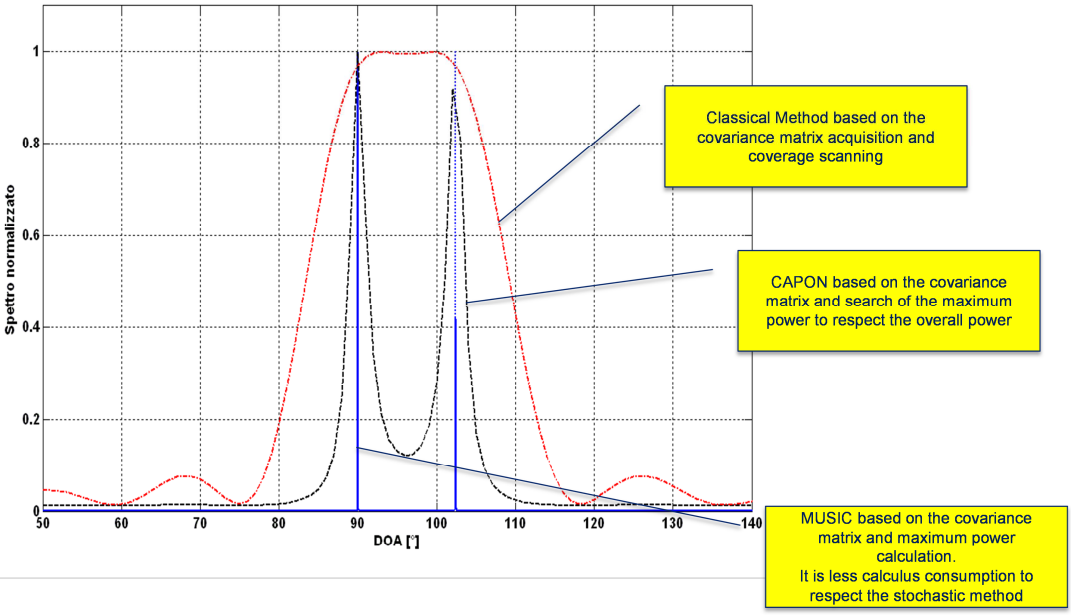

Figure 7-4 Comparison of the three algorithms (red: conventional, black: Capon, blue: MUSIC)

7.1.3 ALGORITHMS BASED ON SPECTRAL ANALYSIS

In order to report the DOA Estimation algorithms based on spectral analysis, such as Conventional and Capon techniques, it has to be defined the output power concept, starting from the definition of the output signal as a linear combination of all the received signals

from the various sensors.

The output signals from the different elements are multiplied by the appropriate weight factors w_l, and subsequently summed.

The output signal of the whole system in the generic instant of time t will then be:

$$y(t) = \sum_{l=1}^{L} w_l^* x_l(t) \qquad \text{Eq. 7-18}$$

Having previously defined as the weight vector as $\mathbf{w} = [w_1, ..., w_L]^T$, it can be written:

$$y(t) = \mathbf{w}^H \mathbf{x}(t) \qquad \text{Eq. 7-19}$$

The average power output can then be written as:

$$P(\mathbf{w}) = \frac{1}{N}\sum_{k=1}^{N} |y(t_k)|^2 = \frac{1}{N}\sum_{k=1}^{N} \mathbf{w}^H \mathbf{x}(t_k)\mathbf{x}^H(t_k)\mathbf{w} = \mathbf{w}^H \hat{\mathbf{R}} \mathbf{w} \qquad \text{Eq. 7-20}$$

It is interesting to note how the power output can be written in function of the estimated covariance matrix.

7.1.4 DOA ESTIMATION ALGORITHM USING CONVENTIONAL TECHNIQUE

The objective of the conventional technique is to maximize the output power of the BFN for a given input signal. For simplicity, it will expose the problem in the case of simplification of two-dimensional space.

The formulation of the problem is:

$$\begin{aligned} \max_{w} P(w) &= \max_{w} E\{w^H x(t) x^H(t) w\} = \max_{w} w^H E\{x(t) x^H(t)\} w \\ &= \max_{w} \left\{ E|s(t)|^2 \left| w^H a(\theta) \right|^2 + \sigma^2 |w|^2 \right\} \end{aligned} \qquad \text{Eq. 7-21}$$

To obtain a non-trivial solution, it is necessary to require that the norm of weight vector **w** is unitary:

$$|\mathbf{w}| = 1 \qquad \text{Eq. 7-22}$$

The vector **w** that maximizes Eq. 7-21 is then:

$$w_{BF} = \frac{a(\theta)}{\sqrt{a^H(\theta) a(\theta)}} \qquad \text{Eq. 7-23}$$

For each direction θ the weight vector calculated according to (7.20) means that the re-

ceived signals from the various sensors in phase.

Substituting Eq. 7-23 in Eq. 7-20, the output power corresponding to each angle of arrival θ is true:

$$P_{BF}(\theta) = \frac{a^H(\theta)\hat{R}a(\theta)}{a^H(\theta)a(\theta)} \qquad \text{Eq. 7-24}$$

By way of example, consider a uniform linear array, with a vector of steering equal to:

$$a_{ULA}(\theta) = \begin{bmatrix} 1 & e^{j\varphi} & \dots & e^{j(L-1)\varphi} \end{bmatrix}^T \qquad \text{Eq. 7-25}$$

where L is the number of elements in the array and:

$$\phi = -kd\ \cos\theta = -\frac{\omega}{c} d\ \cos\theta \qquad \text{Eq. 7-26}$$

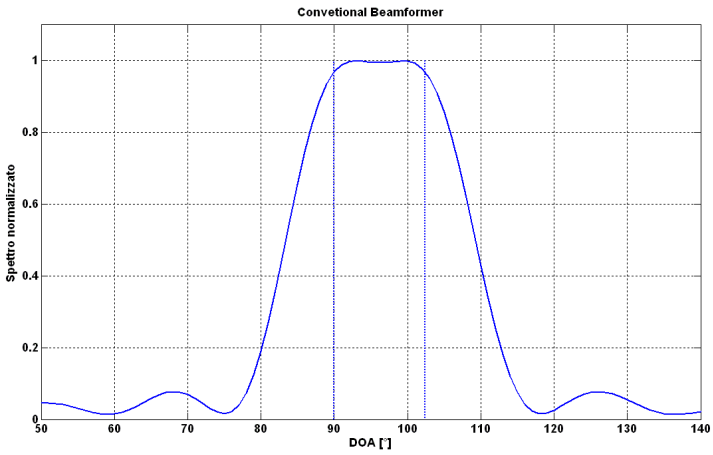

Figure 7-5: Performance of conventional DOA Estimation algorithm

Inserting Eq. 7-26 in Eq. 7-24 it can be calculated the power P(θ). The conventional technique has very low resolution capacity, and these are linked closely to the size of the antenna.

Errore. L'origine riferimento non è stata trovata. Figure 7-5 shows the performance achievable by means of the algorithm of estimation of the directions of the signals realized with the conventional technique. For simplicity, it was considered a uniform linear array.

7.1.5 DOA ESTIMATION ALGORITHM USING CAPON TECHNIQUE

To improve performance in terms of resolution capability, numerous changes have been proposed to conventional technique. One of the alternatives is the Capon technique.

The Capon technique solves signals also very close together, although its resolution capabilities are still closely linked to the size of the array.

The optimization problem of Capon technique can be formulated as follows:

$$\min_{w} P(\mathbf{w}) \qquad \text{subject to} \qquad \mathbf{w}^H \mathbf{a}(\theta) = 1 \qquad \text{Eq. 7-27}$$

It is namely to minimize the power received from directions different from θ, keeping fixed the received power in the direction of observation θ.

Using the technique of Lagrange multipliers, the minimization problem of Eq. 7-27 can be solved. It is obtained:

$$\mathbf{w}_{CAP} = \frac{\hat{\mathbf{R}}^{-1}\mathbf{a}(\theta)}{\mathbf{a}^H(\theta)\hat{\mathbf{R}}^{-1}\mathbf{a}(\theta)} \qquad \text{Eq. 7-28}$$

Inserting (7.25) in (7.17), it can be calculated as follows "spatial spectrum":

$$P_{CAP}(\theta) = \frac{1}{\mathbf{a}^H(\theta)\hat{\mathbf{R}}^{-1}\mathbf{a}(\theta)} \qquad \text{Eq. 7-29}$$

The Capon technique has better performance than the conventional, and makes it possible to resolve signals even very close.

The benefits are, however, still related to the size of the antenna and, of course, to the signal to noise ratio.

Figure 7-6 shows the performance of Capon technique. Comparing Figure 7-6 with **Errore. L'origine riferimento non è stata trovata.**, it is evident how the performance of the Capon algorithm in terms of resolution is much better than those of the conventional.

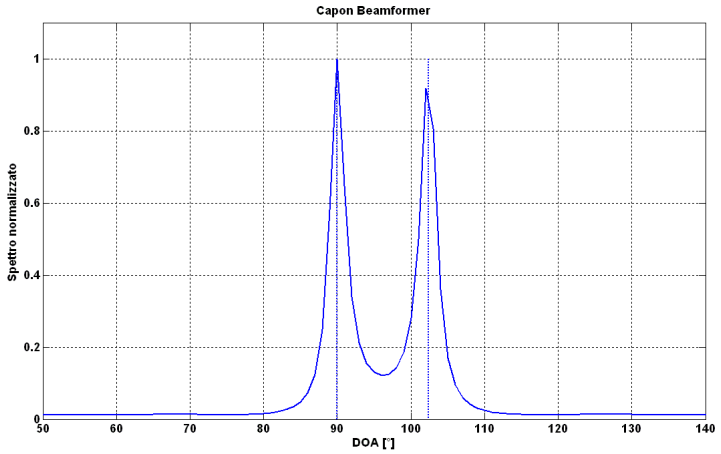

Figure 7-6 Performance of Capon DOA Estimation algorithm

7.1.6 OTHER SUPER-RESOLUTION ALGORITHMS

A large number of other super-resolution algorithms have been formulated and evaluated, giving improved performance over the basic MUSIC algorithm. These include search-free methods such as ESPRIT (Estimation of Signal Parameters by Rotational Invariance Technique) and TAM, one-dimensional parameter search methods such as MUSIC and Capon's MVDR, and multidimensional search schemes such as IMP (Incremental Multi-Parameter), stochastic and deterministic max-likelihood, and WSF.

Table 7-1 shows a classification of these algorithms, into those which works with arrays of arbitrary geometry and those which are formulated for uniformly-spaced linear arrays. The algorithms are also divided into those based on translational invariance, one dimensional parameter searches and multi-dimensional parameter searches.

	Arrays of arbitrary geometry	Equi-spaced linear arrays
Translational invariance	ESPRIT [LS, TLS]*	TAM
One-dimentional parametr search	MVDR (Capon) MUSIC(Schmidt)	Maximum Entropy (Burg) minimum norm (KT)
Multi-dimentional parametr search	IMP (Clarke) WSF Stochastic max. likelihood Deterministic max. likelihood	* Array must process at least one translational invariance

Table 7-1: Classification of super-resolution algorithms

A particular problem occurs when the incident signals are correlated, e.g.in the case with multipath. In this case the MUSIC algorithm does not perform well, and the "pre-whitening" process is necessary to de-correlate the input signals applied to the algorithm. This can be done by taking successive sub-aperture samples of the complete array, and using these as the inputs to the algorithm.

8 ANNEX 2

8.1 ESTIMATION METHOD OF CHANNELS TRANSFER FUNCTION

In order to estimate the channel transfer function, a calibration tone is assumed to be swept over the communication bandwidth. This method has been already used in TAS-I Antenna Nulling Design. Simulation results show the required integration degree for the needed precision achievement in the module and phase estimation.

The following signal will be used:

$$I(nT_s) = A\cos 2\pi \frac{B}{K} knT_s \quad \text{Eq. 8-1}$$

$$Q(nT_s) = A\sin 2\pi \frac{B}{K} knT_s \quad \text{Eq. 8-2}$$

i.e.: $s_{ck}(t) = Ae^{j2\pi f_k t}$ with $t = nT_s$ and $f_k = B/K$ in which B =1 GHz. Hence:

$$s_{ck}(n) = Ae^{j2\pi \frac{B}{K} knT_s} \quad \text{Eq. 8-3}$$

The channel will affect the calibration signal in the following manner:

$$r_{ck}(n) = Ae^{j2\pi \frac{B}{K} knT_s} \left|H(f_k)\right| e^{j\phi(f_k)} \quad \text{Eq. 8-4}$$

i.e., by multiplying the signal by means of |H(f)| and shifting its phase by $\phi(f_k)$; after down-sampling, a single bin (the one where the calibration tone falls, the k-th) of an M points complex DFT will provide a high SNR means to estimate both the channel phase and amplitude attenuation. Hence, defining the received signal as s(n), its DFT at frequency bin k is:

$$S(k) = \sum_{n=1}^{M} s(n) e^{-j2\pi \frac{B}{K} knT_s} = \sum_{n=1}^{M} \left\{ Ae^{j2\pi \frac{B}{K} knT_s} \left|H(f_k)\right| e^{j\phi(f_k)} + n(n) \right\} e^{-j2\pi \frac{B}{K} knT_s} \quad \text{Eq. 8-5}$$

$$S(k) = AM\left|H(f_k)\right| e^{j\phi(f_k)} + \sum_{n=1}^{M} n(n) \quad \text{Eq. 8-6}$$

The obtained SNR is:

$$SNR = \frac{P_{cal}}{P_{noise}} = \frac{A^2 M^2}{M\sigma_{noise}^2} = M\frac{A^2}{\sigma_{noise}^2} \quad \text{Eq. 8-7}$$

The complex multiplier to execute the DFT product with the conjugate of the calibration tone before accumulation will be:

$$\begin{bmatrix} \cos\left(2\pi\frac{B}{K}knT\right) & \text{sen}\left(2\pi\frac{B}{K}knT\right)_s \\ -\text{sen}\left(2\pi\frac{B}{K}knT\right) & \cos\left(2\pi\frac{B}{K}knT\right) \end{bmatrix} \begin{bmatrix} I_{IN} \\ Q_{IN} \end{bmatrix} = \begin{bmatrix} I_{OUT} \\ Q_{OUT} \end{bmatrix} \quad \text{Eq. 8-8}$$

The extraction of the phase and the relative amplitude are simply executed by:

$$|H(f_k)| = \sqrt{\frac{{I_{OUT}}^2 + {Q_{OUT}}^2}{A^2M^2}} = \frac{\sqrt{{I_{OUT}}^2 + {Q_{OUT}}^2}}{AM}$$

and

$$\arg\{H(f_k)\} = arc\tan\frac{Q_{OUT\,k}}{I_{OUT\,k}} \quad \text{Eq. 8-9}$$

The adaptive coefficients calculation can be done by means of Fourier transformation based standard techniques for error minimisation among the synthesised filter response and the desired frequency domain transfer function; least means squares (LMS) algorithm is one of them.

9 ANNEX 3

9.1 CALIBRATION VIA TRANSFER FUNCTION PARAMETERS ESTIMATION

Based on company expertise consolidated in previous projects, is here proposed an adaptive phase equalisation approach based on configurable FIR (Finite Impulse Response) filtering. In order to estimate the FIR coefficients to be dynamically loaded in the Filter architecture, the following steps must be executed:

1. Continuous mode estimation of the complex H(f) describing the overall behaviour of channel processor;
2. Adaptive (continuous mode) calculation of the FIR coefficients for the I and Q branch;
3. Continuous mode operation of the parallel FIR branches data stream equalisation.

The estimation of the overall transfer function of the channel can be obtained by coherent correlation with the discrete-time calibration tone itself on both the I and Q channels. The obtained gain over the noise of useful signal depends on the number *M* of accumulated samples and on the relative power of the applied calibration tone.

By design not all of the functions need to operate at clock equal to the sample rate, since:

1. It is possible (and mandatory) to design the I & Q section adopting architectures capable to reduce its operating speed (e.g. interleaved parallel branches architectures);
2. The FIR filter can be designed in a polyphase parallel architecture whose K branches are operated at a division by K rate
3. Furthermore, in the hypothesis of extraction of the covariance matrix for DoA estimation, using a sub-sampling technique, the required samples processing rate could be one every many, that allows a FIR operation in which only the shift register have to be operated at a full rate speed but decimated speed can be used for Digital Signal Processor

(DSP) multiplying execution in the FPGA. of course, this simplified method can be applied only to the pre-processing stage of a radio-goniometry system and obviously cannot be applied to a true digital transponder with beam forming.

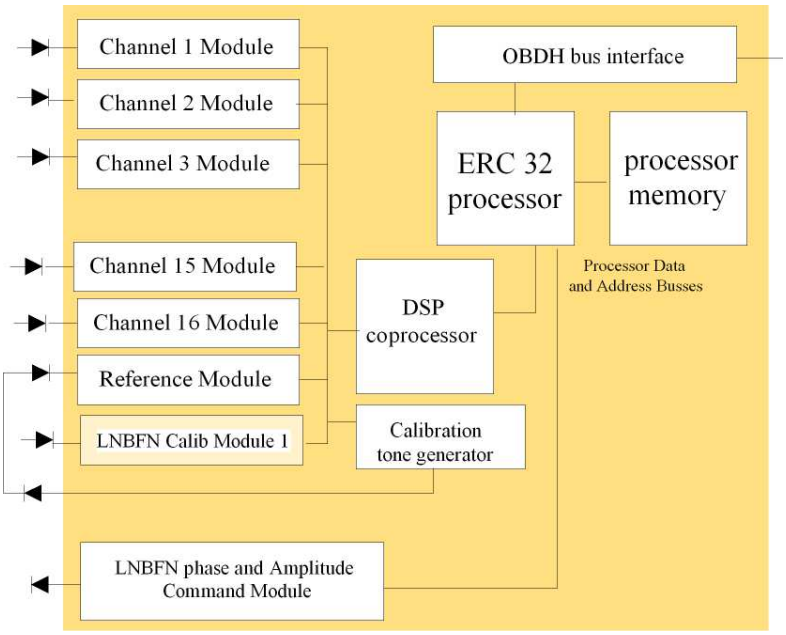

Figure 9-1: Digital part of the Channel Processor coming from Company Heritage System

a) H(f) Phase Behaviour b) H(f) Module Behaviour c) Complex H(f)

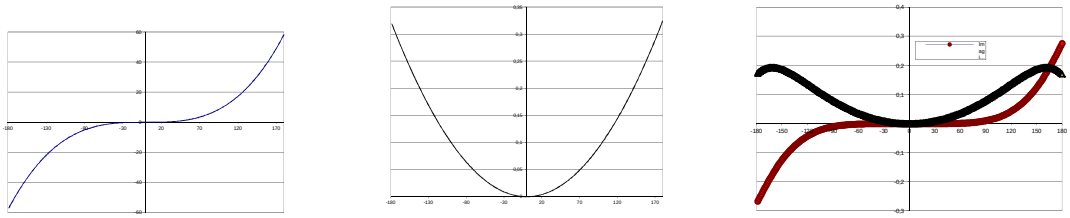

Figure 9-2: a) and b) estimated transfer functions in phase and module form; c) complex transfer function as to be synthesised on I and Q branches

In ANNEX 2 the estimation method of channels transfer function is detailed.

Performance on Phase estimation

A fundamental theorem in statistics states that, given the problem of estimating a set of parameters from a set of noisy observations, there is a lower limit to the variance of any unbiased estimator. This limit is known as the Cramer Rao Bound (CRB).

Since the CRB sets the minimum variance that can be achieved by any unbiased estimator,

its evaluation is important from both a theoretical and practical point of view. While in the general case of the DoA estimation problem the derivation of the CRB is intractable, it can easily be obtained for simple cases. Here it is possible to use the Cramer Rao Bound for phase estimation, i.e.: $\sigma_{\hat{\phi}_e} \geq \frac{1}{\sqrt{SNR}}$

this limit can be easily achieved if estimation is executed onto an un-modulated carrier affected by Additive White Gaussian Noise. Hence:

$$\sigma_{\hat{\phi}_e} \geq \frac{1}{\sqrt{M \frac{A^2}{\sigma^2_{noise}}}} = \frac{1}{\sqrt{2 P_{cal} M / P_{cTot}}} \qquad \text{Eq. 9-1}$$

Where: P_{cal} is the power of the calibration tone and P_{cTot} is the sum of the powers of the user carriers within the 1 GHz Bandwidth (see: Figure 9-3).

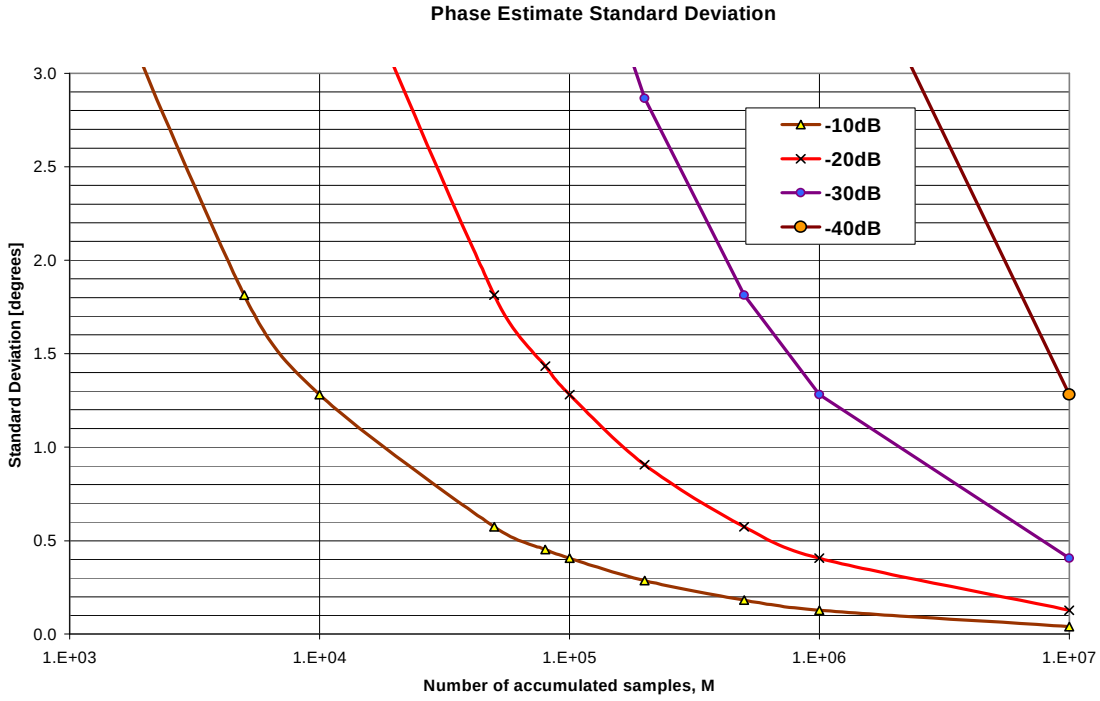

Figure 9-3: Approximate standard deviation of Estimated Phase as a function of the Calibration Tone Power over Total Users Power ratio, i.e., $10 \cdot Log_{10}\left(\frac{P_{cal}}{P_{cTot}}\right)$

The results available in above picture shows that, in the case of 10 dB SNR, the of the required Phase Estimation Accuracy of 0,3 Deg. can be achieved using an integration length of 2 x 10^5 samples.

Performance on Module Estimation

Standard deviation of module can be obtained via similar procedure used for the phase.

To assess the performances of the modulus estimator, we shall calculate the variance of $|H(f)|^2$:

$$\left.\begin{aligned} I_{out} &= AM\,|H(f_k)|\cos(\phi(f_k)) + \sum_{i=1}^{M} n_I; \\ Q_{out} &= AM\,|H(f_k)|\,\mathrm{sen}(\phi(f_k)) + \sum_{i=1}^{M} n_Q; \\ |\hat{H}(f_k)| &= \frac{\sqrt{I_{OUT}{}^2 + Q_{OUT}{}^2}}{AM} \\ \sigma_{|\hat{H}(f_k)|}{}^2 &= E\left\{\left[\,|\hat{H}(f_k)| - |H(f)|\right]^2\right\} = E\left\{\left[|\hat{H}(f_k)|\right]^2\right\} - 2H(f)E\left\{\left[|\hat{H}(f_k)|\right]\right\} + |H(f)|^2 \end{aligned}\right\} \quad \text{Eq. 9-2}$$

$$\left.\begin{aligned} &E\left\{|\hat{H}(f_k)|\right\} = \\ &= \frac{1}{AM} E\left\{\sqrt{\begin{aligned} &A^2M^2\,|H(f_k)|^2\cos^2(\phi(f_k)) + A^2M^2\,|H(f_k)|^2\,sen^2(\phi(f_k)) + \sum_{i=1}^{M} AM\,|H(f_k)|\,n_I\cos(\phi(f_k)) + \\ &+ \sum_{i=1}^{M}\sum_{j=1}^{M} n_I(i)n_I(j) + \sum_{i=1}^{M}\sum_{j=1}^{M} n_Q(i)n_Q(j) + + \sum_{i=1}^{M} AM\,|H(f_k)|\,n_Q sen(\phi(f_k)) \end{aligned}}\right\} = \\ &= \frac{1}{AM} E\left\{\sqrt{\begin{aligned} &A^2M^2\,|H(f_k)|^2 + \sum_{i=1}^{M} AM\,|H(f_k)|\,n_I\cos(\phi(f_k)) + \\ &+ \sum_{i=1}^{M}\sum_{j=1}^{M} n_I(i)n_I(j) + \sum_{i=1}^{M}\sum_{j=1}^{M} n_Q(i)n_Q(j) + \sum_{i=1}^{M} AM\,|H(f_k)|\,n_Q sen(\phi(f_k)) \end{aligned}}\right\} \end{aligned}\right\} \quad \text{Eq. 9-3}$$

Mixed terms ($n_I \bullet \cos(\bullet)$ e $n_Q \bullet \mathrm{sen}(\bullet)$, with increasing M estimate the mean and tend to zero since zero is the mean of n_I e n_Q. On the other hand, the term $n_I \bullet n_Q$ is an estimate of the variance so the above mean of |H(f)| is approximately equal to:

$$\eta = \frac{\sqrt{A^2M^2\,|H(f)|^2 + M\sigma_N{}^2}}{AM} \qquad \text{Eq. 9-4}$$

If σ^2 is much smaller than $A^2M^2|H(f)|^2$ the mean of |H(f)| can be approximated simply with |H(f)|. Let us now calculate $E\{|H(f_k)|^2\}$:

$$
\begin{aligned}
&E\left\{\left[|\hat{H}(f_k)|\right]^2\right\} = E\left\{\frac{I_{OUT}^{\ 2} + Q_{OUT}^{\ 2}}{A^2M^2}\right\} = \\
&= \frac{1}{A^2M^2}E\left\{\begin{aligned}&A^2M^2\,|H(f_k)|^2\cos^2(\phi(f_k)) + A^2M^2\,|H(f_k)|^2\,\mathrm{sen}^2(\phi(f_k)) + \sum_{i=1}^{M} AM\,|H(f_k)|\,n_I\cos(\phi(f_k)) + \\ &+ \sum_{i=1}^{M}\sum_{j=1}^{M} n_I(i)n_I(j) + \sum_{i=1}^{M}\sum_{j=1}^{M} n_Q(i)n_Q(j) + + \sum_{i=1}^{M} AM\,|H(f_k)|\,n_Q\mathrm{sen}(\phi(f_k))\end{aligned}\right\} = \\
&= \frac{1}{A^2M^2}E\left\{A^2M^2\,|H(f_k)|^2\cos^2(\phi(f_k)) + A^2M^2\,|H(f_k)|^2\,\mathrm{sen}^2(\phi(f_k)) + \sum_{i=1}^{M}\sum_{j=1}^{M} n_I(i)n_Q(j) + \ldots.\right\} = \\
&= \frac{A^2M^2\,|H(f_k)|^2 + M\sigma_N^{\ 2}}{A^2M^2} = |H(f_k)|^2 + \frac{\sigma_N^{\ 2}}{A^2M}
\end{aligned}
$$

Eq. 9-5

We can now calculate:

$$\sigma_{|\hat{H}(f)|}^{\ 2} = |H(f_k)|^2 + \frac{\sigma_N^{\ 2}}{A^2M} + |H(f_k)|^2 - 2|H(f_k)|\eta = 2|H(f_k)|^2 + \frac{\sigma_N^{\ 2}}{A^2M} - 2|H(f_k)|\eta \qquad \text{Eq. 9-6}$$

in which η has been above calculated**.**

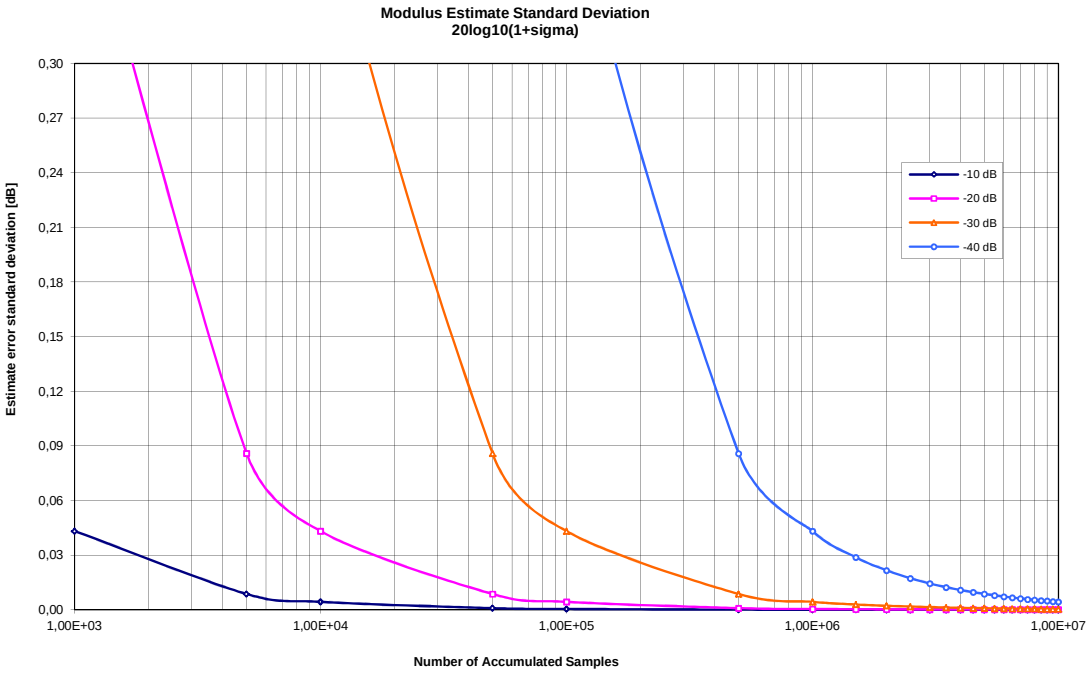

Figure 9-4 : Estimated Module Standard Deviation (20*log10(1+sigma)

Simulation Results

A number of simulations have been made to establish bit-true performances of the DFT processor. These simulations required the external analog environment to be simulated as

well, in order to achieve realistic results. The following RF impairments have been considered in the simulations:

- Calibration tone phase noise (-60 dBc @ 100 Hz, -100 dBc @ 100 kHz, 0,1 rad rms phase jitter) (labelled PNJ in simulation results)
- Sampling clock jitter (1 ns rms) (labelled PNJ in simulation results)
- Mixer IQ unbalance
- Realistic LP filter (5^{th} order Chebishev)

Only two feeds have been considered, focusing on the impacts of different choices of the DFT length on calibration in different situations:

- Calibration tone / useful signal power ratio of -15dB or -20dB
- Presence of phase noise and ADC timing jitter
- Presence of a disturbing signal at +20 dB vs the useful signal

The simulated environment combines the worst case of several parameters. For instance, the actual order of the envisaged LP filter is higher than five while the total phase jitter foreseen for the calibration tone PLL shall be something less than 0.1 rad rms.

Please note that in all the reported simulations the results are related to differential measures (w.r.t. a reference feed). The standard deviation values are thus double than the ones of a single measure.

I&Q unbalance calibration results

In this section the performances of the intra-channel calibration are given. Random values of ρ and φ have been introduced in I&Q unbalance model, and then estimated via Gram-Schmidt formulas using the values of DFT given by the FPGA processor. Statistical properties of the difference between imposed and estimated values have been calculated for a number of simulations, and are shown in the following. It must be pointed out that these

results refer to a single-shot estimation, while the Digital Processing is expected to perform a moving average on several estimates to improve the precision. In Figure 9-5 and Figure 9-6 some simulation results are shown.

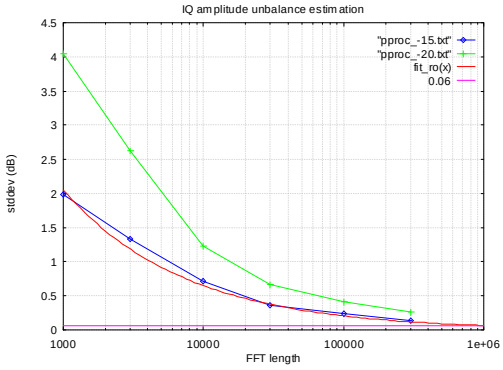

Figure 9-5: Simulated I&Q Amplitude Unbalance estimation

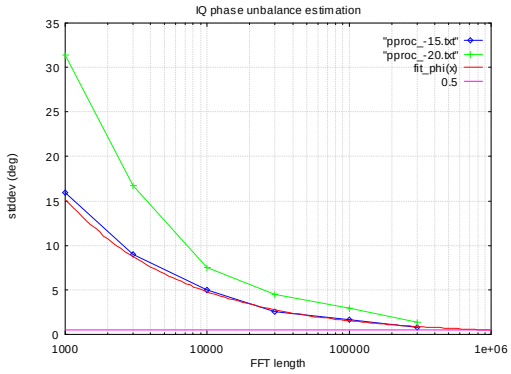

Figure 9-6: Simulated I&Q Phase Unbalance estimation

Feed to feed calibration results

For the feed to feed calibration simulation the same environment as above has been used, and the I&Q unbalance has been introduced, estimated and compensated prior to estimate feed to feed phase and amplitude unbalances. This approach makes the phase and amplitude estimation dependent on the effectiveness of I&Q unbalance compensation (as it is in the realty). However, it must be pointed out that the lack of averaging in this block (that would lead to unbearable simulation times) affects the precision of the estimations. In Figure 9-7and Figure 9-8 some simulation results are shown.

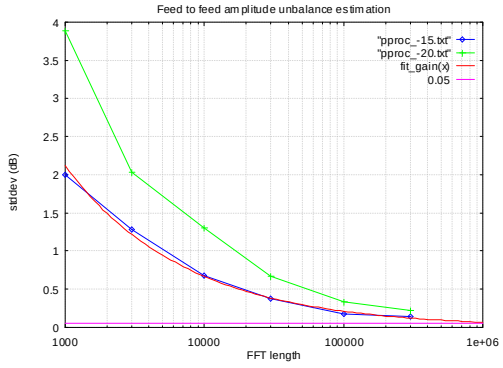

Figure 9-7: Simulated Feed-to-Feed Amplitude Unbalance estimation

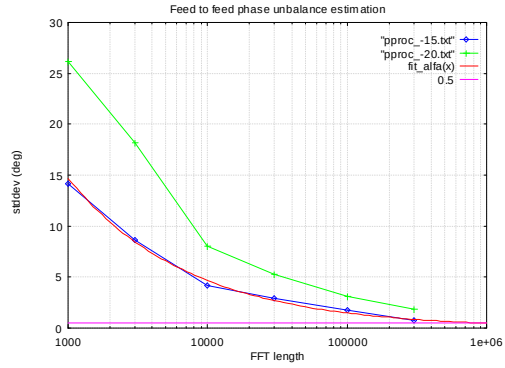

Figure 9-8: Simulated Feed-to-Feed Phase Unbalance estimation

Impact of Phase Noise and Jammer Tone on Gain/Phase Estimation

The impact of phase noise and signal on phase estimation (for 15 dB case only) is given below.

A phase noise term has been added to the calibration tone phase. This term has been simulated by narrow band filtering of a white noise source. The noise mask is depicted in Figure 9-9.

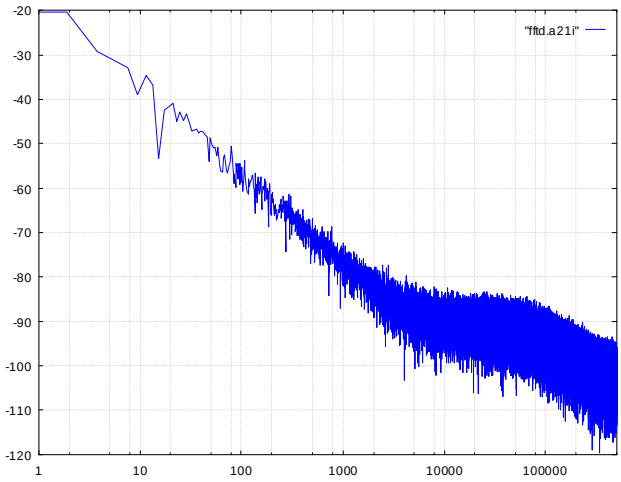

Figure 9-9: Simulated Phase Noise Source

The three lines Blue (baseline), Green (phase noise and timing jitter) and Red (signal at +20 dB vs. the useful signal) show an asymptotic behaviour for high values of the DFT length, both for amplitude and phase estimation.

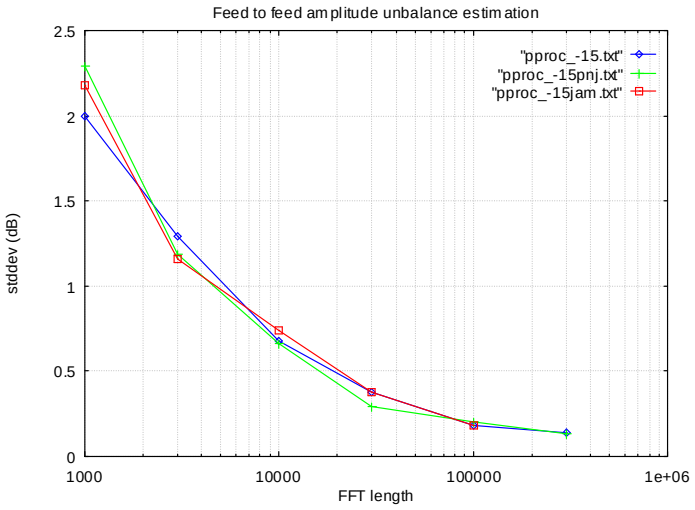

Figure 9-10: Simulated Feed-to-Feed Overall Amplitude Unbalance estimation

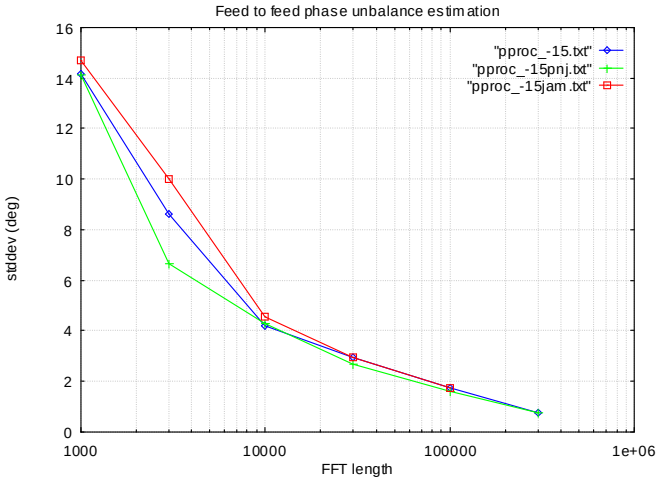

Figure 9-11 : Simulated Feed-to-Feed Overall Phase Unbalance estimation

10 ANNEX 4

In following the MatLAB© [RD 22] code of the main simulation blocks are reported.

Scenario Definition Module

```
%------------------------------
%---- Simulazione Scenario -----
%------------------------------
close all
clear all
clc
% ---Input------
% Coord_int = [41.9 12.416667; 0 11.8; 52.51 13.37]; %Lat e Long Interefrenti
Coord_int = [41.9 12.416667; 0 2.30; 52.51 40.37]; %Lat e Long Interefrenti
% Coord_int = [41.9 12.416667; 0 2.30]; %Lat e Long Interefrenti
% Coord_int = [41.9 12.416667]; %Lat e Long Interefrenti
% Coord_int = [0 11.8; 42 0]; %Lat e Long Interefrenti
% F_int = [29E9; 29.00025E9]; % [Hz]
F_int = [29E9; 29.00025E9; 29.0005E9]; % [Hz]
% F_int = [304.5E6]; % [Hz]
% IPFD_int = [-100; -100]; %dBW/m^2
IPFD_int = [-100; -100; -100]; %dBW/m^2
% IPFD_int = [-100]; %dBW/m^2
%------------------------------

Length_coord = size(Coord_int);
N_int = Length_coord(1); % nemero degli interefernti

figure ('Color','white')
latlim_E = [34, 70];
lonlim_E = [-30, 45];
latlim = [min(latlim_E(1),(min(Coord_int(:,1))-1)), max(latlim_E(2),(max(Coord_int(:,↙
1))+1))];
lonlim = [min(lonlim_E(1),(min(Coord_int(:,2))-1)), max(lonlim_E(2),(max(Coord_int(:,↙
2))+1))];
Map = worlddatamap_mod('cntry02.shp',latlim,lonlim);
land = shaperead('landareas.shp', 'UseGeoCoords', true);
grid on
hold on

title(strcat('Posizione interferenti - Numero Interferenti = ', num2str(N_int)))
plotm(Coord_int(:,1), Coord_int(:,2), 'r*');
hold on

U_V_int = zeros(N_int,2);
for index = 1:1:N_int
    [U,V]= LatLong2uv(Coord_int(index,1),Coord_int(index,2));%Routine per immettere la↙
posizione Lat, Log orbitale del satellite
    U_V_int(index,:) = [U,V];
end
U_V_int

Lat_Long = zeros(N_int,2);
for index = 1:1:N_int
   [lat,lon]=uv2LatLong(U_V_int(index,1),U_V_int(index,2));%Routine per immettere la↙
posizione Lat, Log orbitale del satellite
    Lat_Long(index,:) = [lat,lon];
end
Lat_Long
```

Convolution Matric Module

```
%----------------------------------------
%---- Calcolo Matrice di Covarianza -----
%----------------------------------------
% ------ Costanti ---------------
c = 299792458; % m/s
%---------------------------------

% ------ Input ----------------------------------
% %--Parameters
% U_V_int
F_c = 29E9; % [Hz]
% F_int = [20.050E9; 20.000E9; 20.0100E9]; % [Hz]
% IPFD_int = [-100; -100; -100]; %dBW/m^2
SNR=100;%dB EVENTUALMENTE ELIMINARE E METTERE N DIRETTAMENTE COME INPUT
F_sampl = 1E9; %Hz Frequenza di campionamento
K = 1E6; %Numero Campioni per stima Covarianza
A_eff = 1; %m2 DA RIVEDERE IL VALORE
%-----------------------------------------------
%-----------------------------------------------
IPFD_int_lin = 10.^(IPFD_int./10); %W/m^2
Amp_int = sqrt(IPFD_int_lin.*A_eff);
SNR_lin=10.^(SNR./20);
N = mean(Amp_int)/SNR_lin;
T_sampl = 1/F_sampl; % Tempo di Campionamento
A = SteeringMatrix(U_V_int,F_int);
size_A = size(A);
N_elementi = size_A(1); %Numero Elementi Array
Lambda_int = c./F_int;

%--Data Matrix
%si costruisce la matrice di covarianza R, a partire da
%un segnale random da K punti per ognuna delle interferenti
%e si somma il rumore a dato SNR

% Inizializzazione fasi
phi_0 = 2*pi*rand(N_int,1);

R = zeros(N_elementi,N_elementi);

for k = 1:K
    t = T_sampl*(k-1);
    phi = phi_0 - 2*pi.*F_int.*t;
    s = Amp_int .* exp(1i*phi);
    X = A*s +  N * (randn(N_elementi,1) + 1j*randn(N_elementi,1));
    R = R + X*X';
end

%--Stima matrice di covarianza
R = R/K;
```

MUSIC Algorithm Module

```
% --- MUSIC -------------
passo = 1e-3;

%--EVD and Subspace decomposition
[W, B] = eig(R);
[DD, S] = sort(diag(B),'descend');
Es = W(:,S(1:N_int));
En = W(:,S(N_int+1:end));

%--MUSIC Pseudospectrum
u = -0.13:passo:0.13;
v = -0.13:passo:0.13;
U = length(u);
V = length(v);
Pmusic = zeros(V,U);
for uu = 1:1:U
    for vv = 1:1:V
        U_V = [u(uu), v(vv)];
        an = SteeringMatrix(U_V,F_c);
        Pmusic(vv,uu) = abs(an'*an/(an'*En*En'*an));
%         an = an.';
%         Pmusic(uu,vv) = 1./abs(an*En*En'*an');
    end
end

% Pmusic = Pmusic/max(max(Pmusic));
Pmusic_dB = 10*log10(Pmusic);

figure (2)
% surf(u,v,Pmusic);
mesh(u,v,Pmusic_dB);
xlabel('u')
ylabel('v')
hold on

Lat_grid = zeros(V,U);
Long_grid = zeros(V,U);
for uu = 1:1:U
    for vv = 1:1:V
        [Lat, Long]= uv2LatLong(u(uu),v(vv));
        if (isreal(Lat)&&isreal(Long))
            Lat_grid(vv,uu) = Lat;
            Long_grid(vv,uu) = Long;
        else
            Lat_grid(vv,uu) = real(Lat);
            Long_grid(vv,uu) = real(Long);
        end
    end
end

figure ('Color','white') %figure (3)
latlim = [min(latlim_E(1),min(min((Lat_grid)))), max(latlim_E(2),max((max↙
(Lat_grid))))];
lonlim = [min(lonlim_E(1),min(min((Long_grid)))), max(lonlim_E(2),max((max↙
(Long_grid))))];
```

RFI Geo-Localisation Module

```
%  --Find Peaks------------
tic
[Stima_u_v_int, u_v_index] = FindPeaks(u,v,Pmusic_dB,N_int);
plot_Pmusic_dB = zeros(N_int,1);
real_pos = zeros(N_int,1);
for index =1:1:N_int
    plot_Pmusic_dB(index) = Pmusic_dB(u_v_index(index,2),u_v_index(index,1));
    u_real = find(u>U_V_int(index,1),1,'first');
    v_real = find(v>U_V_int(index,2),1,'first');
    real_pos(index) = Pmusic_dB(v_real,u_real);
end
figure (2)
plot3(Stima_u_v_int(:,1),Stima_u_v_int(:,2),plot_Pmusic_dB,'k+');
hold on
plot3(U_V_int(:,1),U_V_int(:,2),real_pos,'r*');
hold on

Stima_lat_long_int = zeros(N_int,2);
for index = 1:1:N_int
     [Lat, Long]= uv2LatLong(Stima_u_v_int(index,1),Stima_u_v_int(index,2));
     Stima_lat_long_int(index,:) = [Lat, Long];
end
figure (3)
plotm(Stima_lat_long_int(:,1), Stima_lat_long_int(:,2), 'k+');
hold on
toc
```

RFI Position Zoom Module

```
% --- Zoom -----
tic
N_zoom = 10;
passo_zoom = passo/N_zoom;
Stima_u_v_int_zoom = zeros(N_int,2);
Stima_lat_long_int_zoom = zeros(N_int,2);
for index = 1:1:N_int
    u_zoom = (Stima_u_v_int(index,1)-passo) : passo_zoom : (Stima_u_v_int(index,1)
+passo);
    v_zoom = (Stima_u_v_int(index,2)-passo) : passo_zoom : (Stima_u_v_int(index,2)
+passo);
    U = N_zoom*2+1;
    V = N_zoom*2+1;
    Pmusic_Zoom = zeros(V,U);
    for uu = 1:1:U
        for vv = 1:1:V
            U_V = [u_zoom(uu), v_zoom(vv)];
            an = SteeringMatrix(U_V,F_c);
            Pmusic_Zoom(vv,uu) = abs(an'*an/(an'*En*En'*an));
        end
    end
    maximum = max(max(Pmusic_Zoom));
    [vv,uu] = find(Pmusic_Zoom == maximum);
    Stima_u_v_int_zoom(index,:)=[u_zoom(uu), v_zoom(vv)];
    [Lat, Long]= uv2LatLong(Stima_u_v_int_zoom(index,1),Stima_u_v_int_zoom(index,2));
    Stima_lat_long_int_zoom(index,:) = [Lat, Long];
end

figure ('Color','white') %figure (3)
latlim = [min(latlim_E(1),min(min((Lat_grid)))), max(latlim_E(2),max((max
(Lat_grid))))];
lonlim = [min(lonlim_E(1),min(min((Long_grid)))), max(lonlim_E(2),max((max
(Long_grid))))];
Map = worlddatamap_mod('cntry02.shp',latlim,lonlim);
land = shaperead('landareas.shp', 'UseGeoCoords', true);
grid on
hold on
plotm(Coord_int(:,1), Coord_int(:,2), 'r*');
hold on
plotm(Stima_lat_long_int_zoom(:,1), Stima_lat_long_int_zoom(:,2), 'k+');
hold on

% --- quadratini -----
R_pol = 6356.988; %[Km]
R_mean = 6371.005076123; %[Km]
DeltaLat1Km = 360/(2*pi*R_pol); %[deg/Km]
for index = 1:1:N_int
    lat = Coord_int(index,1);
    long = Coord_int(index,2);
    R_lat = R_mean * cos(lat*pi/180);
    DeltaLong1Km = 360/(2*pi*R_lat); %[deg/Km]
    Lat_quad = [lat+DeltaLat1Km, lat+DeltaLat1Km, lat-DeltaLat1Km, lat-DeltaLat1Km,
lat+DeltaLat1Km];
    Long_quad = [long-DeltaLong1Km, long+DeltaLong1Km, long+DeltaLong1Km, long-
DeltaLong1Km, long-DeltaLong1Km];
```

Position Accuracy Improvement Module

```
% --- Zoom dello Zoom -----
tic
N_zoom = 10;
passo_zoom_old =  passo_zoom;
Stima_u_v_int_zoom_old = Stima_u_v_int_zoom;
passo_zoom = passo_zoom/N_zoom;
Stima_u_v_int_zoom = zeros(N_int,2);
Stima_lat_long_int_zoom = zeros(N_int,2);
clear u_zoom;
clear v_zoom;
clear Pmusic_Zoom;
for index = 1:1:N_int
    u_zoom = (Stima_u_v_int_zoom_old(index,1)-passo_zoom_old) : passo_zoom :↙
(Stima_u_v_int_zoom_old(index,1)+passo_zoom_old);
    v_zoom = (Stima_u_v_int_zoom_old(index,2)-passo_zoom_old) : passo_zoom :↙
(Stima_u_v_int_zoom_old(index,2)+passo_zoom_old);
    U = N_zoom*2+1;
    V = N_zoom*2+1;
    Pmusic_Zoom = zeros(V,U);
    for uu = 1:1:U
        for vv = 1:1:V
            U_V = [u_zoom(uu), v_zoom(vv)];
            an = SteeringMatrix(U_V,F_c);
            Pmusic_Zoom(vv,uu) = abs(an'*an/(an'*En*En'*an));
        end
    end
    maximum = max(max(Pmusic_Zoom));
    [vv,uu] = find(Pmusic_Zoom == maximum);
    Stima_u_v_int_zoom(index,:)=[u_zoom(uu), v_zoom(vv)];
    [Lat, Long]= uv2LatLong(Stima_u_v_int_zoom(index,1),Stima_u_v_int_zoom(index,2));
    Stima_lat_long_int_zoom(index,:) = [Lat, Long];
end

figure ('Color','white') %figure (3)
latlim = [min(latlim_E(1),min(min((Lat_grid)))), max(latlim_E(2),max((max↙
(Lat_grid))))];
lonlim = [min(lonlim_E(1),min(min((Long_grid)))), max(lonlim_E(2),max((max↙
(Long_grid))))];
Map = worlddatamap_mod('cntry02.shp',latlim,lonlim);
land = shaperead('landareas.shp', 'UseGeoCoords', true);
grid on
hold on
plotm(Coord_int(:,1), Coord_int(:,2), 'r*');
hold on
plotm(Stima_lat_long_int_zoom(:,1), Stima_lat_long_int_zoom(:,2), 'k+');
hold on

% --- quadratini -----
R_pol = 6356.988; %[Km]
R_mean = 6371.005076123; %[Km]
DeltaLatlKm = 360/(2*pi*R_pol); %[deg/Km]
for index = 1:1:N_int
    lat = Coord_int(index,1);
    long = Coord_int(index,2);
    R_lat = R_mean * cos(lat*pi/180);
```

11 REFERENCE DOCUMENTS

[RD 1] ESA Study Project "Low Cost Anti-Interference Techniques for SATCOM Commercial Satellites (LoCATe)", "*Final Report*", Contract n. 4000103706-11-NL-NR), http://telecom.esa.int/telecom/www/object/index.cfm?fobjectid=32877

[RD 2] ESA Study Project "Low Cost Anti-Interference Techniques for SATCOM Commercial Satellites (LoCATe)", "*TN#1.2: Definition and Justification of Reference Scenarios for Victim Commercial Satellite Networks*", Contract n. 4000103706-11-NL-NR), http://telecom.esa.int//telecom/www/object/index.cfm?fobjectid=32877

[RD 3] ESA Study Project "Low Cost Anti-Interference Techniques for SATCOM Commercial Satellites (LoCATe)", "*TN#1.3: Definition and Justification of Reference Interference Scenario*", Contract n. 4000103706-11-NL-NR), http://telecom.esa.int//telecom/www/object/index.cfm?fobjectid=32877

[RD 4] ESA Study Project "Low Cost Anti-Interference Techniques for SATCOM Commercial Satellites (LoCATe)", "*TN#1.4: Assessment of effects of unmitigated interference*", Contract n. 4000103706-11-NL-NR), http://telecom.esa.int//telecom/www/object/index.cfm?fobjectid=32877

[RD 5] October 25th, 2011, Martin Coleman, WBU-ISOG 2011-Zagreb, "Satellite Interference...The Carrier ID Process".

[RD 6] V. Schena, G. Losquadro, V. Pascale; "*Low Cost Anti Interference Techniques and Performance for Commercial TLC SatCom Missions*"; 18th Ka and Broadband Communications, Navigation and Earth Observation Conference Proceedings; September 24-27, 2012; Ottawa (Canada),pages 459-466.

[RD 7] "*SICRAL Sistema Italiano Per Le Comunicazioni Militari*", Aerospazio, la Difesa e la Sicurezza (AIAD); broschure edited by TELSPAZIO S.p.A.

[RD 8] Recommendation ITU-R V.431-8 (08/2015); "*Nomenclature of the frequency and wavelength bands used in telecommunications - V Series Vocabulary and related subjects*"; ITU-R; August 2015.

[RD 9] April 12th, 2006, Rausch H., CACI Inc., Information Assurance, 2006, IWIA

2006, " *Jamming commercial Satellite communications during wartime an empirical study*".

[RD 10] T. Pratt and C. W. Bostian; "Satellite Communications"; John Wiley and Sons Inc.; USA 1986 (ISBN 0-471-87837-5); pages 113-119.

[RD 11] M. Coleman, 'Satellite Interference! ..Carrier ID, Jamming, and VSAT Statistics', WBU-ISOG Forum, Los Angeles (CA), 29 May 2013.

[RD 12] G. Maral; "VSAT Networks"; Second Edition; John Wiley and Sons Ltd.; UK 2003 (ISBN 0-470-86684-5); pages 173-178.

[RD 13] R. Poisel; "Modern Communications Jamming Principles and Techniques"; Second Edition; Artech House; USA 2011; (ISBN-13 978-1-60807-165-4); pages 121-239.

[RD 14] "*Summary Characteristics of the Hot Bird*^{TM} *Satellites*"; Edited by EUTELSAT S.A. (France); year 2013.

[RD 15] "*Dimostratore di Antenna Nulling Adattivo (Di.A.N.A.)*"; Italia Ministro of Defence (IT-MoD), Contract n. 8905, 16 December 2002.

[RD 16] P. Angeletti, G. Gallinaro, M. Lisi, A. Vernucci, "On-ground digital beamforming techniques for satellite smart antennas", proceedings of the 19th AIAA International Communications Satellite Systems Conference (ICSSC 2001), Toulouse, France, April 2001.

[RD 17] http://www.telespazio.com/it/programmes-programmi/sicral.

[RD 18] Krim, H., Viberg, M., "Sensor Array Signal Processing: Two Decades Later"; Massachusetts Institute of Technology, Laboratory for Information and Decision Systems; Report no.: LIDS-P ; 2282; http://hdl.handle.net/1721.1/3398; January 1995.

[RD 19] https://en.wikipedia.org/wiki/Thruster.

[RD 20] V. Schena, G. Fittipaldi, A. Di Stefano, D. Giancristofaro; "ESA Study on a Flexible and Robust Spread Spectrum Solution Managing Satellite Payload Control and Configuration"; 17th Ka and Broadband Communications, Navigation and Earth Observation Conference Proceedings; October 3-5, 2011; Palermo (Italy); pages 401-408.

[RD 21] G. Maral and M. Bousquet; "Satellite Communiations Systems: Systems, Techniques and Technology", Fifth Edition; John Wiley & Sons Ltd.; 2009; pp. 163-246.

[RD 22] MatLAB© version 2016b (9.1.0.441655) 64-bit, License number: STUDENT; by MathWork

12 LIST OF ACRONYMS

BB	Base Band
BFN	Beam Forming Network
BSS	Broadcasting Satellite Service
CONS	Disadvantage
CRB	Cramer Rao Bound
CW	Continuous Wave
DSP	Digital Signal Processor
DVB	Digital Video Broadcasting
DVB-RCS	Digital Video Broadcasting – Return Channel Satellite
DVB-RCS2	Digital Video Broadcasting – Return Channel Satellite 2
DVB-S2	Digital Video Broadcast by Satellite, Second Generation
EIRP	Effective Isotropic Radiated Power
EoC	Edge of Coverage
ESA	European Space Agency
FFT	Fast Fourier Transform
FGU	Frequency Generation Unit
FIR	Finite Impulse Response
FoM	Figure of Merit
FPGA	Field Programmable Gate Array
FSS	Fixed Satellite Service
FWD	Forward
GBFN	Ground Beam Forming Network
GEO	Geostationary Earth Orbit
GS	Ground Segment
GTW	Gateway
HPA	High Power Amplifier
I/F	Interface
IF	Intermediate Frequency
ITU	International Telecommunication Union
LFM	Linear Frequency Modulation
LHCP	Left Hand Circular Polarisation
LNA	Low Noise Amplifier

LO	Local Oscillator
Lo.C.A.Te.	Low Cost Anti-Interference Techniques for Commercial SATCOM
LOS	Line Of Sight
MCPC	Multiple Channel Per Carrier
MSS	Mobile Satellite Service
MUSIC	Multiple Signal Classification
OMT	Ortho-Mode Transducer
P/L	Payload
PCC	Payload Control and Configuration
PROS	Advantage
QoS	Quality of Service
RaFISS	Radio Frequency Interferometer Sensor System
RD	Reference Document
RF	Radio Frequency
RFI	Radio Frequency Interference
RHCP	Right Hand Circular Polarisation
RTN	Return Link
RX	Receiver or Receiving
SATCOM	Satellite Communications
SICRAL	Satellite Italiano Comunicazioni Riservate ed ALlarmi
SML	Stochastic Maximum Likelihood
SNR	Signal to Noise Ratio
SotA	State-of the-Art
SSPA	Solid State Power Amplifier
TAS-I	Thales Alenia Space Italia
TC	Telecommand
TCR	Telemetry, Command and Ranging
TLC	Telecommunications
TM	Telemetry
TRL	Technology Readiness Level
TTC&R	Tracking, Telemetry, Command and Ranging
TWTA	Travelling Wave Tube Amplifier
TX	Transmission